University of Alberta

TEMPERATURE DEPENDENCE OF PROTEIN AND ORGANELLE TRANSPORT IN THE SCIATIC NERVE OF THE AMPHIBIAN *XENOPUS LAEVIS*

by

RACHEL MELANIE OATES ©

A thesis submitted to the Faculty of Graduate Studies and Research in partial fulfilment of the requirements for the degree of **MASTER OF SCIENCE**

DEPARTMENT OF ANATOMY AND CELL BIOLOGY

EDMONTON, ALBERTA

FALL 1995

National Library
of Canada

Acquisitions and
Bibliographic Services Branch

395 Wellington Street
Ottawa, Ontario
K1A 0N4

Bibliothèque nationale
du Canada

Direction des acquisitions et
des services bibliographiques

395, rue Wellington
Ottawa (Ontario)
K1A 0N4

Your file Votre référence

Our file Notre référence

THE AUTHOR HAS GRANTED AN IRREVOCABLE NON-EXCLUSIVE LICENCE ALLOWING THE NATIONAL LIBRARY OF CANADA TO REPRODUCE, LOAN, DISTRIBUTE OR SELL COPIES OF HIS/HER THESIS BY ANY MEANS AND IN ANY FORM OR FORMAT, MAKING THIS THESIS AVAILABLE TO INTERESTED PERSONS.

L'AUTEUR A ACCORDE UNE LICENCE IRREVOCABLE ET NON EXCLUSIVE PERMETTANT A LA BIBLIOTHEQUE NATIONALE DU CANADA DE REPRODUIRE, PRETER, DISTRIBUER OU VENDRE DES COPIES DE SA THESE DE QUELQUE MANIERE ET SOUS QUELQUE FORME QUE CE SOIT POUR METTRE DES EXEMPLAIRES DE CETTE THESE A LA DISPOSITION DES PERSONNE INTERESSEES.

THE AUTHOR RETAINS OWNERSHIP OF THE COPYRIGHT IN HIS/HER THESIS. NEITHER THE THESIS NOR SUBSTANTIAL EXTRACTS FROM IT MAY BE PRINTED OR OTHERWISE REPRODUCED WITHOUT HIS/HER PERMISSION.

L'AUTEUR CONSERVE LA PROPRIETE DU DROIT D'AUTEUR QUI PROTEGE SA THESE. NI LA THESE NI DES EXTRAITS SUBSTANTIELS DE CELLE-CI NE DOIVENT ETRE IMPRIMES OU AUTREMENT REPRODUITS SANS SON AUTORISATION.

ISBN 0-612-06514-6

Canada

University of Alberta

Library Release Form

Name of Author:	RACHEL MELANIE OATES
Title of Thesis:	TEMPERATURE DEPENDENCE OF PROTEIN AND ORGANELLE TRANSPORT IN THE SCIATIC NERVE OF THE AMPHIBIAN *XENOPUS LAEVIS*
Degree:	MASTER OF SCIENCE
Year this Degree Granted:	1995

Permission is hereby granted to the University of Alberta Library to reproduce single copies of this thesis and to lend or sell such copies for private, scholarly, or scientific research purposes only.

The author reserves all other publication and other rights in association with the copyright in the thesis, and except as hereinbefore provided, neither the thesis nor any substantial portion thereof may be printed or otherwise reproduced in any material form whatever without the author's prior written permission.

Rachel Oates

Rachel Melanie Oates
5716-144 Street
Edmonton, AB T6H 4H4

dated: July 31, 1995

Finish every day and be done with it.
You have done what you could;
Some blunders and absurdities crept in -
Forget them as soon as you can.
Tomorrow is a new day.
You shall begin it well and serenely,
And with too high a spirit
To be encumbered with your old nonsense.

Ralph Waldo Emerson

The University of Alberta

Faculty of Graduate Studies and Research

The undersigned certify that they have read, and recommend to the Faculty of Graduate Studies and Research for acceptance, a thesis entitled TEMPERATURE DEPENDENCE OF PROTEIN AND ORGANELLE TRANSPORT IN THE SCIATIC NERVE OF THE AMPHIBIAN *XENOPUS LAEVIS* submitted by RACHEL OATES in partial fulfillment of the requirements for the degree of MASTER OF SCIENCE.

Richard S. Smith

Dr. R. S. Smith (supervisor)

Richard E. Snyder

Dr. R. E. Snyder (co-supervisor)

David G. Begg

Dr. D. Begg

Tessa Gordon

Dr. T. Gordon

95/07/26

To Honey, Kirsten, Rosie, and Gene,

The world is so empty,
If one thinks only
Of mountains, rivers, and cities;

But to know someone
Here and there
Who thinks and feels with us and

Who, though distant,
Is close to us in spirit,
This makes the earth for us
An Inhabited Garden...

Anonymous

ABSTRACT

The temperature dependence of the fast anterograde transport of newly synthesized proteins and organelles was investigated in the sciatic nerve of the amphibian, *Xenopus laevis*. Fast axonal transport of ^{35}S-methionine labelled proteins was detected with a position-sensitive detector of ionizing radiation. Fast transport of membrane-bounded organelles was visualized in isolated sciatic axons using computer-enhanced video microscopy. The velocity of newly synthesized proteins and small vesicles had a similar exponential dependence on temperature over a range of 6.5-25°C. Below 6.5°C the velocity of protein transport dropped to zero but transport resumed on rewarming the nerve. The drop in protein transport velocity at 6.5°C correlated with a 3-4 fold increase in the amount of labelled protein lost to a stationary phase. Small vesicles continued to move to 0°C; rod-shaped organelles ceased moving at 10°C. The temperature dependence of anterograde and retrograde organelle transport was compared. Control experiments revealed that the detector used in the protein transport experiments could significantly affect the results under some conditions. The work shows that the dynamics of protein transport may, under some conditions, differ from those of organelle transport, the findings support the hypothesis that a loose, reversible, association exists between newly synthesized proteins and their carrier vesicles.

TABLE OF CONTENTS

1. INTRODUCTION

1. 0. General introduction 1
1. 1. The properties of protein and organelle transport 5
    1. 1. 0. Anterograde protein transport 5
    1. 1. 1. Retrograde protein transport 9
    1. 1. 2. Anterograde and retrograde organelle transport 9
1. 2. Protein and organelle transport: evidence to support their relationship 12

2. EFFECTS OF TEMPERATURE ON THE ANTEROGRADE TRANSPORT OF PROTEINS IN THE FROG SCIATIC NERVE

2. 0. Introduction 18
2. 1. Methods 18
    2. 1. 0. Nerve preparation 19
    2. 1. 1. Radiolabelled pulse creation 19
    2. 1. 2. Data acquisition and analysis 23
    2. 1. 3. Methods of studying rapid anterograde transport of proteins 28
    2. 1. 4. Further analysis 30
    2. 1. 5. Liquid scintillation analysis 31
2. 2. Results
    2. 2. 0. The effects of temperature on protein transport rates by Method 1 32
    2. 2. 1. The effects of temperature on protein transport rates by Method 2 32
    2. 2. 2. The effects of temperature upon protein deposition 36
2. 3. Summary 45

3. FACTORS THAT MAY ACCOUNT FOR THE DIFFERING RESULTS OBTAINED FROM THE TWO EXPERIMENTAL APPROACHES

3. 0. Introduction 47
3. 1. Methods
    3. 1. 0. Approaches to monitoring temperature 48
    3. 1. 1. A procedure to mimic both experimental approaches 48
3. 2. Results
    3. 2. 0. Temperature readings 51
    3. 2. 1. Protein transport along the newly constructed press 52
3. 3. Summary 56

4. THE EFFECTS OF TEMPERATURE ON FAST AXONAL TRANSPORT OF ORGANELLES MOVING IN THE ANTEROGRADE AND RETROGRADE DIRECTIONS

4. 0. Introduction 57
4. 1. Methods 57
4. 1. 0. Nerve preparation 58
4. 1. 1. Temperature measurement and control 59
4. 1. 2. Computer-enhanced video light microscopy 59
4. 1. 3. Other methods 60
4. 1. 4. Data analysis of organelle transport 61
4. 2. Results
4. 2. 0. The effects of temperature on organelles with circular images 63
4. 2. 1. The effects of temperature on the transport of rod-shaped organelles 68
4. 2. 2. Q_{10} values and the apparent E_a values 73
4. 2. 3. Organelle transport after 14 hours cooling 73
4. 3. Summary 77

5. DISCUSSION

5. 0. Main findings 81
5. 1. Protein transport 85
5. 2. Organelle transport 86
5. 3. Possible mechanisms of organelle and protein transport 89
5. 4. Difference in results obtained from Methods 1 and 2 92
5. 5. General conclusion 95

6. REFERENCES 97

LIST OF TABLES

Chapter 2.

Table 2. 1. Mean percentage values of protein deposition from Method 1-treated nerves before, during, and after a 14-hour cooling period...38

Table 2. 2. Mean percentage values of protein deposition from Method 2-treated nerves during and after a 48-hour cooling period.....39

Chapter 4.

Table 4. 1. Organelle classification.....62

Table 4. 2. Q_{10} values and apparent activation energies.....74

LIST OF FIGURES

Chapter 2.

Figure 2. 1. Diagram of pulse creation..... 20
Figure 2. 2. Selected counts-vs-time plots from Method 1 and analysis..... 24
Figure 2. 3. Selected counts-vs-time plots from Method 2 and analysis..... 26
Figure 2. 4. Anterograde protein transport vs. temperature (Method 1 analysis)..... 33
Figure 2. 5. Semilog plot of Figure 2. 4..... 34
Figure 2. 6. Anterograde protein transport vs. temperature (Method 2 analysis)..... 35
Figure 2. 7. Semilog plot of Figure 2. 6..... 37
Figure 2. 8. Deposition rate (Method 1) before, during, and after cooling..... 40
Figure 2. 9. Comparison of deposition rates obtained from Methods 1 and 2.. 41
Figure 2. 10. Deposition rate (Method 2) during and after cooling..... 43

Chapter 3.

Figure 3. 1. Diagram of experimental set up with modified press..... 50
Figure 3. 2. Percent distribution of TCA-insoluble radioactivity in each 3.18-mm nerve segment..... 54

Chapter 4.

Figure 4. 1. Mean velocity of anterogradely- and retrogradely-moving vesicles vs. temperature..... 64
Figure 4. 2. Semilog plot of Figure 4. 1..... 66
Figure 4. 3. Mean velocity of anterogradely- and retrogradely-moving rod-shaped organelles vs. temperature..... 69
Figure 4. 4. Semilog plot of Figure 4. 3..... 71
Figure 4. 5. Mean vesicle transport in nerves cooled for 2 hours and 14 hours with or without a press..... 75
Figure 4. 6. Vesicle transport in taxol-untreated and treated nerves..... 78

Chapter 5.

Figure 5. 1. Comparison of protein transport from this work with previous studies 81
Figure 5. 2. Relationship between deposition rate and protein/vesicle transport 84
Figure 5. 3. Dynamics of protein and vesicle transport in relation to temperature 93

LIST OF ABBREVIATIONS

AChE	acetylcholinesterase
DBH	dopamine-β-hydroxylase
DRG	dorsal root ganglion
DWLS	distance-weighted least squares smoothing curve
E_a	apparent activation energy
LC	large, circular
LR	large, rod-shaped
LSC	liquid scintillation counting
MPC	multiple proportional chamber
SC	small, circular
SDS-PAGE	sodium dodecyl sulphate-polyacrylamide gel electrophoresis
SEM	standard error of the mean
SR	small, rod-shaped
TCA	trichloroacetic acid

1 INTRODUCTION

1.0 General introduction

The neuron is a highly specialized cell with a cell body and long cytoplasmic processes, namely the axon and dendrites. Since the protein synthesis machinery is confined to the neuronal cell body (Lasek, 1968; Ochs and Ranish, 1969; Ochs and Hollingsworth, 1971; Edström and Mattsson, 1972), an efficient transport system has developed to shuttle proteins between the cell body, the axons, and the nerve terminals. This system is called axonal transport. The axonal transport of proteins can be divided into two major phases that are distinguished by the speed of movement and the types of proteins carried. Cytoskeletal proteins are the major components of the slow axonal transport, moving at approximately 1-5 mm/day. Fast axonal transport, the subject of this thesis, refers to the movement of membrane-associated materials, namely proteins, lipids, and some other materials (*e.g.*, non-protein transmitter agents and tRNA), at speeds of up to 400 mm/day in mammals (Grafstein and Forman, 1980).

Proteins destined for fast anterograde axonal transport are synthesized on ribosomes associated with the rough endoplasmic reticulum (Hammerschlag *et al.*, 1982) and then routed through the Golgi apparatus where they are glycosylated and sulfated (Stone and Hammerschlag, 1987). These materials then leave the Golgi apparatus via the trans Golgi network in a manner similar to the formation of secretory vesicles (Griffiths and Simons, 1986; Bauerfeind and Huttner, 1993; Rothman, 1994). In axons the carrier organelles are believed to be membrane-bounded organelles 50-100 nm in diameter (Smith, 1980; Tsukita and Ishikawa, 1980). Subsequently, these organelles are actively

transported along microtubule tracks by the action of an ATP-driven motor, presumed to be kinesin, towards the nerve terminals (Vale *et al.*, 1985a, 1985b; Hirokawa *et al.*, 1991). There is also a return (retrograde fast transport) of membrane-bounded organelles towards the neuronal cell body. These organelles carry materials presumed to be destined for degradation, recycling or signalling towards the cell body (Bisby, 1985). The motor responsible for retrograde transport of membrane-bounded organelles is believed to be cytoplasmic dynein (Schnapp and Reese, 1989; Schroer *et al.*, 1989).

The exact relationship between the fast axonal transport of membrane-bounded carrier organelles and that of newly synthesized proteins is not clearly understood. Two models have been proposed to explain this relationship. The first model assumes that, as with secretory proteins (Bauerfeind and Huttner, 1993), the association between proteins and organelles is very stable such that newly synthesized proteins are lost from their carrier organelles only when the organelles fuse with an existing membrane, such as the axolemma or endoplasmic reticulum (Luzio and Banting, 1993; Rothman, 1994). This model predicts that transport properties of newly synthesized proteins will exactly match those of organelles. Evidence to support this view is the finding that most rapidly transported proteins are integral membrane proteins (Bennett *et al.*, 1973; Droz *et al.*, 1973; Giamberardino *et al.*, 1973; Morin *et al.*, 1991), and hence the association between proteins and organelles must be stable. Moreover, the velocities of rapidly transported proteins generally correspond with those of organelles (Smith and Snyder, 1992), although comparisons of the data are difficult because of differences in the time and spatial scales of experimental measurements, and in the rates of axonal transport between nerves in a single species as well as between different taxonomic groups of animals.

The second model proposes that the association of rapidly-transported, newly-synthesized proteins with their carrier organelles is loose, so that these proteins may be lost from the organelles under some circumstances. This model allows for the uptake of free cytosolic proteins by carrier vesicles, an event that has been observed in a study by Ambron and his colleagues (1992). The weakness of this model is that the molecular mechanisms by which such a two-way association/dissociation can take place between organelles and proteins are completely unknown. However, a considerable amount of evidence supports this model. A more detailed review of this evidence will be presented in Section 1. 2. Here, it is sufficient to point out that the evidence rests on demonstrating differences in the transport properties of newly-synthesized radiolabelled proteins and organelles. For instance, deposition of a portion of labelled proteins from the moving phase to a stationary phase has been described (Gross and Beidler, 1975; Muñoz-Martínez, 1982), but no corresponding loss of rapidly transported organelles has been detected (Snyder *et al.*, 1990). In addition, the finding of differences in the anterograde-to-retrograde reversal of protein and organelle transport at nerve lesions suggests that proteins are lost from carrier organelles during transport reversal (Smith and Snyder, 1991; Snyder *et al.*, 1994).

As a means of further understanding the relationship between proteins and organelles, one may consider examining the relationship between the velocity of fast axonal transport and temperature. Studies on fast anterograde transport of radiolabelled proteins in amphibian (Edström and Hanson, 1973; Brimijoin *et al.*, 1979) and mammalian (Ochs and Smith, 1975; Cosens *et al.*, 1976) sciatic nerves describe an exponential relationship between the velocity of protein transport and temperature down to a critical 5-10°C temperature range, below which the velocity of protein transport abruptly drops. No corresponding measurements of the temperature sensitivity of anterogradely

transported organelles have been made prior to the present work. Consequently, the following possibilities are:

a) in line with the first model outlined above, the properties of protein transport reflect the properties of organelle transport and thus all anterograde organelle transport ceases at the critical temperature;

b) in line with the second model, organelle transport does not cease at the critical temperature, but newly synthesized proteins are lost from moving organelles.

The goal of this project was to examine the temperature dependence of the fast anterograde transport of newly synthesized proteins and organelles in sciatic axons of the amphibian, *Xenopus laevis*. A position-sensitive detector of ionizing radiation was used to monitor the movement of newly-synthesized proteins in the anterograde direction; computer-enhanced video microscopy was used to image organelle transport. With these techniques, a confirmation was first sought for the presence of the documented discontinuity at a low critical temperature in the velocity-temperature relationship of rapidly anterogradely-transported proteins. Two experimental approaches were used to determine the effects of temperature on the rate of fast anterograde protein transport (Chapter 2). However, discrepancies in the results obtained from these two approaches resulted in the design of a set of experiments that would enable us to use both approaches simultaneously on the same nerve (Chapter 3). Secondly, the following hypotheses were tested:

1) the reported discontinuity in the velocity of fast axonal transport of proteins at the critical temperature is caused by the deposition of rapidly transported proteins to a non-transportable, stationary phase, or

2) the discontinuity is caused by cessation of anterograde organelle transport at the critical temperature.

In addition to this goal, the opportunity was taken to study the velocity of fast retrograde organelle transport so that the properties of anterograde and retrograde organelle transport could be compared in the same axons, a study that has also not been done prior to the present work (Chapter 4).

1. 1 The properties of protein and organelle transport

In order to consider comparing the dynamics of protein and organelle transport, one must be acquainted with the transport properties of anterogradely- and retrogradely-moving proteins and organelles. First, a review of the literature will be given which describes the role and importance of the cell body and of ATP and microtubules, components necessary for maintaining fast axonal transport within neurons. This will be followed by the evidence to support the two models described in the previous section.

1. 1. 0 Anterograde protein transport

As mentioned briefly in the general introduction, the neuronal cell body is the source of rapidly transported proteins, but it is not essential for the fast transport of these proteins along axons. Early autoradiographic studies showed that radiolabel could only be incorporated into newly synthesized proteins if applied to the neuronal cell body (Lasek, 1968; Edström and Mattsson, 1972). In addition, liquid scintillation counting (LSC) studies in which the dorsal root ganglion (DRG) was ligated from the sciatic nerve showed that fast transport occurs independently of the cell body (Ochs and Ranish, 1969; Ochs and Hollingsworth, 1971; Edström and Mattsson, 1972). These results show that the neuronal cell body is the site at which rapidly transported proteins are synthesized, but its removal does not interfere with the continuation of their transport.

Pharmacological, morphological, and liquid scintillation counting studies have all provided evidence that the fast axonal transport of proteins is an ATP- and microtubule-dependent process. After an *in vivo* incubation with a radiolabelled protein precursor, the nerve, devoid of its DRG, is excised and placed in a chamber to which various drugs of interest are added. At different incubation times, the nerve is processed for LSC analysis. Protein transport halts in the presence of sodium cyanide and dinitrophenol (Ochs and Hollingsworth, 1971; Hanson and Edström, 1977). Sodium cyanide prevents oxidative phosphorylation by affecting the action of cytochrome a_3, and dinitrophenol uncouples phosphorylation in the oxidative chain, suggesting that ATP plays a role in the transport of proteins. Its importance is emphasized by observing the effects of iodoacetic acid and pyruvate. Application of iodoacetic acid to nerves results in the slowing down and eventual cessation of protein transport (Ochs and Smith, 1971; Hanson and Edström, 1977). Iodoacetic acid blocks a step in glycolysis by diminishing the supply of metabolites necessary for ATP production in the citric acid cycle. Addition of pyruvate counteracts the inhibitory effects of iodoacetic acid (Ochs and Smith, 1971). It has also been observed that ATP utilization is local: anoxic conditions applied to a small length of nerve results in a build up of radiolabelled proteins against the anoxic block (Ochs, 1971). Resumption of fast transport of these radiolabelled proteins occurs upon removal of the block.

The fast transport of proteins is also blocked upon addition of colchicine (Ochs, 1971; Heslop and Howes, 1972; Hanson and Edström, 1977) and vinblastine (Edström and Mattsson, 1972; Hanson and Edström, 1977), suggesting the involvement of microtubules in fast protein transport. Colchicine and vinblastine prevent tubulin polymerization and also induce the disassembly of assembled microtubules. Thus, the effects of drugs upon the axonal transport

system have shown that the transport mechanism is both ATP- and microtubule-dependent, but the mechanism of conversion of chemical energy to mechanical energy remains to be elucidated.

Studies of the kinetics of protein transport have involved the use of the ligature and reversible cold block techniques. The ligature technique is simple to use both *in vivo* and *in vitro*. Anterogradely-transported radiolabelled proteins can be accumulated against a single ligature. Processing these ligated nerves for LSC at different times after introducing the radiolabel yields an accumulation rate from which a protein transport rate can be determined. The other technique is the reversible cold block. This involves cooling a portion of the nerve so that anterogradely-transported proteins can accumulate at a sharp warm-cold boundary to form a pulse of radiolabelled proteins. Rewarming the cooled nerve portion releases the cold block, allowing the pulse to travel along the nerve. Results from the use of such techniques indicate that most transport velocities of radiolabelled proteins are exponentially related to temperature over 10-28°C in the mollusc *Anodonta cygnea* (Heslop and Howes, 1972), the frog *Rana temporaria* (Edström and Hanson, 1973), and the cat (Ochs and Smith, 1975). However, in the garfish *Lepisosteus osseus* protein transport velocities are linearly related to temperature over 10-25°C (Gross, 1973; Gross and Beidler, 1975). Cosens *et al.* (1976) suggested that "some unusual feature of neurons in the garfish or, perhaps, of olfactory neurons in general" may have resulted in this linear velocity-temperature relationship. Despite this exception, it appears that in most species protein transport is exponentially related to temperature over a range from 5-10°C up to about 37°C. In both amphibian (Brimijoin *et al.*, 1979; Hanson, 1979) and mammalian nerves (Brimijoin, 1975; Cosens *et al.*, 1976; Hanson, 1978) the transport rate and dynamics of individual enzymes, such as dopamine-β-hydroxylase (DBH) and acetylcholinesterase (AChE), are similar to

those of all newly synthesized radiolabelled proteins: at 37°C the transport rate of these enzymes is 300-400 mm/d, and the transport velocity of DBH is exponentially related to temperature over a similar range as that of radiolabelled proteins (Cosens *et al.*, 1976; Brimijoin *et al.*, 1979). Above and below the extremes of this temperature range (5-37°C), the velocity drops. Possible explanations for the cessation below certain critical temperatures will be discussed in Section 1.2.

Liquid scintillation counting analysis of protein transport described above yields only a static view of this process. Thus, several position-sensitive detectors of ionizing radiation have been developed to monitor the transport of radiolabelled proteins in live nerve preparations (Snyder *et al.*, 1976; Takenaka *et al.*, 1978; Snyder and Smith, 1982). Similar to the results of LSC analysis, the velocity of radiolabelled proteins in a live bullfrog nerve is exponentially related to temperature over a range of 5-24°C (Takenaka *et al.*, 1978). The detector developed and used in this laboratory is the multiple proportional counter (MPC). It serves to detect the β-particles emitted from ^{35}S-methionine labelled proteins at 3.18-mm intervals along a nerve (Snyder and Smith, 1982). The protein transport rate is calculated by determining the displacement of the radioactive front from the origin and the time elapsed during this displacement. Although the relationship between velocity and temperature has not previously been observed with the MPC, it has been shown that at 23-25°C the transport rate of the fastest moving proteins is 180-190 mm/d (Snyder *et al.*, 1976; Snyder, 1986a; Snyder *et al.*, 1990). These rates are similar to those found in garfish (Gross, 1973; Gross and Beidler, 1973), frog (Edström and Mattsson, 1972), and cat (Ochs and Smith, 1975) at similar temperatures. In addition, LSC and MPC analyses show that the migration of the front is accompanied by a 2%/mm loss of radioactivity along the length of the nerve, suggesting that labelled

components are deposited behind the migrating wave (Edström and Hanson, 1973; Gross and Beidler, 1975; Hanson and Edström, 1977; Snyder *et al.*, 1990).

1. 1. 1 Retrograde protein transport

Fast retrograde transport is also an ATP- and microtubule-dependent process. It is sensitive to many of the ATP- and microtubule-inhibiting drugs of fast anterograde protein transport (Grafstein and Forman, 1980; Schwab and Thoenen, 1983), but lower concentrations of these drugs are required to inhibit its transport. Further indication of this difference is in the transport rates. In comparison to anterograde transport rates of 300-400 mm/d at 37°C, the rates of retrograde transport of AChE and DBH are 220 mm/d in cat (Ranish and Ochs, 1972) and 288 mm/d in rabbit (Brimijoin and Helland, 1976). In *X. laevis* the velocity of the fast retrograde transport of radiolabelled proteins is about 100-160 mm/d at 23°C (Snyder, 1986a); anterograde protein transport occurs at 180-190 mm/d at 23°C in the same animal (Snyder *et al.*, 1976; Snyder *et al.*, 1990). Thus, it appears that retrograde protein transport is slower than anterograde protein transport. In addition, a fraction of radiolabelled material is deposited behind a retrogradely-migrating wave of proteins (Snyder, 1989), suggesting that proteins can be lost from both fast anterograde and retrograde transport systems.

1. 1. 2 Anterograde and retrograde organelle transport

The local cold block technique used to study protein transport, and electron and video microscopy have been applied extensively to examine the morphology and behaviour of organelle transport. Many anterogradely-moving organelles are morphologically distinct from retrogradely-moving organelles. Anterogradely-moving organelles consist of small circular vesicles (50-100 nm in diameter), vesiculo-tubular structures, and long tubular mitochondria, while

retrogradely-moving organelles consist of dense lamellar bodies, multivesicular bodies, and vesicles (80-200 nm in diameter) (Smith, 1980; Tsukita and Ishikawa, 1980; Fahim *et al.*, 1985; Miller and Lasek, 1985). Similar to protein transport, the difference in anterograde and retrograde transport of organelles can be distinguished by studying their dynamics. It has been shown that in amphibia anterogradely-moving organelles move much faster (1.3-1.7 μm/s) than retrogradely-moving organelles (0.6-1.0 μm/s) (Cooper and Smith, 1974; Forman *et al.*, 1977b; Smith and Forman, 1988). However, in lobster (*Homarus americanus*) intact axons and extruded lobster axoplasm, retrograde organelle transport is faster than anterograde transport (Forman *et al.*, 1983; Smith and Forman, 1988). Studies examining the effects of pharmacological agents upon the two directions of organelle movement provide further evidence to support that the anterograde and retrograde organelle transport use different transport motors. Vanadate ions and EDTA reversibly and completely inhibit retrograde transport of microscopically visible organelles at lower concentrations than anterograde transport (Smith, 1988). Erythro-9-[3-(2-hydroxynonyl)] adenine has been shown to selectively inhibit only the retrograde transport of organelles in the lobster (Forman *et al.*, 1983).

Direct evidence that fast axonal transport of organelles is ATP-dependent has been obtained from video microscopy studies (Adams, 1982; Brady *et al.*, 1982; Forman *et al.*, 1984; Lasek and Brady, 1985). Giant axons from crab (*Carcinus meanus*), squid (*Loligo pealei*), or lobster (*Homarus americanus*) were permeabilized and then bathed in supportive buffer solutions. Organelle movement was visualized by video microscopy. Addition of buffer without ATP reduced and eventually halted organelle movement in both directions (Adams, 1982; Forman *et al.*, 1983; Smith and Forman, 1988). Resupplying these permeabilized axons with ATP or ADP restored organelle movement (Adams,

1982). In addition, organelle transport is halted in the presence of vanadate ions and the nonhydrolyzable ATP analogue, AMP-PNP (Forman *et al.*, 1984; Smith, 1988). Experiments using extruded axoplasm from the giant axons of squid have also shown that fast organelle transport is both an ATP-and microtubule-dependent process (Gilbert and Sloboda, 1984; Vale *et al.*, 1985b, 1985d).

Electron and video microscopy studies have also shown that microtubules serve as tracks for organelle movement. In electron microscopy (EM) studies, the motors responsible for anterograde and retrograde movement of organelles are seen as "cross-bridges" that contact microtubules (Smith, 1971; Miller and Lasek, 1985; Smith and Forman, 1988). Video microscopy studies have shown that colchicine (Cooper and Smith, 1974; Hammond and Smith, 1977; Kendal *et al.*, 1983; Smith and Kendal, 1985) and vinblastine (Chang, 1972), halt retrograde organelle transport before anterograde transport. Addition of taxol, a drug that stabilizes microtubules and protects them from depolymerization by cold, colchicine, and vinblastine, does not alter organelle transport in either direction (Forman, 1982; Smith and Kendal, 1985; Smith, 1988). Miller *et al.* (1987) further characterized this association between circular or elliptical organelles (vesicles) and microtubules through cold block EM studies of lobster axons. Based on the observation that these vesicles associate with only some of the many available microtubules, they describe two subclasses of microtubules: architectural and vesicle transport-supporting.

Unlike the number of studies showing the relationship between temperature and fast anterograde transport of proteins, very few studies have demonstrated the effects of temperature on fast anterograde and retrograde transport of microscopically visible organelles. Before the major improvements in video microscopy that enabled the detection of the smallest anterogradely-moving organelles (Smith, 1988), Forman *et al.* (1977b), Smith and Cooper (1981)

observed in isolated myelinated sciatic axons of *R. catesbeiana* and *X. laevis* that the average mean speed of microscopically visible, retrogradely-moving organelles increases exponentially within a temperature range of 5-36.9°C. All visible movement ceased roughly at around 37°C. Smith and Cooper (1981) did detect some anterograde organelle movement which stops at 37.3°C, 0.4°C higher than the more visible retrograde organelle transport. The velocity of organelle transport below 5°C has not been measured.

1. 2 Protein and organelle transport: evidence to support their relationship

From the account given in the above sections, both protein and organelle transport appear to share similar transport properties: both are ATP- and microtubule-dependent and are exponentially related to temperature over a similar range of temperatures, and anterograde and retrograde protein transport rates generally correspond with anterograde and retrograde organelle transport rates. Further confirmation that anterograde protein and organelle transport rates correspond with one another is given by Abe and his colleagues (1973) and Longo and Hammerschlag (1980) who showed that radiolabelled proteins and lipids are transported together at the same rate. These similarities suggest that organelles are protein carriers. Circular or elliptical organelles, otherwise known as vesicles (50-100 nm in diameter), particularly appear to be responsible for carrying proteins. Electron microscopy studies have shown that fast anterogradely- and retrogradely-transported radiolabelled proteins colocalize with vesicle accumulations at the proximal and distal sites of a crush or ligature, respectively (Schwab and Thoenen, 1978; Tsukita and Ishikawa, 1980). In addition, LaVail *et al.* (1980) found that DBH associates with the membranes of transmitter storage vesicles of adrenergic neurons. Video microscopy studies have also shown that the transport of organelles with round or elliptical images

is similar to the transport of radiolabelled proteins (Kirkpatrick *et al.*, 1972; Forman, 1982). So, from these observations it appears that microscopically visible vesicles are responsible for carrying proteins, but as eluded to already, their exact relationship is not clearly understood.

Evidence to support the model that a stable association exists between newly synthesized proteins and vesicles is based, in part, on sodium dodecyl sulphate-polyacrylamide gel electrophoresis (SDS-PAGE) analyses of subcellularly fractionated vesicles. These analyses have demonstrated that rapidly transported proteins are integrally associated with fractions related to the plasma membrane and/or components of the plasma membrane, such as synaptic vesicles (Elam and Agranoff, 1971; Edström and Mattsson, 1972; Bennett *et al.*, 1973; Droz *et al.*, 1973; Giamberardino *et al.*, 1973; Levine and Willard, 1980; Brimijoin, 1981; Morin *et al.*, 1991). Tytell and his colleagues (1981) have suggested that polypeptides assemble as discrete units and that these units may represent a long-term association between the polypeptides and their carrier vesicles. This integral association implies a tight, stable association such that to translocate these integral membrane proteins from one membrane to another would require a fusion of the carrier vesicle to the receiving plasma membrane. This would lead to a loss of the carrier vesicle and its cargo of newly synthesized proteins from the fast axonal transport system. From the results it may also be postulated that a subset of membrane-bounded vesicles carries newly synthesized proteins which can be lost from a moving phase to a stationary phase. For this possibility to hold, however, the protein-carrying subset would have to be a sufficiently small fraction of all anterogradely-moving organelles such that its loss is undetectable by video microscopy.

On the other hand, it is possible that newly synthesized proteins may be loosely associated with their carrier vesicles and therefore can be off-loaded

from them. As stated previously, much of the evidence to support this model is derived from studies of the dynamics of protein and organelle transport. Snyder and his colleagues (1990) compared the loss of proteins and the number of anterogradely-transported vesicles at two different locations along the length of a sciatic nerve. The assumption was that if proteins were lost along with their carrier vesicles, then one should observe a corresponding loss in the number of vesicles at two locations distanced from one another. Finding no difference in vesicle traffic at the two locations, they concluded that there was no loss of vesicles from the moving phase and favoured the alternative model whereby newly synthesized proteins may be lost from their carrier vesicles. Also supporting this model is the evidence that anterograde-to-retrograde transport reversal of newly synthesized proteins at a nerve lesion is prevented by inhibitors of Ca^{2+}-dependent proteolytic enzymes (Sahenk and Lasek, 1988; Smith and Snyder, 1991), but the reversal of vesicle traffic is not affected (Smith and Snyder, 1991). These findings imply that the proteolytic enzymes, somehow, cause newly-synthesized proteins to be lost from moving vesicles during transport reversal. In addition, the dynamics of transport reversal differ for proteins and vesicles: vesicles are observed to reverse their direction in no greater than 15-30 minutes while protein turnaround requires about 2 hours (Snyder *et al.*, 1994). These findings imply that there must be a loose, short-term association between proteins and vesicles such that proteins may be off-loaded from their carrier vesicles and up-loaded to different moving vesicles. Furthermore, it has been shown that organelle transport continues in the complete absence of any cargo of newly synthesized proteins (Smith *et al.*, 1994), suggesting that a transient association does exist between proteins and organelles. However, it is not known and difficult to determine what proportion of this observed continued organelle transport is derived from the cell body

because it also includes organelles that have been recycled from the population of retrogradely-transported organelles.

It is possible that the off-loading and up-loading of proteins described above may not only involve proteolytic processing, but also depend upon the destination of the proteins. Anterogradely-moving proteins are deposited from a moving phase to a stationary phase within an axon at a rate of about 2% per mm (Edström and Hanson, 1973; Gross and Beidler, 1975; Muñoz-Martínez, 1982; Snyder *et al.*, 1990). This value appears to occur at the same rate in axons ranging from about 7 cm in length in frog to about 22 cm in length in garfish. This deposited material may represent proteins and glycoproteins that renew membrane components undergoing turnover, while the remainder is destined for the nerve terminals (Hendrickson, 1972; Bennett *et al.*, 1973; Droz *et al.*, 1973; Brimijoin, 1981). For instance, 85% of rapidly transported AChE remains within the axon, specifically the axolemma (Brimijoin, 1981). AChE deposition to a small area of the axolemma can be prevented by local application of echothiophate (Brimijoin *et al.*, 1978). Since the boundaries of this inhibition remained "sharp", the investigators concluded that very little lateral diffusion occurs, implying that the source of new AChE must be from the rapidly transported pool. Morin and his colleagues (1991) also described a similar situation in regards to the presence of the glucose transporter in both a stationary and a mobile peak. These observations showed that rapidly transported proteins may be deposited to a stationary phase for the function of renewing membrane components.

Evidence to support that up-loading of proteins depends upon protein destination is provided by the work done by Ambron and his colleagues (1992). These investigators injected human serum albumin, a protein that is usually not transported retrogradely (Schwab and Thoenen, 1978), tagged with a nuclear

import signal into the axoplasm of marine mollusc (*Aplysia californica*) neurons. The result was that the protein was retrogradely transported through the axon to the cell body and then into the nucleus (Ambron *et al.*, 1992). The implication from these results is that proteins in the cytosol may be taken up by retrogradely-moving organelles. Thus, it is possible that the two-way association/dissociation of newly synthesized proteins and their carrier vesicles may require a protein targeting sequence and some form of proteolytic processing.

As stated in Section 1.0, the objective of this thesis was to further understand the relationship between newly synthesized proteins and organelles by investigating the temperature dependence of fast axonal transport of proteins and organelles. Studies on fast anterograde transport of radiolabelled proteins in amphibian (Edström and Hanson, 1973; Brimijoin *et al.*, 1979) and mammalian (Ochs and Smith, 1975; Cosens *et al.*, 1976) sciatic nerves describe an exponential relationship between the velocity of protein transport and temperature down to a critical temperature in the range 5-10°C. In this range the velocity of protein transport abruptly drops. Muñoz-Martínez (1982) suggested that the sudden drop in protein velocity at low temperature is related to an increase in the amount of material that is deposited from the rapidly moving phase to a stationary phase. Previous investigations in which nerves have been cooled and rewarmed have shown that upon rewarming, fast transport of radiolabelled proteins or specific proteins, such as the enzymes DBH and AChE, resumes and leaves behind a trail of proteins (Lasek, 1968; Ochs and Ranish, 1969; Ochs, 1971; Edström and Hanson, 1973; Brimijoin, 1975; Ochs and Smith, 1975; Cosens *et al.*, 1976; Hanson, 1978; Hanson, 1979; Snyder *et al.*, 1990). Some investigators have noted that an accumulation remains at the site of cooling upon migration of radiolabelled proteins or DBH following rewarming (Edström and Hanson, 1973; Brimijoin, 1975). This suggests that proteins may be dropped off to a stationary

phase while others may be picked up for further transport in the rapidly moving phase (Edström and Hanson, 1973; Brimijoin, 1975; Brimijoin, 1981; Ochs, 1983). The *in vivo* situation, however, differs. Performing a cold block in rats and rabbits *in vivo*, Hanson (1978) observed no persistent accumulation of AChE at the cooling site upon rewarming, indicating that local cellular conditions *in vivo* must aid in the "complete" cold recovery which is lacking in the *in vitro* experiments.

Thus, both protein and organelle transport share the same mechanisms and have the same properties. This thesis will show that this statement is only partially true since the dynamics of protein transport may, under some conditions, differ from those of organelle transport, thus providing further evidence to support the second model, namely that the association between the carrier organelles and newly synthesized proteins is not rigidly fixed.

2 EFFECTS OF TEMPERATURE ON THE ANTEROGRADE TRANSPORT OF PROTEINS IN THE FROG SCIATIC NERVE

2.0 Introduction

Earlier work has demonstrated that in vertebrates the velocity of the anterograde axonal transport of proteins changes exponentially with temperature down to some low temperature at which point a sudden drop in velocity occurs. Brimijoin *et al.* (1979) showed that the velocity of protein transport in bullfrog sciatic nerve dropped abruptly at about 10°C. In cat and rabbit sciatic nerves, the velocity of protein transport fell abruptly at 11-13°C (Ochs and Smith, 1975; Cosens *et al.*, 1976; Brimijoin *et al.*, 1979). Muñoz-Martínez (1982) has suggested that the sudden drop in protein velocity at low temperature is related to an increase in the amount of material that is deposited from the rapidly moving phase to a stationary phase.

This chapter presents the results of experiments that were designed to determine whether a sudden discontinuity in the transport rate of proteins occurs in the sciatic nerve of *Xenopus laevis* as temperature drops through the range 15-3°C and whether such a discontinuity is accompanied by an increased rate of protein deposition.

2.1 Methods

Two experimental approaches were adopted to determine the effects of temperature on the rate of fast anterograde transport of newly synthesized proteins in the frog sciatic nerve. Both approaches involved the use of the MPC to study the propagation of a pulse of radiolabelled proteins transported in the anterograde direction. The first approach involved

recording the movement of protein transport on the MPC at room temperature before and after altering the nerve temperature (usually below room temperature). No recordings were obtained during the cooling interval. A second approach was adopted to verify the protein transport rates determined by the first approach. This involved enclosing the MPC in a thermoregulated refrigerator, thus allowing the direct observation of protein transport throughout the cooling period.

2. 1. 0 Nerve Preparation

Adult female *Xenopus laevis* toads were anaesthetized by immersion in a 2% solution of urethane (Sigma Chemical Co.). An 80-85 mm length of sciatic nerve, in continuity with its 8th or 9th DRG, was removed and a ligature was tied at the distal end of the nerve (Step 1 of Figure 2.1). During the dissection and the pulse formation, the nerve and its ganglion were bathed in oxygenated physiological saline of composition: NaCl, 112 mM; KCl, 2.9 mM; $CaCl_2$, 2.2 mM; $MgSO_4$, 1.6 mM; glucose, 5.5 mM; hydroxyethylpiperazine-N-2-ethanesulfonic acid (HEPES), 3.0 mM; pH 7.40.

2. 1. 1 Radiolabelled Pulse Creation

After dissection, the nerve preparation was mounted in a two-compartment tray so that the DRG was separated from the bulk of the sciatic nerve by a barrier of inert grease (Step 2 of Figure 2.1). A 25-μL solution of oxygenated physiological saline containing L-[^{35}S]-methionine (0.25 mCi, specific activity of 1200 Ci/mmol, Dupont, NEN Research Products) was added to the compartment containing the DRG. A period of 1.5 hours was

Figure 2. 1. Schematic representation of the steps taken to create a pulse of radiolabelled proteins in the sciatic nerve of an adult *Xenopus laevis* and to detect and analyze the anterograde transport of the pulse by a position-sensitive detector (MPC) and later a liquid scintillation counter.

Step 1. Dissection of a sciatic nerve with either the 8th or 9th dorsal root ganglion (DRG) to the peroneal and tibial nerves.

Step 2. Mounting of sciatic nerve in a two-compartment tray so that the DRG was separated from the bulk of the nerve by a barrier of inert grease. The DRG was then incubated in 25-μL physiological saline containing L-[^{35}S]-methionine; the bulk of the nerve was bathed in radioactive-free physiological saline. After 1.5 hours, the DRG saline was replaced with radioactive-free saline. Three hours later, the DRG and a 3-mm proximal portion of the nerve were removed to create a pulse of radiolabelled proteins. Subsequently, the nerve was desheathed and rinsed for 2.5 hours, after which 10 mm of the proximal end of the nerve was removed. The nerve preparation now consisted of a desheathed sciatic nerve containing a clean pulse of radiolabelled proteins.

Step 3. Experimental set up. The nerve preparation was secured by proximal and distal ligatures to a nerve chamber and then placed in apposition to the window of the counting chamber (MPC). A nerve press gently pressed the nerve preparation against the MPC window to increase the efficiency of detecting β-particles emitted from the L-[^{35}S]-methionine labelled proteins. Physiological saline containing non-radioactive methionine bathed the nerve throughout the duration of the experiment.

Step 4. Detection of radiolabelled protein pulse and subsequent data acquisition.

Step 5. Liquid scintillation processing. At the conclusion of each experiment, the nerve preparation was cut into 3.18-mm segments and processed for liquid scintillation counting.

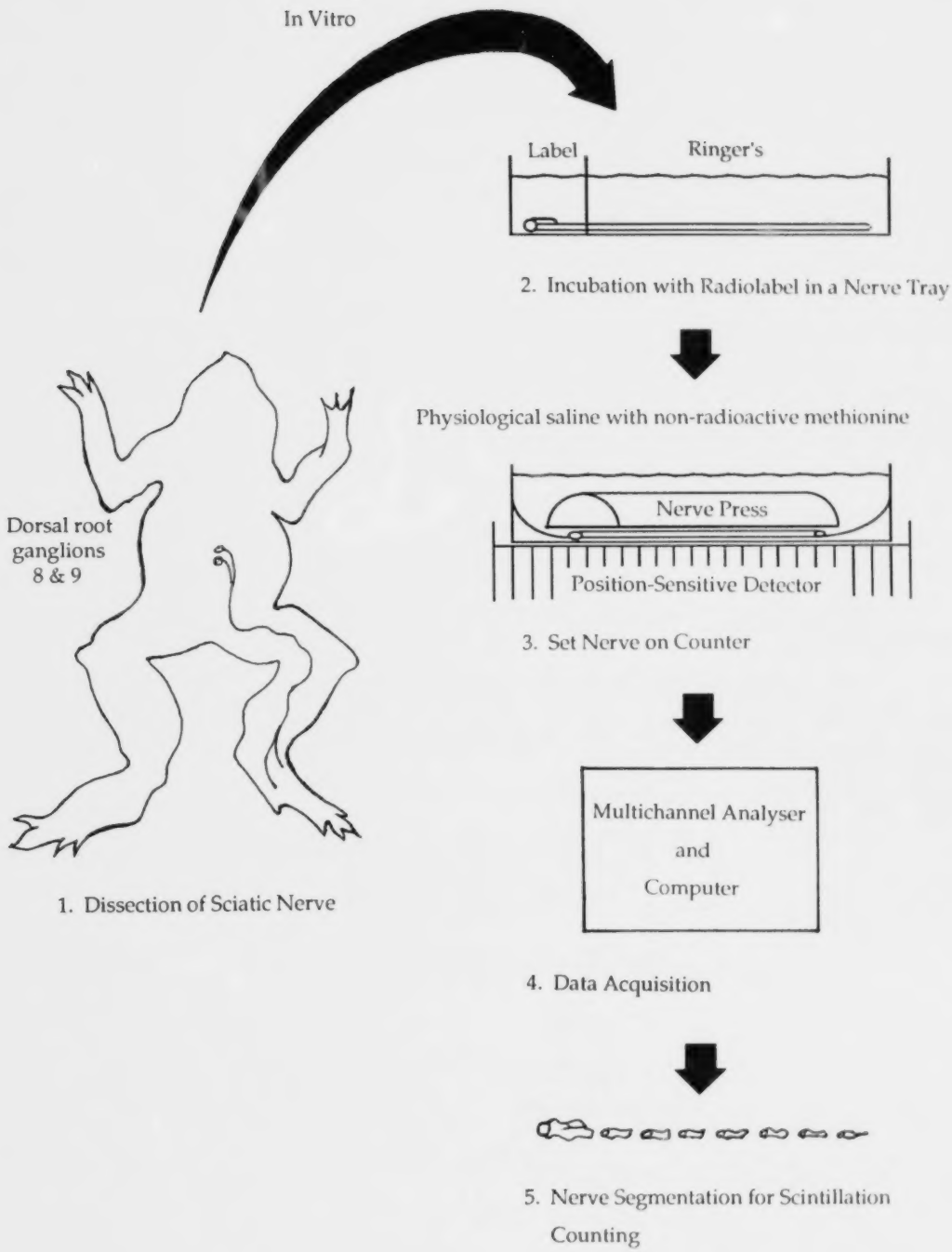
In Vitro
Label
Ringer's
2. Incubation with Radiolabel in a Nerve Tray
Physiological saline with non-radioactive methionine
Nerve Press
Position-Sensitive Detector
3. Set Nerve on Counter
Multichannel Analyser
and
Computer
4. Data Acquisition
5. Nerve Segmentation for Scintillation
Counting
Dorsal root
ganglions
8 & 9
1. Dissection of Sciatic Nerve

allowed for the incorporation of the label into proteins before the DRG compartment was rinsed and replaced with 25 μL of radioactive-free physiological saline. Three hours later the entire nerve was removed from the two-compartment tray, and the DRG and a 3-mm proximal portion of nerve were removed to create a pulse of radiolabelled proteins. Once the length of the sciatic nerve was measured and noted, the distal ligature was removed and the sciatic nerve desheathed via the "slit-desheathing" method described by Chan *et al.* (1980) and retied at the distal end. After a 2.5-hour rinse in 100 mL of physiological saline containing 1.0-mM non-radioactive methionine, 10 mm of the proximal end of the nerve was removed and the nerve ligatured. This reduced the possibility of radiolabel entering the sciatic nerve by a means other than rapid axonal transport (*e.g.*, diffusion). The nerve preparation now consisted of a 70-75 mm sciatic nerve containing a pulse of labelled proteins. The nerve preparation was transferred and secured by the proximal and distal ligatures to a nerve chamber (Step 3 of Figure 2.1) having a 3.6-μm thick mylar floor that allowed β-particles emitted from the nerve to be detected by the MPC. Temperature was continually monitored by fine thermocouples. These temperature readings were noted and used later to calculate the mean and standard deviation of the temperature. The nerve was tensioned to 70-75 mm and then placed in apposition to the aluminized mylar window of the MPC. A coarse gauze wrapped tightly around a plastic frame gently pressed the nerve against the MPC window in order to increase the efficiency of detecting β-particle emissions. Physiological saline containing 1-mM non-radioactive methionine bathed the nerve throughout the duration of the experiment.

2. 1. 2 Data acquisition and analysis

The MPC is a gas-filled (argon-carbon dioxide mixture) proportional counter that serves to detect the β-particles emitted from ^{35}S-methionine labelled proteins in each 3.18-mm region of nerve through an aluminized mylar window. Counts-versus-position spectra were recorded for times up to 20 hours or more in 1000 second blocks (Step 4 of Figure 2.1). Prior to securing the nerve in the chamber, two to five spectra were obtained with the chamber and the press positioned on the MPC window. These spectra served as background runs. The average counting rate from these runs was subtracted from all subsequent spectra to correct for the increased counting rates due to background radiation. At the conclusion of each experiment, another two to five spectra were recorded after the nerve was removed from the chamber. These served as post-experiment background runs to evaluate the radioactivity released from the nerve during the experiment. All the recordings were converted to counts-versus-time plots in which the counting rate for each 3.18-mm region of nerve was plotted as a function of time (Figure 2.2A-D and 2.3A-D). It was from these plots that the progress of the front end of the pulse through each 3.18-mm nerve segment could be monitored for the duration of the experiment. The front end was used to determine a protein transport rate. From these data, the time that the front of the pulse reached each segment was calculated by determining the intersection of the baseline and the slope of the pulse front (Figure 2.2A-D and 2.3A-D, small arrows). These times were plotted as a function of position. A regression line was fitted through these time-versus-position points by a weighted least squares method (Figures 2.2E and 2.3E). The reciprocal of the slope of the fitted line represented the protein transport rate.

Figure 2. 2.

A - D: Counts-versus-time plots showing the anterograde propagation of a pulse of radiolabelled proteins at room temperature before (A and B) and after (C and D) the nerve was cooled to 7°C. The data points show the time course of radioactivity through 3.18-mm segments of nerve. The distance of each segment from the proximal end of the nerve is given in mm on each plot. For this particular nerve, 23 counts-versus-time plots were obtained; 4 are presented here. The error bars represent ± 1 standard error of the mean (SEM). The open squares represent the background activity of the nerve chamber before and after the experiment. The area designated by the double-headed arrow and the dotted vertical lines represent the cooling period. Note that no recordings were taken during this interval because the nerve chamber was removed from the MPC window. The vertical arrows indicate the time at which the front of the pulse reached each segment of nerve.

E: Time-versus-position plot. The circles represent the times at which the front of the pulse entered each nerve segment before the cooling period; the open circles specify the times determined from plots A and B. The squares represent the data gathered after the cooling period; the open squares indicate the times determined from plots C and D. The weighted least squares method was employed to fit the regression lines (solid lines) to the time-versus-position points obtained at room temperature. The dotted line is defined by end points which are derived from the noted stop and start times of the cooling period. The reciprocal of the slope of this line gave the protein transport rate at 7°C, namely 24.1 ± 4.5 mm/d.

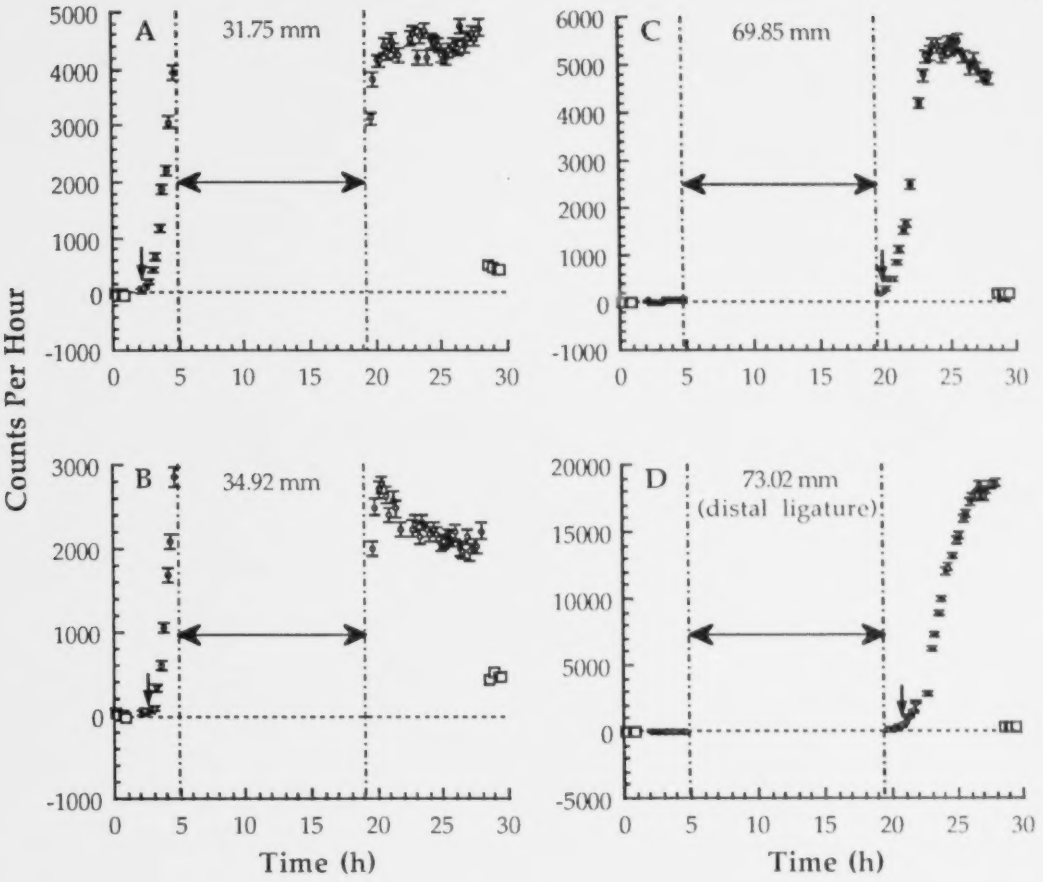
A
31.75 mm
B
34.92 mm
C
69.85 mm
D
73.02 mm
(distal ligature)
Counts Per Hour
Time (h)
Time (h)

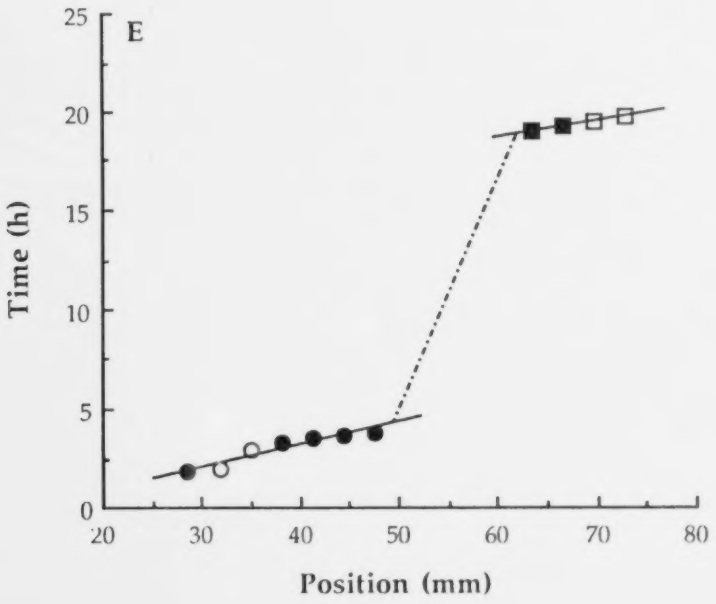
E
Time (h)
Position (mm)

Figure 2. 3.

A - D: Counts-versus-time plots showing the anterograde transport of a pulse of radiolabelled proteins during a 7°C cooling period of 48 hours. The circles show the course of radioactivity, already corrected for background activity, through 3.18-mm segments of nerve. As in Figure 2.2., the distance of each segment from the proximal end of the nerve is given in mm on each plot. For this particular nerve, 23 counts-versus-time plots were obtained; 4 are presented here. The error bars represent ± 1 SEM. The vertical arrows indicate the time at which the front of the pulse reached each segment of nerve.

E: Time-versus-position plot. The open circles represent the values indicated by the arrows in Panels A-D. The filled circles represent the values obtained from similar plots as above. The protein transport rate at 7°C was calculated from the reciprocal of the regression line fitted to these time-versus-position points by the weighted least squares method. The transport rate here was 19.7 ± 2.4mm/d.

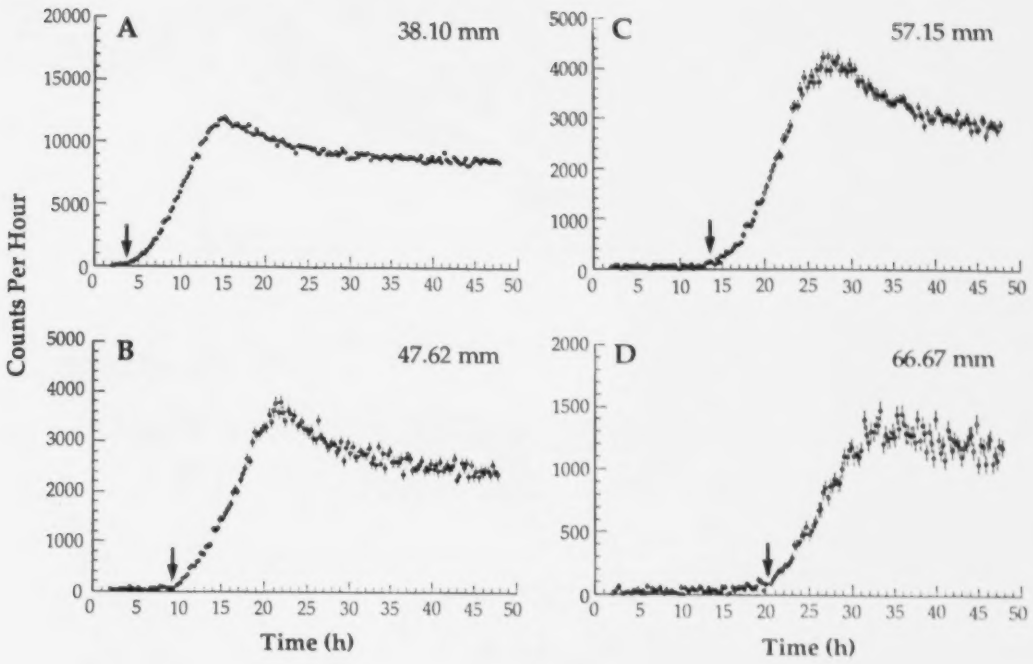
A
38.10 mm
B
47.62 mm
C
57.15 mm
D
66.67 mm
Counts Per Hour
Time (h)
Time (h)

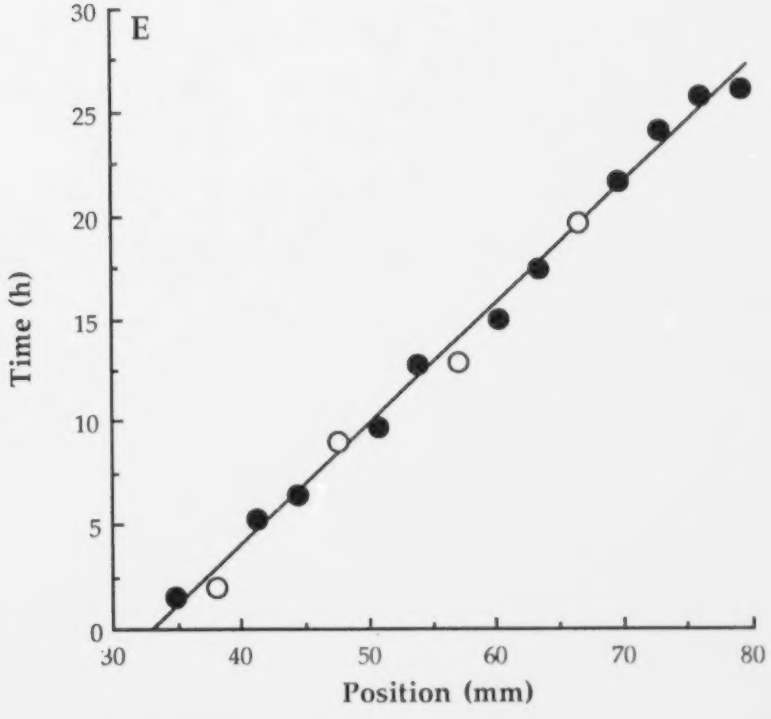
E
Time (h)
Position (mm)

2. 1. 3 Methods of Studying Rapid Anterograde Transport of Proteins

As described briefly at the beginning of this methods section, two experimental approaches were used to evaluate the effects of temperature on the transport rate of protein.

Method 1. Similar to the procedure outlined by Snyder (1986a, 1986b), the counts-versus-position spectra were recorded on the MPC at room temperature before and after the temperature of the nerve was altered and then converted to counts-versus-time plots (Figure 2.2A-D). No recordings were taken during the cooling period (usually 14 hours) (indicated by the double-headed arrows in Figure 2.2A-D). To ensure that the entire nerve preparation was cooled to the desired temperature, the alignment of the nerve on the floor of the chamber was first noted, and then the nerve chamber was removed from the MPC window and the nerve preparation was gently lifted from the bottom of the nerve chamber. Physiological saline, containing 1-mM non-radioactive methionine, was quickly cooled to the temperature of interest by a cold bath and circulated throughout the nerve chamber. During cooling, the temperature was continually monitored by fine thermocouples placed at the proximal and distal nerve ends. Finally, the preparation was returned to room temperature ("warm-up"), the nerve chamber repositioned on the MPC window, and the nerve realigned on the floor of the MPC. The thermocouples were then placed on the proximal and distal ends of the nerve, the press replaced on the nerve, and the counts-versus-position spectra recorded. To determine the protein transport rate during the cooling period, the "start" and "stop" times at which the nerve reached and remained at the desired temperature until warm up were noted. Thus, the transition intervals (15-35 minutes), the length of time the nerve preparation equilibrated to the desired temperature, were not included in

calculating the protein transport rate. The times recorded were then used to determine the position of the front of the pulse at the start and stop of the cooling period. This was achieved by substituting the times noted into the appropriate equations for the slope of the regression line fitted through the time-versus-position points at room temperature (solid lines in Figure 2.2E). The protein transport rate during the cooling period (dotted line in Figure 2.2E) was calculated as:

$$(1) \qquad \text{Protein transport rate} = \frac{P_2 - P_1}{t_2 - t_1}$$

where P_1 and P_2 are the positions measured from the proximal end of the nerve to the front of the pulse at the start and stop of the cooling period, and t_1 and t_2 are the respective times.

Method 2. This approach was designed to observe the movement of protein transport during the cooling period. This involved keeping nerve preparations in apposition with the aluminized mylar window of the MPC for the duration of the experiment. Thus, the MPC was enclosed in a thermoregulated refrigerator to ensure that the entire nerve remained cooled at the desired temperature. This compensated for the errors (± 1 mm) included in the calculation of the protein transport rate in Method 1, namely the realignment of the nerve on the floor of the nerve chamber and the repositioning of the nerve chamber on the MPC. In three experiments, the nerve preparations were cooled for 14 hours and the rest for 24-48 hours in order to collect enough MPC data to calculate a protein transport rate, especially at very low temperatures (2-6°C). The counts-versus-position

spectra were collected on the MPC throughout the cooling period and during the following warm-up. Temperature was continually monitored by fine thermocouples placed under the 8th branch of the sciatic nerve and between the branches of the peroneal and tibial nerves. The data collected from the warm up were used to check the nerve's viability. These data were converted to counts-versus-time plots (Figure 2.3A-D). A protein transport rate was calculated from the reciprocal of the regression line that was directly obtained from the time-versus-position plot (Figure 2.3E).

2. 1. 4 Further Analysis

Calculation of E_a and Q_{10} values were used to evaluate the influence of temperature on the velocity of anterograde axonal transport of proteins. The E_a is the apparent activation energy necessary for a given reaction to occur, and was derived from the following equation:

(2) $$E_a = \frac{-2.3R\ (\log V_2 - \log V_1)}{\frac{1}{T_2} - \frac{1}{T_1}}$$

where V_1 and V_2 are the protein transport rates in μm/s at the corresponding absolute temperatures, T_1 and T_2, in kelvins (K) and R is the gas constant of 1.98 cal/mole.

The Q_{10} value, the factor by which a reaction velocity is increased for a rise of 10°C, was calculated by the following equation:

(3) $$Q_{10} = \left(\frac{V_1}{V_2}\right)^{\frac{10}{t_1 - t_2}}$$

where V_1 and V_2 are the protein transport rates in μm/s at the respective temperatures, t_1 and t_2, in degrees Celsius (°C).

2. 1. 5 Liquid Scintillation Analysis

At the conclusion of each experiment the nerve preparation was cut into 3.18-mm segments, corresponding to the spacing of the MPC detectors (Step 5 of Figure 2.1). Each segment was first treated with 1 mL of 5% trichloroacetic acid (TCA) solution for one hour at 80°-85°C to extract the soluble protein. The segments were then completely solubilized overnight in 600 μL of Scintigest (Fisher Scientific). After 10 mL of fluor (Scinti-Verse II, Fisher Scientific) and 25 μL of glacial acetic acid were added to the TCA-insoluble protein samples, radiation counts were recorded in a Beckman LS-230 β-counter system and the acid insoluble label in each segment was determined by LSC analysis. The results were expressed as counts of TCA-insoluble activity per hour per segment.

The fraction of material that the pulse of radiolabelled proteins left behind as it moved along the nerve was calculated as the % TCA-insoluble activity or % deposition per millimetre segment of nerve. This was defined as:

$$(4) \qquad \%\ \text{deposition / mm for segment i} = \frac{1}{3.18}\left[\frac{C_i}{\sum_{j=i}^{n} C_j}\right] \times 100\%$$

where C_i represents the amount of radioactivity (counts of TCA-insoluble activity per hour per segment) in segment i (usually 1-23 nerve segments), n

represents the last nerve segment, and $\sum_{j=i}^{n} C_j$ represents the total amount of radioactivity from segments i to n.

2. 2 Results

2. 2. 0 The effects of temperature on protein transport rates by Method 1

Figure 2.4 shows the results derived from the analysis shown in Figure 2.2. The protein transport rates were plotted as a function of temperature. Over the range of 6.5-25°C the transport rate was fitted by the equation for a simple exponential curve as $V=0.142\ (1.12)^T$ where V is the velocity in μm/s and T is the temperature in °C. Figure 2.5 is a semilog plot of the data in Figure 2.4. The protein transport rates from 6.5-25°C fitted well with a straight line and its 95% confidence intervals, confirming that the relationship between the velocity of protein transport and temperature is reasonably described by an exponential curve over a range of 6.5-25°C. The Q_{10} value (± SEM) between 6.5°C and 25°C was 3.0 ± 0.1 with an E_a of 18.2 ± 0.8 kcal/mole. Two deviations from the exponential curve were observed. At 25°C the velocity of protein transport apparently reached its maximum as indicated by the difference in velocity of protein transport from 25-31.2°C. At 6.5°C the rate of protein transport rapidly dropped to zero.

2. 2. 1 The effects of temperature on protein transport by Method 2

Figure 2.6 shows the rate of protein transport over a range of 2-10°C. Particular attention was directed to this temperature range in order to assess whether a sudden discontinuity existed at 6.5°C as observed in Method 1. Protein transport continued to at least 2°C as an exponential function of temperature with no sudden discontinuity observed at 6.5°C. The equation

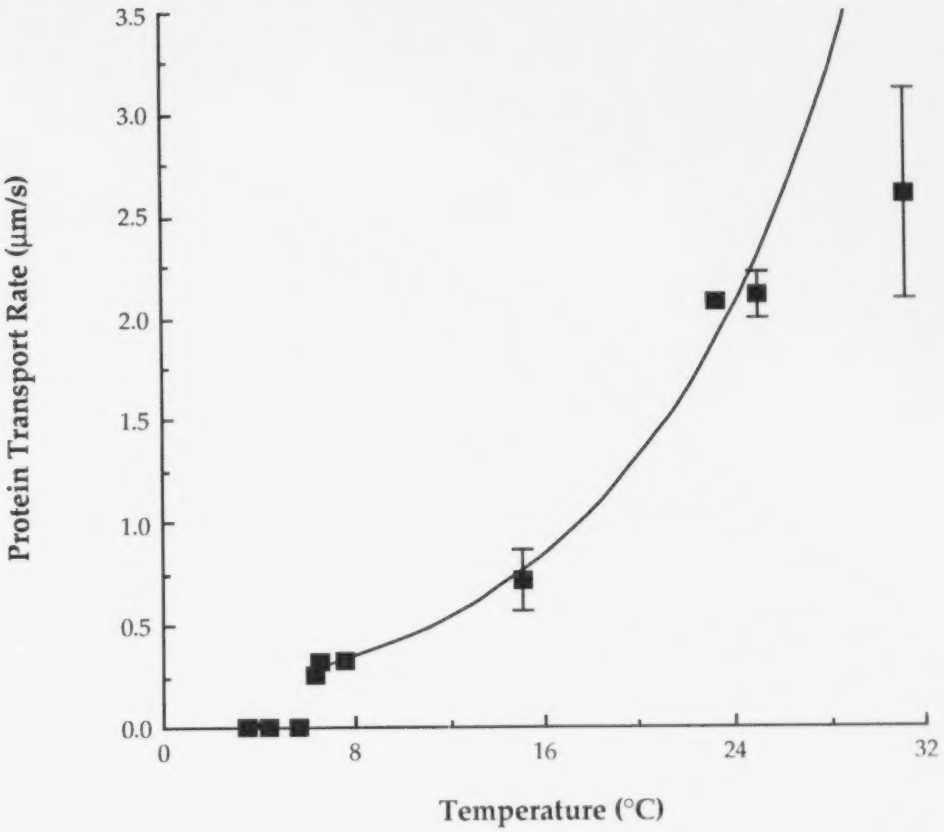

Figure 2. 4. Anterograde protein transport rates from Method 1 at different temperatures. Each solid square represents the protein transport rate obtained from the positions of the radiolabelled pulse of newly synthesized proteins at the beginning and the end of a cooling period (ranging from 3 1/2 hours at 31°C to 14 hours below 8°C) at the given temperature. The exponential curve was a least squares fit to the data points between 6.5°C and 25°C. Below 6.5°C protein transport dropped rapidly to zero.

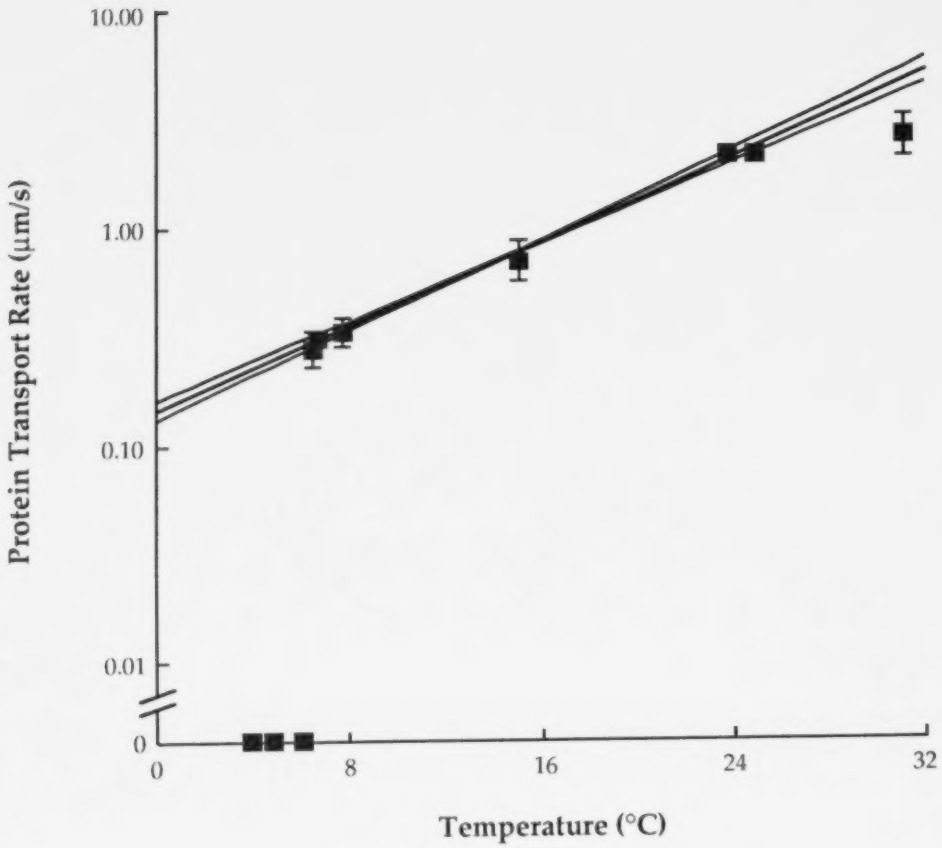

Figure 2. 5. Semilog plot of the data from Figure 2.4. Anterograde protein transport rates were plotted on a logarithmic scale against temperature. The regression line is fitted to the data points over a temperature range of 6.5-25°C. The curved lines above and below the regression line represent the 95% confidence intervals for the mean transport rate. Note that the velocity of protein transport was exponentially related to temperature from 6.5-25°C. There were two distinct discontinuities in the relationship between velocity and temperature for fast anterograde transport of proteins. These discontinuities occurred at 6.5°C and above 25°C.

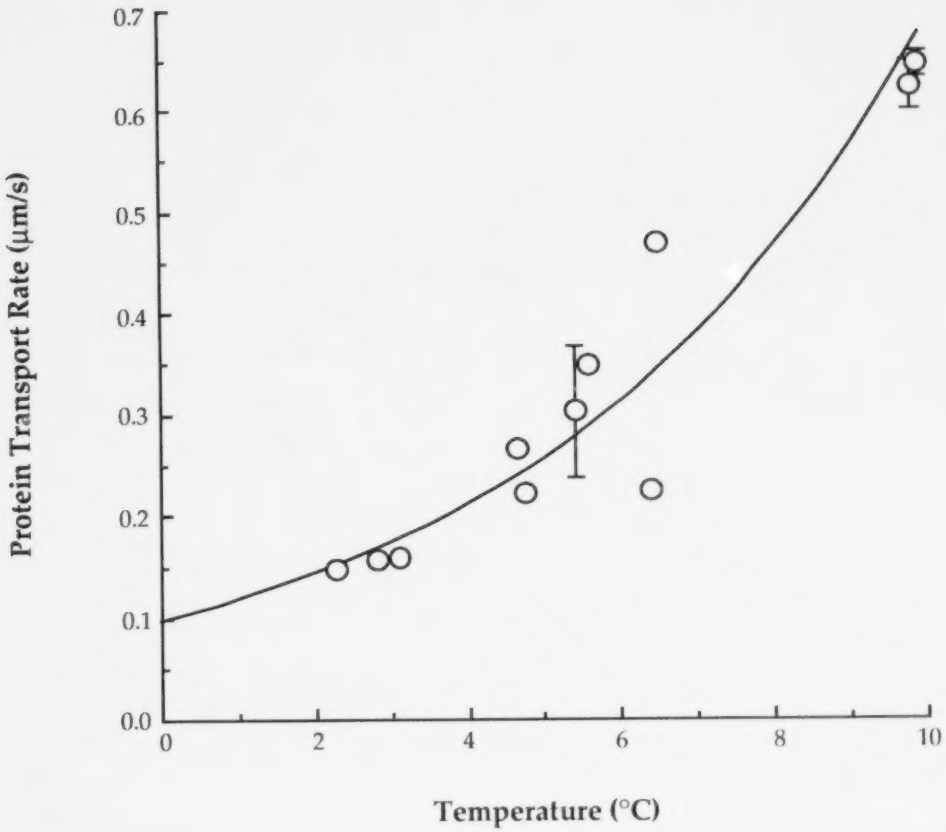

Figure 2. 6. Anterograde protein transport rates from Method 2 at temperatures from 2-10°C. Here, each circle represents the protein transport rate derived as shown in Figure 2.3E. The error bar of each point indicates ± 1 SEM associated with the fitting of the slope in Figure 2.3E. The curve fitted to the data is an exponential. Note that the velocity of protein transport was smoothly related to temperature over a range of 2-10°C. No sudden discontinuity was observed at around 6.5°C. Protein transport continued to at least 2°C.

that described the relationship between protein transport rate and temperature was $V=0.146\ (1.12)^{T}$. The Q_{10} value (± SEM) between 2°C and 10°C was 3.2 ± 0.4 with an E_a of 17.7 ± 1.8 kcal/mole. Figure 2.7 is the data from Figure 2.6, but plotted on a logarithmic scale. The entire set reasonably fitted an exponential curve, and showed no sudden discontinuity at around 6.5°C.

2. 2. 2 The effects of temperature upon protein deposition

To examine the effects of temperature upon the amount of material left behind by the migrating pulse required analysis of MPC and LSC data. For Method 1, the counts-versus-time spectra from the MPC analysis were used to define the number of segments the pulse travelled before and after the cooling period (Table 2.1). Similarly for Method 2, the counts-versus-time spectra were used to determine the number of segments during and after cooling (Table 2.2). It must be noted that in Table 2.2 the cooled segments are separated into start-cold deposition and cold deposition to maintain a consistency in comparing a similar number of segments between the two methodologies. The % deposition per mm in both methodologies was derived from equation (4). Pre-cold (deposition at room temperature), cold, and warm-up depositions of Method 1 and cold and warm-up depositions of Method 2 represented the amount (%) of material, on average, that was deposited by the pulse per mm. The mean % deposition rates were plotted as a function of temperature to observe the effects of various temperatures upon protein deposition (Figures 2.8, 2.9, 2.10).

Method 1. The mean % pre-cold deposition rate (derived from the segments of several experiments shown in Table 2.1) was 4.8 ± 0.6%/mm, a value 2.4 times higher than calculated by Snyder *et al.* (1990). Their rate of deposition

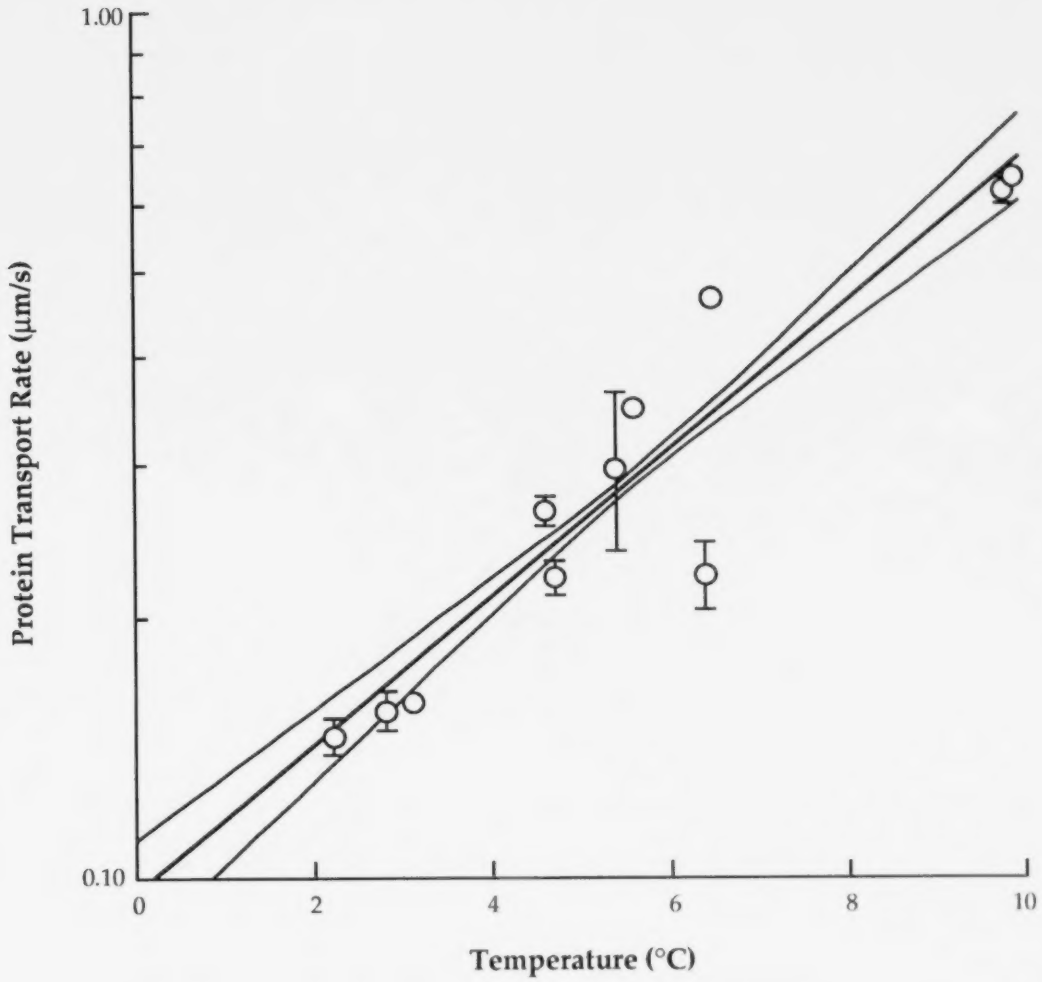

Figure 2. 7. Semilog plot of the entire data set from Figure 2.6. Protein transport rates were plotted on a logarithmic scale as a function of temperature. The curved lines above and below the regression line represent the 95% confidence intervals. The entire data set was exponentially related to temperature over a range of 2°C to 10°C. No sudden discontinuity was observed, especially at 6.5°C.

Table 2. 1.

Mean percentage values of radiolabelled protein deposition in a collection of 3.18-mm segments of Method 1-treated nerves before, during, and after a 14-hour cooling period

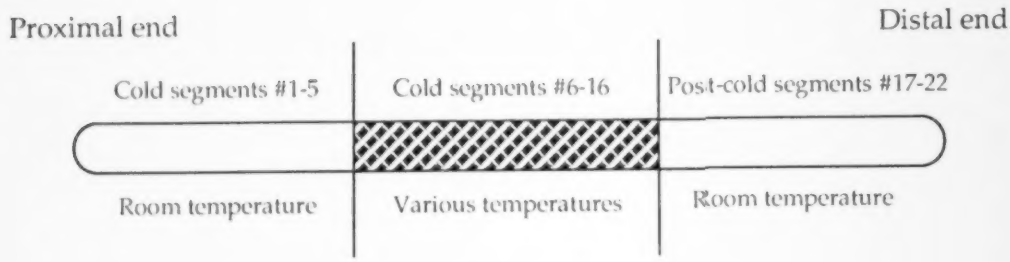

Temperature (°C)	Cold deposition (%/mm ± SEM)	Cold deposition (%/mm ± SEM)	Post-cold deposition (%/mm ± SEM)
3.9	3.6 ± 0.4	6.7 ± 0.8	4.0 ± 0.7
4.7	6.0 ± 0.8	4.6 ± 0.6	5.0 ± 0.6
6.0	3.8 ± 0.6	3.2 ± 0.4	4.6 ± 0.7
6.5	3.3 ± 0.3	3.3 ± 0.3	5.1 ± 0.6
7.7	5.5 ± 0.7	2.4 ± 0.6	5.2 ± 1.2
15.4*	2.6 ± 0.6	3.4 ± 0.5	4.5 ± 0.6
31.2*	5.9 ± 0.6	1.9 ± 0.3	5.4 ± 0.8

*The length of time spent at 15.4°C and 31.2°C was about $3\ ^1/_2$ and $1\ ^1/_2$ hours, respectively.

Table 2. 2.

Mean percentage values of radiolabelled protein deposition in a collection of 3.18-mm segments of Method 2-treated nerves during and after a 48-hour cooling period

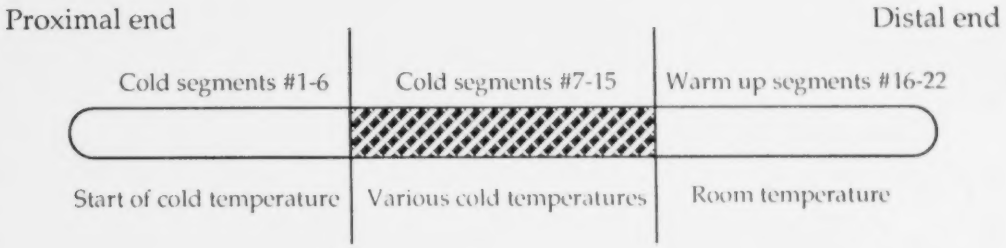

Temperature (°C)	Start cold deposition (%/mm ± SEM)	Cold deposition (%/mm ± SEM)	Warm-up deposition (%/mm ± SEM)
2.4	6.9 ± 0.7	13.9 ± 1.4	5.3 ± 0.4
3.3	7.7 ± 1.1	11.4 ± 1.2	7.1 ± 1.2
5.2	6.5 ± 1.0*	4.2 ± 0.4	4.3 ± 0.3
6.0	5.9 ± 0.7*	5.5 ± 0.6	4.0 ± 0.8
6.1	5.2 ± 0.8	5.6 ± 0.4	8.1 ± 0.4**
6.9	6.5 ± 0.8	4.8 ± 0.7	5.8 ± 0.6

* Deposition of radiolabelled proteins in 3.18-mm nerve segments #1-6 at room temperature.

** Deposition of radiolabelled proteins in 3.18-mm nerve segments #16-22 at 6.1°C. The nerve here remained at 6.1°C for the duration of the experiment.

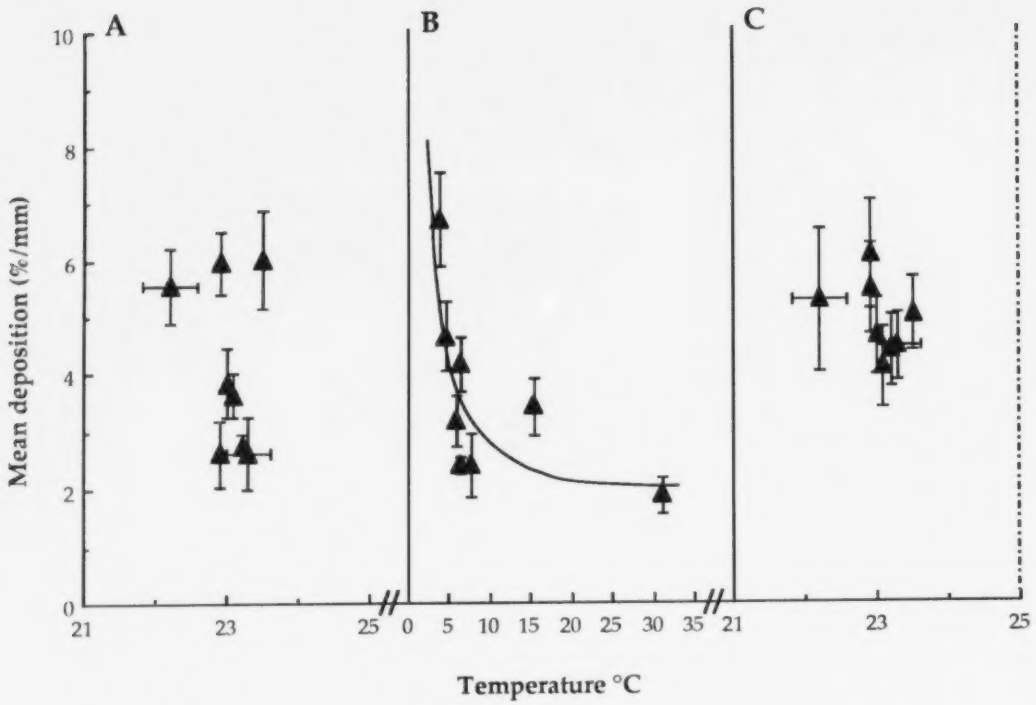

Figure 2. 8. Rate of protein deposition per millimetre of Method 1-treated nerves (%/mm) as a function of temperature. Each point represents the mean deposition value of a number of segments that was defined according to the temperature at which radiolabelled proteins were off-loaded from a pulse travelling in the anterograde direction (see Table 2.1). The horizontal and vertical bars of each point indicate ± 1 standard deviation in temperature and ± 1 SEM % deposition, respectively.

A: Here, the rate of deposition before the cooling period was 4.8 ± 0.6 %/mm.

B: A distance-weighted least squares (DWLS) smoothing curve fitted to the data points was used to describe the curve presented in the figure. The curve shows that as the temperature was lowered, the amount of protein deposited increased non-linearly.

C: Once the nerve was warmed up, the deposition rate was 4.8 ± 0.2 %/mm.

Figure 2. 9.

A: Mean rate of protein deposition per millimetre (%/mm) of nerve as a function of temperature. Both Method 1- (black bars) and Method 2-treated (shaded bars) nerves were cooled for a period of 14 hours at 6.5°C before being warmed up to 23°C. The error bars indicate ± 1 SEM. A Student's t-test showed no statistical difference in the mean rate of protein deposition of Method 1- and Method 2-treated nerves cooled at 6.5°C and then warmed up to 23°C.

B: Subsequent comparison of cold and warm-up depositions of Method 1-treated (solid triangles) and Method 2-treated nerves (open triangles). Both Method 1-treated and Method 2-treated nerves were cooled for about 14 hours before being warmed up. The DWLS curve shown also in Figure 2.8. is presented here to demonstrate that the differences in the two approaches effected no distinct change in the cold deposition rates of either Method 1-treated or Method 2-treated nerves. Both nerves followed a similar trend outlined by the curve. Warm up deposition rates also were not affected by the different approaches. Mean deposition rates after cooling ranged between 4 and 6%/mm.

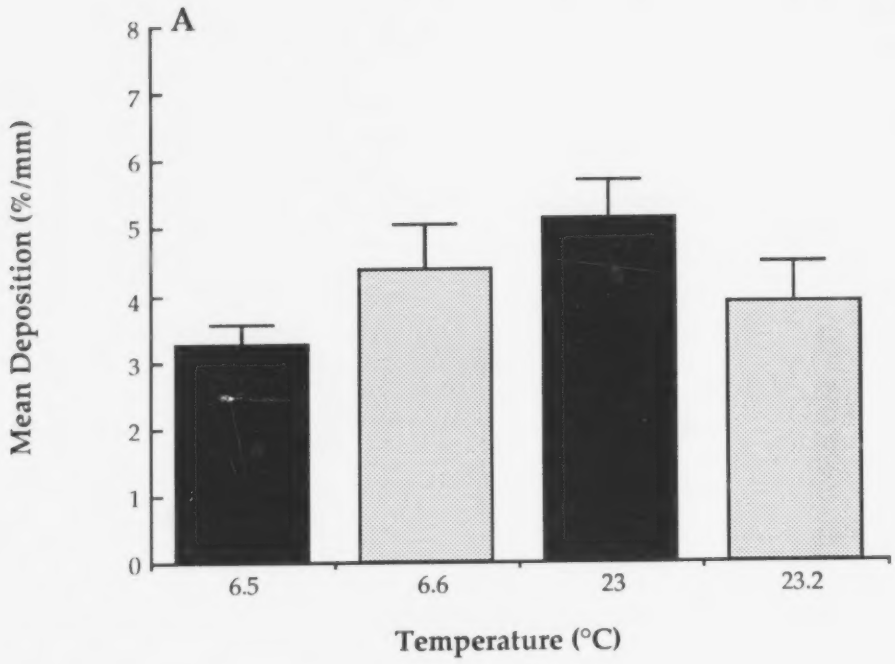
A
Mean Deposition (%/mm)
8
7
6
5
4
3
2
1
0
6.5
6.6
23
23.2
Temperature (°C)

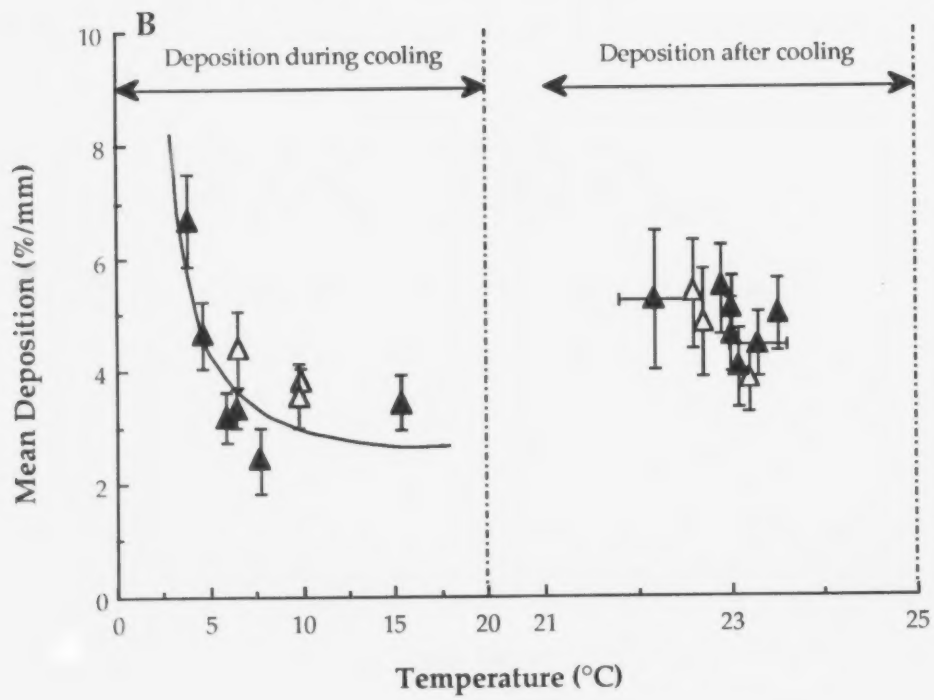
B
Deposition during cooling
Deposition after cooling
Mean Deposition (%/mm)
10
8
6
4
2
0
0
5
10
15
20
21
23
25
Temperature (°C)

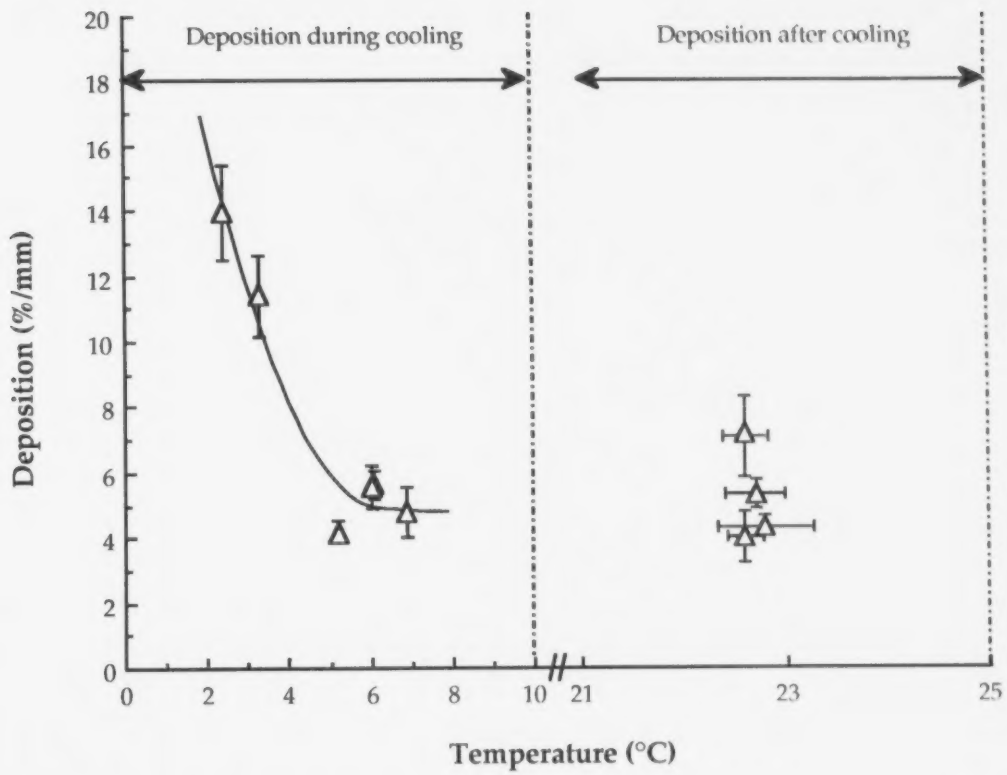

Figure 2. 10. Mean percentage of protein deposited per millimetre as a function of temperature. Nerves treated in the manner outlined in Method 2 over a 48-hour cooling period. A DWLS curve was fitted to the data to indicate the trend that the rate of deposition per millimetre increased with decreasing temperatures. Moreover, in comparison to the 14-hour experiment, the deposition per millimetre increased with longer exposure to low temperatures, especially at 2-3°C. However, despite the extended exposure to these cold temperatures, the warm up deposition rates did not change. The rate of deposition remained at 4-6%/mm.

(± 1 SEM), which excluded those segments with branch endings, was 2.0 ± 0.7%/mm at room temperature. This may imply that some branch endings were included in the values observed in this work. A robust locally weighted regression curve, otherwise known as a distance-weighted least squares smoothing (DWLS) curve (Cleveland, 1985), was fitted to the mean percentages obtained for cold deposition (Figure 2.8) using Systat 5.2.1 (SYSTAT, Inc.) to illustrate the general trend of deposition in Method 1-treated nerves. As the temperature decreased from 31°C to 4°C, the amount of radiolabelled proteins lost from the pulse increased from 1.9%/mm to 6.7%/mm (Table 2.1), particularly at around 5-10°C. This suggested that the sudden drop in protein velocity at 6.5°C may be related to an increase in the amount of protein lost by the pulse. After the nerve was warmed up, the mean deposition rate was 4.8 ± 0.2%/mm. The same deposition rate of 4.8%/mm before and after the nerve was cooled indicated that similar to protein transport which resumes at the same velocity as before cooling, protein deposition also resumes at the same rate as before cooling.

As stated in Section 2.1, Method 2 was adopted to verify the results of Method 1. However, the cessation of transport at 6.5°C in the results of Method 1 (Figures 2.4 and 2.5) did not occur in the results of Method 2 (Figures 2.6 and 2.7). It was thought that this difference may be associated with a higher percentage of radiolabelled protein left behind the migrating pulse during the cooling period of Method 1 than Method 2. To test whether the deposition rates from Methods 1 and 2 differed, three experiments were conducted at 6.5°C to 10°C in the manner outlined in Method 2 with a 14-hour cooling period, followed by a warm-up. A Student's t-test comparison of the deposition rates at 6.5°C and 23°C revealed no significant difference in

the mean deposition rates obtained between Method 1- and Method 2-treated nerves at the 0.05 level ($t = -1.69$, $P = 0.10$) (Figure 2.9A). Figure 2.9B also shows that the mean deposition values of 14-hour cooled Method 2-treated nerves at 6.5°C and 10°C fell within the general trend of the DWLS curve fitted to those values from Method 1-treated nerves, indicating that there must be another explanation for the velocity-temperature relationship seen in Figure 2.6.

Method 2. LSC analysis of nerves cooled beneath a press for 38-48 hours showed that the trend illustrated in Figure 2.8 was also observed in Figure 2.10; as the temperature decreased, the amount of radiolabelled proteins lost from the pulse increased, particularly at around 4-7°C. This indicated that both methodologies show an increase in the rate of deposition at around the low critical temperature range of 5-10°C. In addition, after the nerve was warmed up, the deposition per millimetre was around 5.8 ± 0.6%, a value slightly higher than the warm-up deposition rate of Method 1-treated nerves. This may be due to the increase in the length of the cooling time of Method 2-treated nerves.

2.3 Summary

In both sets of data gathered from Methods 1 and 2, the relationship between protein transport velocity and temperature was approximately exponentially related over a range of 6.5°-25°C. The Q_{10} value (3.0) and E_a value (18.2 kcal) for Method 1-treated nerves between 6.5°C and 25°C corresponded with those values for Method 2-treated nerves (Q_{10} value of 3.2 and E_a value of 17.7 kcal between 2°C and 10°C). The main difference between the two sets of data was the sudden discontinuity in the velocity of protein

transport observed only in the results of Method 1. This discontinuity occurred at 6.5°C.

Liquid scintillation counting analysis of Method 1- and Method 2-treated nerve preparations both showed a similar non-linear relationship between the rate of protein deposition and temperature despite the difference in the way the nerve was cooled and the length of the cooling period. Both analyses showed that as the temperature decreased, the amount of material lost by the pulse increased, particularly around 5-10°C. It is this temperature range at which proteins cease to be transported.

3 FACTORS THAT MAY ACCOUNT FOR THE DIFFERING RESULTS OBTAINED FROM THE TWO EXPERIMENTAL APPROACHES

3. 0 Introduction

The previous chapter and earlier work (Edström and Hanson, 1973; Ochs and Smith, 1975; Cosens *et al.*, 1976; Brimijoin *et al.*, 1979) show that as the temperature was lowered, the velocity of protein transport decreased exponentially. Method 1 of the previous chapter produces the result that a sudden drop in the velocity of protein transport occurred at 6.5°C, and this result is in agreement with the earlier work referenced above. However, this cessation of transport at the low critical temperature of 6.5°C was not observed when using Method 2, an approach adopted to verify the results of the first approach. Unlike Method 1, nerves in Method 2 remained in contact with the mylar floor of the MPC throughout the 24-48 hour cooling period for direct observation of protein transport. It follows then that perhaps the press and/or the MPC itself allowed protein transport to occur below 6.5°C.

This chapter presents the results of experiments designed to investigate: a) whether the temperature along the length of Method 2-treated nerve preparations was markedly different from Method 1-treated nerve preparations to allow protein transport to occur below the critical temperature of 6.5°C, and b) whether the experimental apparatus, namely the MPC, in some way permitted protein transport to continue below 6.5°C using Method 2.

3. 1 Methods

3. 1. 0 Approaches to monitoring temperature

In Method 1, the temperature during cooling was recorded from fine thermocouples placed a few millimetres from the proximal and distal ends of a raised nerve preparation. At room temperature it was recorded from above or beneath the proximal and distal ends of the nerve in a pressed situation. In Method 2, the temperature was noted from fine thermocouples, one secured beneath the 8th branch of the sciatic nerve at the proximal end, and the other placed between the branches of the peroneal and tibial nerves at the distal end.

To test whether a temperature gradient existed along the length of Method-2 treated nerves, allowing protein transport to continue below 6.5°C, the temperature around an unlabelled nerve preparation was monitored and recorded from thermocouples tied or placed in different locations along the length of the nerve. The position of one thermocouple remained secured at the proximal end of the pressed nerve while the other was varied: above, below, and distal. The temperature between the 3.6-μm thick mylar of the nerve chamber and the MPC window was also measured and recorded. In addition, a thermocouple was inserted in the outflow line of the gas-filled MPC to measure the temperature of the gaseous mixture of argon and carbon dioxide flushing through the MPC system.

3. 1. 1 A procedure to mimic both experimental approaches

The techniques used to dissect the sciatic nerve, to create a pulse of radiolabelled proteins, and to acquire and analyze data from the MPC were as described in Section 2.1.

A press was designed to mimic both methodologies (Methods 1 and 2) simultaneously. Coarse gauze was wrapped tightly around the ends of an 80-

mm long plastic frame, exposing a 6-mm centre region (Figure 3.1). A "peephole" was made at the top of the frame. Once a radiolabelled nerve preparation was secured in the nerve chamber, it was gently pressed against the MPC window while a small piece of polyethylene intramedic tubing (1.01 mm in outside diameter) was passed through the "peephole" and beneath the nerve. Elevation of the nerve at this "peephole" prevented its contact with the floor of the chamber and MPC window and allowed physiological saline to circulate throughout the entire unpressed region of the nerve. Temperature was continuously monitored by fine thermocouples, one secured beneath the 8th branch and the other a few millimetres from the exposed region of nerve. Protein transport rates derived from both methodologies in Chapter 2 were used in these experiments to predict the length of time that the pulse of radiolabelled proteins would take: a) to reach the transition between the proximal pressed region and the unpressed mid-region of the nerve and, b) possibly to pass into the distal portion of the nerve. These experiments were performed in the absence or presence of the MPC to examine its effects on protein transport. It must be noted that the MPC remained enclosed in the thermoregulated refrigerator throughout these experiments. The presence of the MPC refers to the situation where the nerve tray was positioned on the MPC so that the nerve was gently pressed against the MPC window. In the absence of the MPC, the nerve tray was placed on a 2-inch thick Styrofoam block so that the nerve was gently pressed against the mylar floor of the tray, but was not in contact with the MPC or its window.

At the conclusion of this set of experiments, the transition points between the pressed and unpressed regions of nerve were marked with charcoal powder (Sigma Chemical Co.) and the nerve was subsequently processed for LSC analysis (Section 2.1.5). The percent distribution of TCA-insoluble

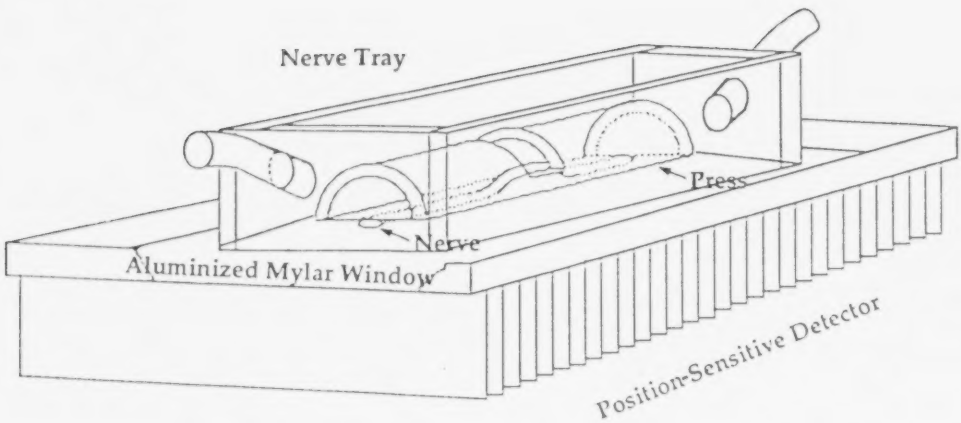

Figure 3. 1. Schematic representation of the arrangement used to detect a radioactively-labelled pulse of proteins in the sciatic nerve of an adult *Xenopus laevis*. In this particular case, a press was constructed to mimic the two experimental approaches (Methods 1 and 2) simultaneously. Throughout the duration of a 40-hour cooling period, both the proximal and distal ends of the nerve preparation (70-75 mm in length) were gently pressed against the aluminized mylar window of the position-sensitive detector, thus mimicking Method 2. A small piece of plastic tubing was inserted beneath a 6-mm mid region of the nerve to prevent contact with the MPC window and to allow physiological saline to circulate around this middle region, thus mimicking Method 1. At the conclusion of the experiment, the nerve was segmented according to its position on the MPC window and processed for liquid scintillation counting.

radioactivity in each 3.18-mm nerve segment was calculated using the following equation:

$$(5) \qquad \% \text{ of radioactivity in segment } i = \frac{1}{3.18}\left[\frac{C_i}{\sum_{j=1}^{n} C_j}\right] X\ 100\%$$

where C_i represents the amount of radioactivity in segment i (usually 1-23 nerve segments), n represents the last nerve segment, and $\sum_{j=1}^{n} C_j$ represents the total amount of radioactivity from segments 1 to n.

3. 2 Results

3. 2. 0 Temperature readings

In nine experiments performed in the manner outlined in Section 2.1.3 (Method 1), the temperature difference between the proximal and distal ends of the nerve at room temperature or a desired low temperature was 0.4 ± 0.2°C. A similar temperature difference was observed at room temperature for Method 2-treated nerve preparations (n=14) in which one thermocouple was secured beneath the 8th branch of the sciatic nerve and the other between the branches of the peroneal and tibial nerves. During the cooling period in the thermoregulated refrigerator, the temperature difference between proximal and distal ends was 0.3 ± 0.1°C. These results indicate that the temperature along the length of Method 2-treated nerves is not markedly different from Method 1-treated nerves.

In unlabelled Method 2-treated nerve preparations (n=4) (Section 2.1.3), the temperature difference between two proximally-located thermocouples, one beneath the nerve and the other between the mylar of the

nerve chamber and the MPC mylar window, was 0.3 ± 0.1°C. A 0.1-0.2°C difference was observed between a thermocouple situated above or below the proximal end of the nerve and another placed beneath the mid-region of the nerve. In two experiments, the nerve preparation remained unlabelled and sheathed in order to insert and secure a thermocouple at the proximal end of the nerve. Since the branches of the peroneal and tibial nerves were too narrow, the second thermocouple was placed and secured beneath them. A temperature difference of 0.3 ± 0.2°C was observed. This result suggested that the entire length of Method 2-treated nerves was not markedly different between the proximal and distal ends.

The temperature of the interior of the refrigerator and the gas differed only by 0.1°C, indicating that temperature of the gas probably did not raise the nerve temperature enough to allow protein transport to continue below 6.5°C. Thus, it appears that the difference in the velocity-temperature relationship between Methods 1 and 2 cannot be explained by temperature differences.

3. 2. 1 Protein transport along the newly constructed press

These experiments were conducted at 2-3°C because protein transport ceases at this low temperature in Method 1, but not Method 2. The press was constructed (Figure 3.1) with a "peephole" to test whether the state of the nerve, either pressed or raised, would affect protein transport. First, three nerve preparations were cooled for 38-42 hours in the absence of the MPC and then processed for LSC analysis. In all three nerve preparations the proximal pressed region of nerve was 0.3 ± 0.1°C cooler than the middle raised region of nerve. The prediction was that if the press alone insulated the nerve preparation at cold temperatures, then protein transport should occur in the pressed proximal region of nerve at a rate of about 13 mm/d as seen in Method 2, but not the raised

region as observed in Method 1. At 13 mm/d, the distance travelled by the pulse should be 21-23 mm (6-7 segments) in 38-42 hours. Since all the experiments from Chapter 2 show that a pulse of radiolabelled proteins spanned about 7-8 nerve segments and the modified press covered only 10-11 segments of the proximal end of the nerve, it was expected that an accumulation would be observed at the transition site between the proximal pressed and raised regions of the nerve.

Figure 3.2A represents results from an experiment performed without the presence of the MPC. Here, the percentage of TCA-insoluble radioactivity was examined in each 3.18-mm nerve segment, particularly at the transition between the pressed (segments 9-11) and raised (segments 12-13) portion of the nerve. The low percent distribution of radioactivity in segments 10-19 seemed to indicate that at 2.8 ± 0.1°C the pulse of radiolabelled proteins did not move either in the pressed or raised region of nerve. Hence, these results suggested that the press alone does not allow protein transport to continue below 6.5°C as seen in Method 2.

Secondly, three experiments were conducted in the presence of the MPC. MPC and LSC data were collected from nerves cooled for 38-42 hours to determine the effects of both the MPC and the modified press upon the movement of protein transport. In all three nerve preparations the proximal pressed region of nerve was 0.5 ± 0.2°C cooler than the middle raised region of nerve. MPC data from one experiment revealed that the rate of protein transport in the proximally pressed region of the nerve was within the range of 12-16 mm/d (0.14-0.18 μm/s), values which were not only predicted but also similar to protein transport rates in Method-2 treated nerves at 2-3°C (Figure 2.6). With the exception of this experiment, however, no information concerning the rate of protein transport was derived from the MPC data collected due to technical and

Figure 3. 2.

Percentage of TCA-insoluble radioactivity in each 3.18-millimetre segment of nerve, particularly segments 9-19, as assayed by liquid scintillation. The segments before and after the broken lines represent the proximal and distal pressed regions of nerve. The area between the broken line represents the elevated nerve segments.

A: This panel represents a nerve preparation cooled for 42 hours at 2-3°C with only the modified press present (no MPC present) and then processed for liquid scintillation analysis. The low percentage distribution of TCA-insoluble radioactivity from segments 11-19 shows that the radiolabelled pulse did not move in the pressed proximal region or into the elevated region (6 mm in length). This result indicated that the pressed or raised condition of the nerve was not a factor in allowing protein transport to occur at 2-3°C.

B: Here both MPC and LSC data were collected from a nerve preparation cooled at 2-3°C for 45 hours. In comparison to the above panel, the high percentage of TCA-insoluble radioactivity in nerve segments 9-12 shows that the radiolabelled proteins were transported through the pressed proximal region (segments 9-10) into the elevated region (9mm in length) of the nerve. This indicated that the MPC was somehow allowing protein transport to occur at 2-3°C.

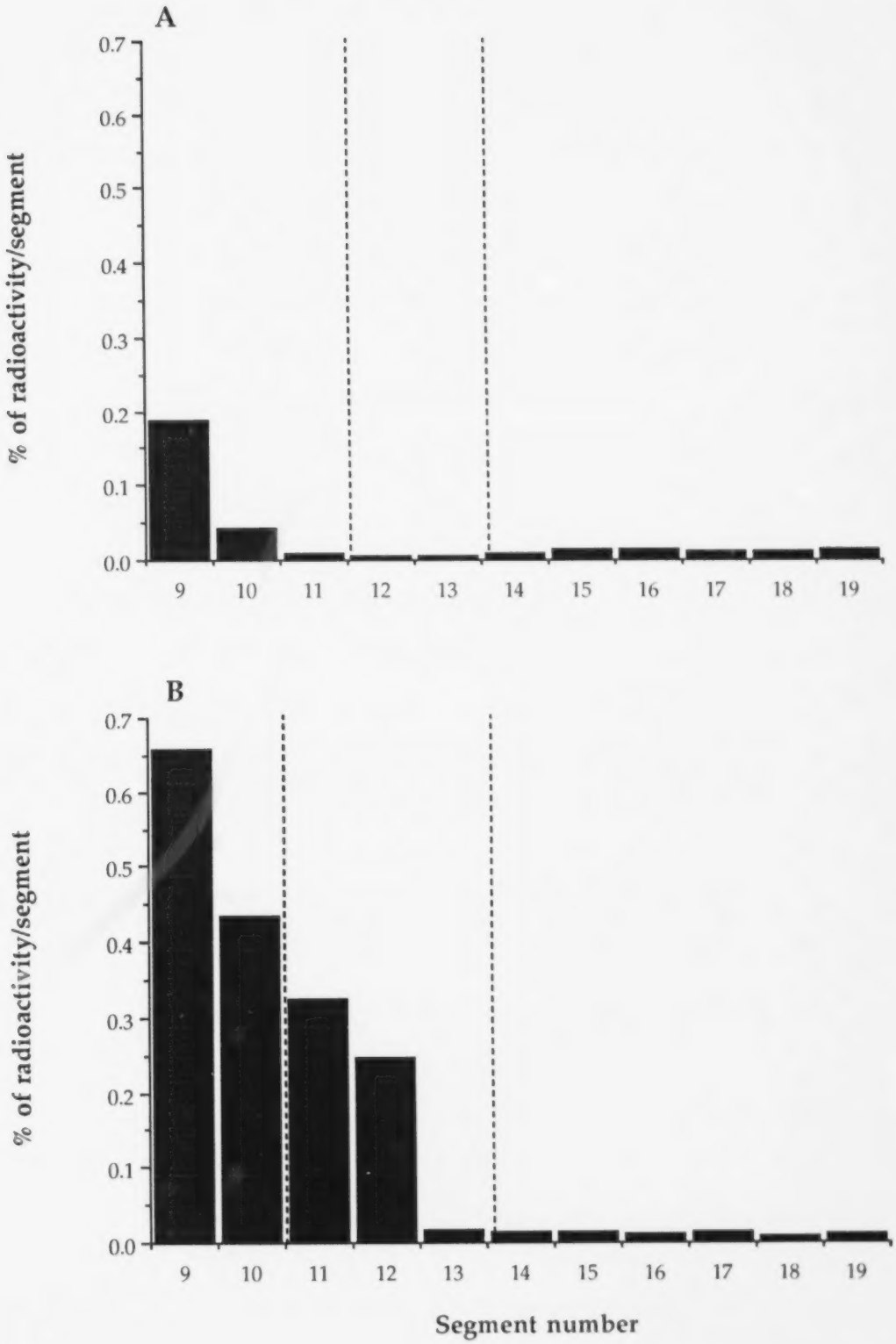
A
% of radioactivity/segment
0.7
0.6
0.5
0.4
0.3
0.2
0.1
0.0
9
10
11
12
13
14
15
16
17
18
19
B
% of radioactivity/segment
0.7
0.6
0.5
0.4
0.3
0.2
0.1
0.0
9
10
11
12
13
14
15
16
17
18
19
Segment number

computational difficulties. Figure 3.2B represents the LSC analysis of a nerve preparation on the MPC during cooling at 2.4 ± 0.4°C in which the percentage of TCA-insoluble radioactivity was determined in each 3.18-mm nerve segment. It shows a redistribution of radioactivity from the pressed proximal region (segments 9-10) of the nerve into the unpressed region (segments 11-12), indicating that some radiolabelled proteins may have been transported at 2-3°C. The low level of radioactivity in the raised nerve segment 13 and in the distal nerve segments (14-19) indicated that the pulse did not migrate into the distal pressed portion of the nerve.

3. 3 Summary

The investigation of temperature along the length of several nerves, both labelled and unlabelled, revealed that the temperature difference between the proximal and distal nerve ends was no greater than around 0.4°C in both Method 1- and 2-treated nerve preparations. This result indicated that temperature could not explain the difference in results between Methods 1 and 2. In addition, the temperature of the MPC window and the quenching gas could not have raised the temperature of the nerves sufficiently to allow protein transport to continue below 6.5°C.

In the set of experiments performed with only the modified press, no protein transport was detected at 2-3°C. However, in the presence of the MPC and the modified press, some movement of protein transport was detected at 2-3°C in the pressed proximal region, which was expected, and in the raised middle portion of the nerve preparation, which was not expected. These results suggest that the MPC itself was somehow affecting the rate of protein transport in Method 2 for reasons that will be discussed later.

4 THE EFFECTS OF TEMPERATURE ON FAST AXONAL TRANSPORT OF ORGANELLES MOVING IN THE ANTEROGRADE AND RETROGRADE DIRECTIONS

4. 0 Introduction

The work described in this chapter was undertaken primarily to produce a description of the transport dynamics of organelles in sciatic axons of *Xenopus laevis* over a range of temperatures so that a comparison might be made between the temperature dependences of protein transport and of organelle transport. Of particular interest was whether a sudden decrease in organelle velocity occurs as the temperature is dropped below 6.5°C (see Chapter 2).

The temperature dependence of the velocity of retrograde organelle transport has been described earlier using optical techniques that did not detect anterogradely-transported sub-resolution organelles (Forman *et al.*, 1977b; Smith and Cooper, 1981). Therefore, the opportunity was taken to compare the temperature dependences of anterograde and retrograde organelle transport using imaging techniques capable of detecting sub-resolution structures (Smith, 1989).

4. 1 Methods

The effects of various temperatures on the velocity of fast anterograde and retrograde organelle transport were observed for different cooling periods. In the first case, observations and comparison of transport in both the anterograde and retrograde directions over a range of 0-40°C were made in nerves acclimated to a desired temperature for no longer than 30 minutes. The effects of increasing and decreasing the temperature upon organelle transport

were also examined in some nerve preparations. The second case was designed specifically to determine the effects of prolonged periods of low temperatures (0-10°C) on the transport of small, circular organelles in both directions. Nerves were treated in a similar manner as outlined previously (Section 2.1.3) for a 14-24 hour cooling period. In addition, some nerves were bathed in oxygenated physiological saline containing taxol (10μmol/L), a drug that stabilizes microtubules and protects them from cold depolymerization (Smith and Snyder, 1995), for 1 hour at room temperature before the taxol-containing saline was cooled for 16-20 hours.

4.1.0 Nerve Preparation

Adult female *Xenopus laevis* toads were anaesthetized by immersion in a 2% solution of urethane (Sigma Chemical Co.). A 50-60 mm length of sciatic nerve was dissected out from the hip to just below the knee joint. The perineural sheath was removed according to the method outlined by Chan *et al.* (1980) to expose a bundle of single myelinated axons. During dissection and desheathing, the nerve was bathed in an oxygenated physiological saline of the same composition as in the protein studies (Section 2.1.0). The desheathed nerve was mounted on a microscope slide and gently teased at the centre of its length with two fine needles to reveal individual axons.

During the experiment, a thin layer of physiological saline bathed the entire nerve. Since the detection of the smallest moving organelles required a mechanically stable preparation, a drop of inert silicone fluid (Dow Corning 710) was applied to the teased axons. A #0 coverslip was applied over the nerve and the microscope slide. To support it above the nerve, the coverslip was ringed with a thin layer of silicone grease (Dow Corning Silicone Lubricant).

4. 1. 1 Temperature Measurement and Control

To measure the temperature of the nerve preparation, a fine thermocouple was passed through the thin layer of silicone grease so that its tip rested in the drop of the silicone fluid close to the isolated axons. Temperatures above the specimen's ambient temperature (23°C) were achieved by heating the microscope stage with a thermostatically actuated infra-red lamp. Experiments below the specimen's ambient temperature were performed in a cold room at 4°C. Altering the temperature of the nerve preparation between 0° and 23°C within the cold room required either heating the microscope stage with the infra-red lamp or cooling the stage with pieces of dry ice. After the nerve preparation was acclimated for a maximum of 30 minutes to the desired temperature, computer enhanced video microscopy was used to image organelles undergoing transport in isolated myelinated axons.

4. 1. 2 Computer Enhanced Video Light Microscopy

The basic optical system for imaging organelles has been described in detail by Allen *et al.* (1981) and Inoué (1986). Briefly, isolated axons were viewed by Zeiss differential interference-contrast (DIC) optics using a 63x oil immersion objective with a numerical aperture of 1.4. Illumination was provided by a 50 W mercury arc lamp and a green interference filter (60 nm bandpass centred at 550 nm), heat filters were also placed in the light path. The microscope image was detected with a DAGE Newvicon target television camera, the output of which was electronically processed with digital processors (Quantex Corp.) to detect the smallest, 50-100 nm diameter, organelles travelling in the anterograde direction. A full description of the digital processing procedure is given in detail elsewhere (Smith, 1989). Essentially, the microscope image obtained with DIC optics was obscured by low frequency shadows and highlights emanating from the myelin

sheath. To attenuate these low spatial frequencies and to accentuate fine detail, the DIC microscope image was subject to high-pass spatial filtering. The resulting filtered image displayed few diffraction images of the 50-100 nm anterogradely-moving organelles. Consequently, detection of these images was achieved by a subtraction method of motion detection. A running exponential average of adjacent high-pass filtered TV frames (about 16 frames) was produced to obtain an image of the stationary parts of the axis cylinder. To eliminate the stationary structural detail of the axon from the image, its representation was continuously updated in computer memory and subtracted from the spatially filtered, but unaveraged, image of the current TV frame. This resulted in an image of moving organelles only. Attenuating the background noise in this "subtracted" image was achieved by running a short exponential time average; the black level and gain were adjusted to increase contrast. The enhanced real-time images of moving organelles were then recorded on video tape for subsequent analysis.

4. 1. 3 Other Methods

A variation on the above methods was to treat the nerves under the conditions of previous methods. Excluding the radiolabelling step and the runs at room temperature, the same procedure outlined in Section 2.1.3 was followed. Once secured in the nerve tray, the nerve was immediately cooled for 14 hours to a desired low temperature either with or without the press. Temperature was continually monitored throughout the experiment by fine thermocouples. After cooling, the nerve was removed from the tray. To maintain the desired temperature of the unlabelled nerve, the desheathing of the nerve and its subsequent preparation for visualizing organelle transport were performed in a cold room at 4°C.

4. 1. 4 Data Analysis of Organelle Transport

The classification of organelles on the basis of their direction of transport, their apparent size (sub or supra resolution), and their shape (circular or rod-shaped) (Table 4.1) was achieved by visualizing the organelles from a television display at a magnification of 10,000x. Organelle speeds were estimated by recording transit times in seconds across a 5 to 10 μm "gate." Cricket Graph 1.3.2 (Cricket Software) was used to fit a simple exponential curve through the collected data points. The influence of temperature on the reaction involved in the mechanism of anterograde and retrograde transport was also evaluated by determining the Q_{10} value and E_a from the mean organelle velocities. The E_a could be derived from equation (2) where V_1 and V_2 were the mean organelle velocities in μm/s at the corresponding absolute temperatures (K), or from the slope of the line (b) of an Arrhenius plot ($b=-E_a/2.3R$) in which the natural logarithm of mean organelle velocity was plotted as a function of the reciprocal of the absolute temperature (K). The Q_{10} value was calculated by equation (3) where V_1 and V_2 were the mean organelle velocities in μm/s at the respective temperatures (°C). These values were later compared to those values obtained from the protein transport studies.

To determine whether there was a reduction in the number of organelles transported anterogradely at 6.5°C, organelle flux over 0-12°C was estimated by recording the number of organelles passing a vertically-placed 10 μm "gate" in a 2-3 minute interval. The organelle flux over 0-12°C was normalized to 6.5°C. This was done by dividing it by the corresponding mean vesicle velocity and then multiplying it by the mean vesicle velocity at 6.5°C.

Statistical comparison of data sets was carried out using Systat 5.2.1 (SYSTAT, Inc.).

Table 4. 1.

Characterization of rapidly transported organelles on the basis of their apparent image size and shape (NA = not applicable)

Organelle type	Image Diameter (μm)	Length (μm)
Small, circular (SC)	~ 0.2	NA
Large, circular (LC)	> 0.2	NA
Small, rod-shaped (SR)	~ 0.2	< 1.3
Large, rod-shaped (LR)	> 0.2	> 1.3

4. 2 Results

4. 2. 0 The effects of temperature on organelles with circular images

Figure 4.1 shows the results obtained from 20 nerve preparations that were acclimated for a maximum of 30 minutes to the desired temperature before organelle transport was visualized for up to 1.5 hours. Organelle speeds in both anterograde and retrograde directions were studied between 0°C and 37°C. From these speeds, the mean velocities of small circular (SC) (Figures 4.1A and 4.1B) and large circular (LC) vesicles (Figures 4.1C and 4.1D) in the anterograde and retrograde directions were plotted as a function of temperature. Over a range of 5-30°C, the mean velocities of anterogradely-moving SC and LC vesicles were fitted by simple exponential curves, $V=0.227(1.09)^T$ and $V=0.156(1.10)^T$, respectively, where V is the velocity in μm/s. Over the same range of temperatures, the equations describing the temperature dependent properties of retrogradely-moving SC and LC vesicles were $V=0.151(1.11)^T$ and $V=0.116(1.10)^T$, respectively. These results were reproducible when the nerve temperature was decreased and then warmed up. In both classes of circular vesicles the correlation coefficients (r) for the exponential fits were greater than 0.9.

Figure 4.2 shows semilog plots of the same data. The mean velocities in both directions from about 5-30°C fitted well with a straight line, indicating that the anterograde and retrograde transport of the circular vesicles was exponentially related with temperature. Although the slope of the lines were similar, the shift in the position of the lines indicated that anterogradely- and retrogradely-moving LC vesicles (solid line) were transported at slower mean velocities than anterogradely- and retrogradely-moving SC vesicles (broken line).

An analysis of residuals about the fitted lines indicated two possible deviations from the exponential curve in both classes of vesicles. Between 25° and 30°C the mean vesicle velocities apparently reached their maximum as

Figure 4. 1.

Mean velocities of anterograde (Panels A and C) and retrograde (Panels B and D) transport of small (open circle and triangles) and large (solid circles and triangles) circular organelles, otherwise known as vesicles, over a temperature range of 0°-40°C. The error bar of each point represents ± 1 SEM. The exponential curve for each graph was a least squares fit to the data points between 5°C and 30°C.

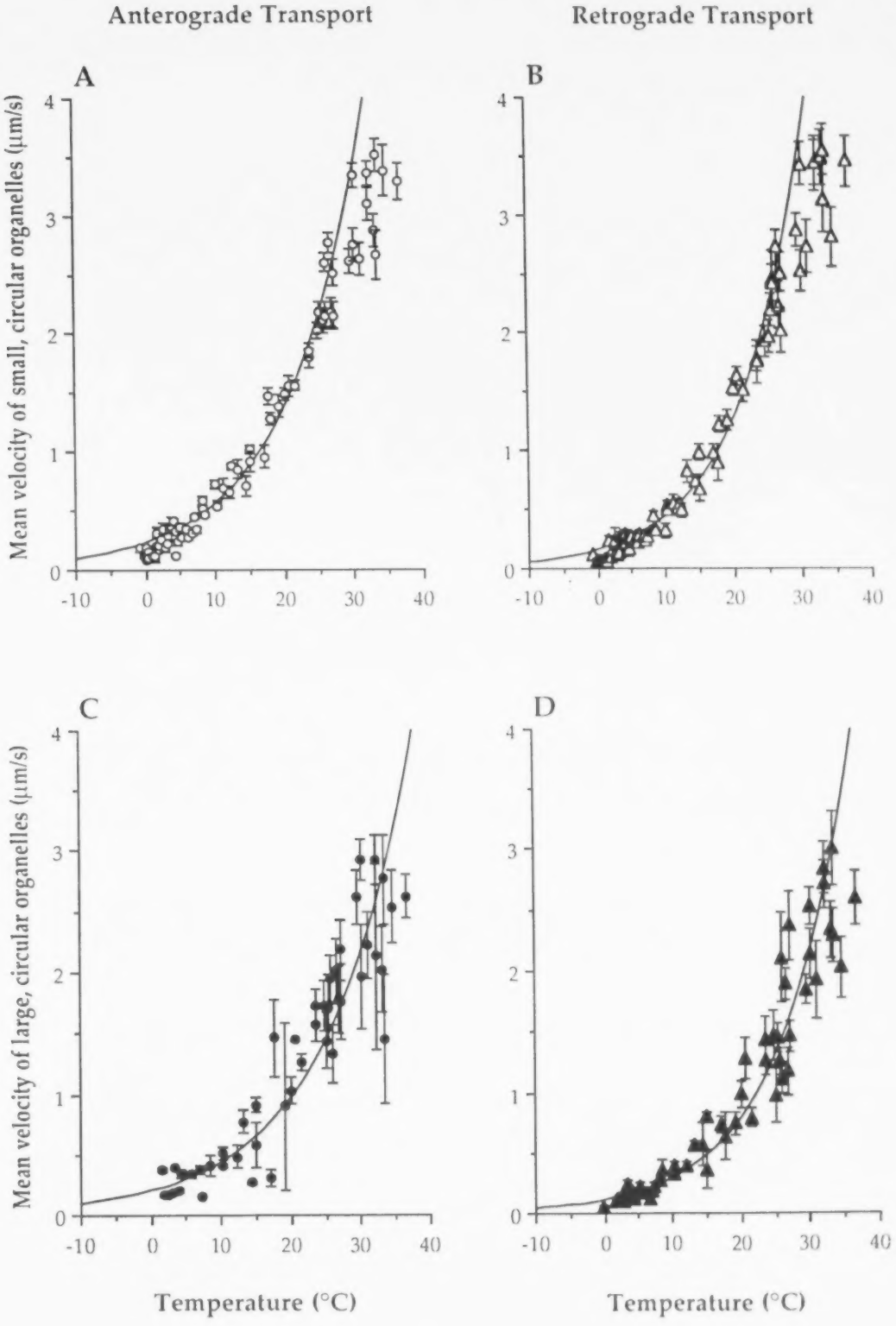
Anterograde Transport
Retrograde Transport
A
B
C
D
Mean velocity of small, circular organelles (μm/s)
Mean velocity of large, circular organelles (μm/s)
0
1
2
3
4
-10
0
10
20
30
40
Temperature (°C)
Temperature (°C)

Figure 4. 2.

Semilog plot of the data from Figure 4.1. Mean velocities of anterogradely- (A) and retrogradely-transported (B) vesicles were plotted on a logarithmic scale against temperature.

A: The open circles represent mean velocities of small vesicles whose relationship with temperature is described by the dotted line. The solid circles represent mean velocities of large vesicles. Their relationship with temperature is described by the solid line. Note that the mean anterograde vesicle velocity was exponentially related to temperature over a range of 5-30°C. The shift in the position of the lines indicates that at all temperatures anterogradely-transported large vesicles moved on average more slowly than small vesicles. Two possible discontinuities in the relationship between velocity and temperature occurred below about 5°C and above 30°C.

B: The triangles and lines here correspond to the same classes of organelles as in A but in the retrograde direction. Note that the influence of temperature upon the velocity of retrogradely-transported small and large vesicles was similar to that of anterogradely-transported vesicles.

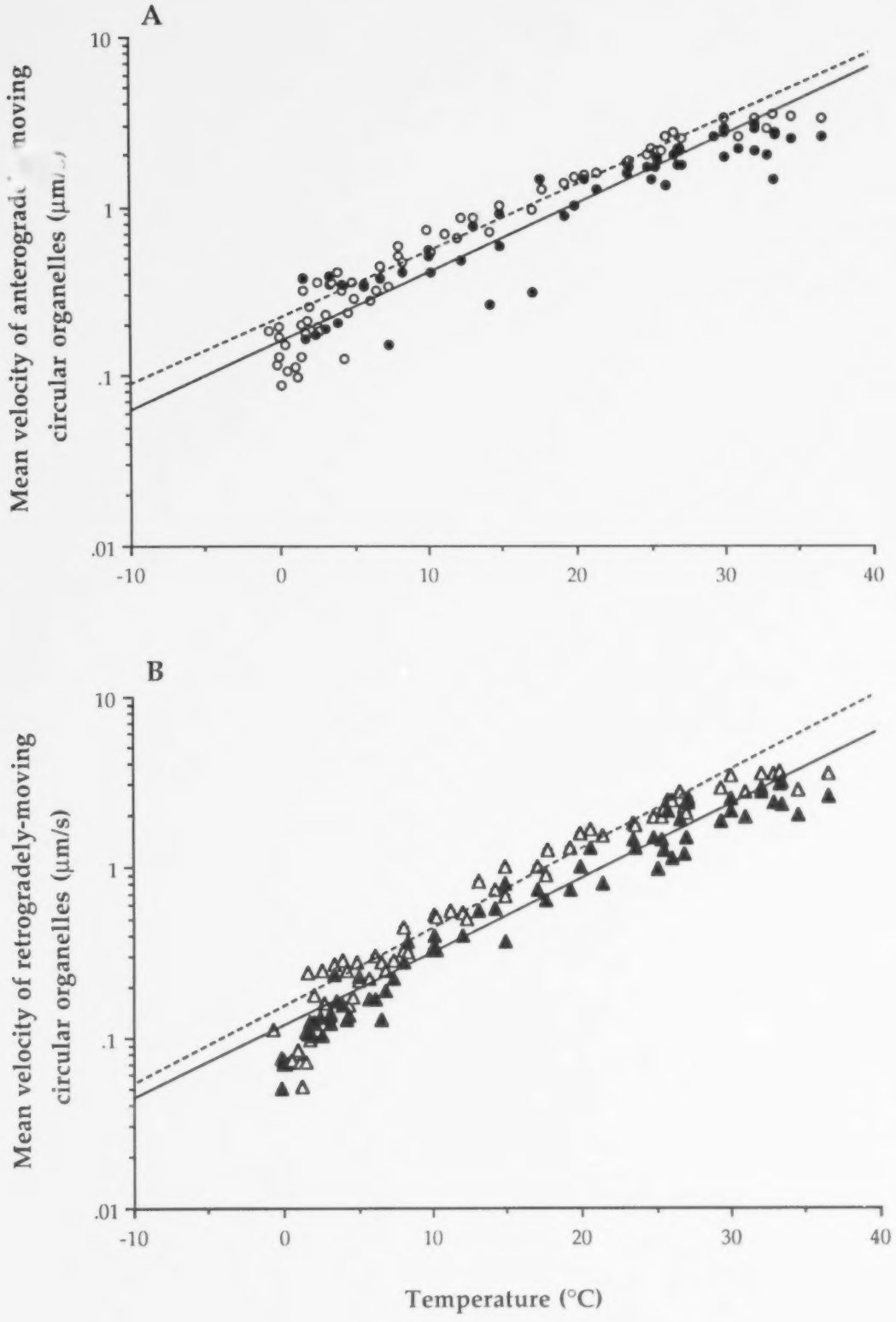
A
Mean velocity of anterograde moving circular organelles (µm/s)
10
1
.1
.01
-10
0
10
20
30
40
B
Mean velocity of retrogradely-moving circular organelles (µm/s)
10
1
.1
.01
-10
0
10
20
30
40
Temperature (°C)

indicated by the deviation in velocity from the straight line. Between 5° and 0°C vesicle velocities showed a deviation from the fitted line such that vesicles moved more slowly than the fitted line predicted. However, vesicles continue to move in the anterograde and retrograde directions down to 0°C.

There was no statistical difference observed between the mean number of SC vesicles above and below 6.5°C based on a one-tailed Student's t-test ($p>0.05$). If there was a reduction in vesicle traffic below 6.5°C, it was less than 15%. This indicated that the observed deviation in mean vesicle velocity was not accompanied by a reduction in vesicle numbers.

4. 2. 1 The effects of temperature on the transport of rod-shaped organelles

Between 10° and 30°C, an exponential curve seemed to fit the mean velocities calculated for anterogradely- and retrogradely-moving small rod-shaped (SR) organelles (Figures 4.3A and B). The equations describing these fits were $V=0.281(1.08)^T$ and $V=0.135(1.11)^T$, with r values of 0.95 and 0.92, indicating that the anterograde and retrograde transport of SR organelles were exponentially related with temperature. However, a simple exponential curve was not a good fit to the mean velocities of large rod-shaped organelles in either the anterograde ($r=0.16$) or retrograde direction ($r=0.77$) (Figures 4.3C and D). This can be clearly observed in Figure 4.4 which shows semilog plots of the same set of data illustrated in Figure 4.3. The mean velocities of anterogradely- and retrogradely-transported LR organelles were scattered about the best-fit line. Similar to the circular classes of organelles, at around 30°C the mean velocity of SR organelles apparently reached its maximum as indicated by the drop in velocity at that temperature. Below 10°C no rod-shaped organelles of either size were observed to move, demonstrating that rod-shaped organelles could not be the carriers of newly synthesized proteins.

Figure 4. 3.

Mean velocities of anterograde (Panels A and C) and retrograde transport (Panels B and D) of small (open squares and diamonds) and large (solid squares and diamonds) rod-shaped organelles over a temperature range of 3°-37°C. The error bar of each point indicates ± 1 SEM. The exponential curve for each graph was a least squares fit to the data points between 10°C and 30°C.

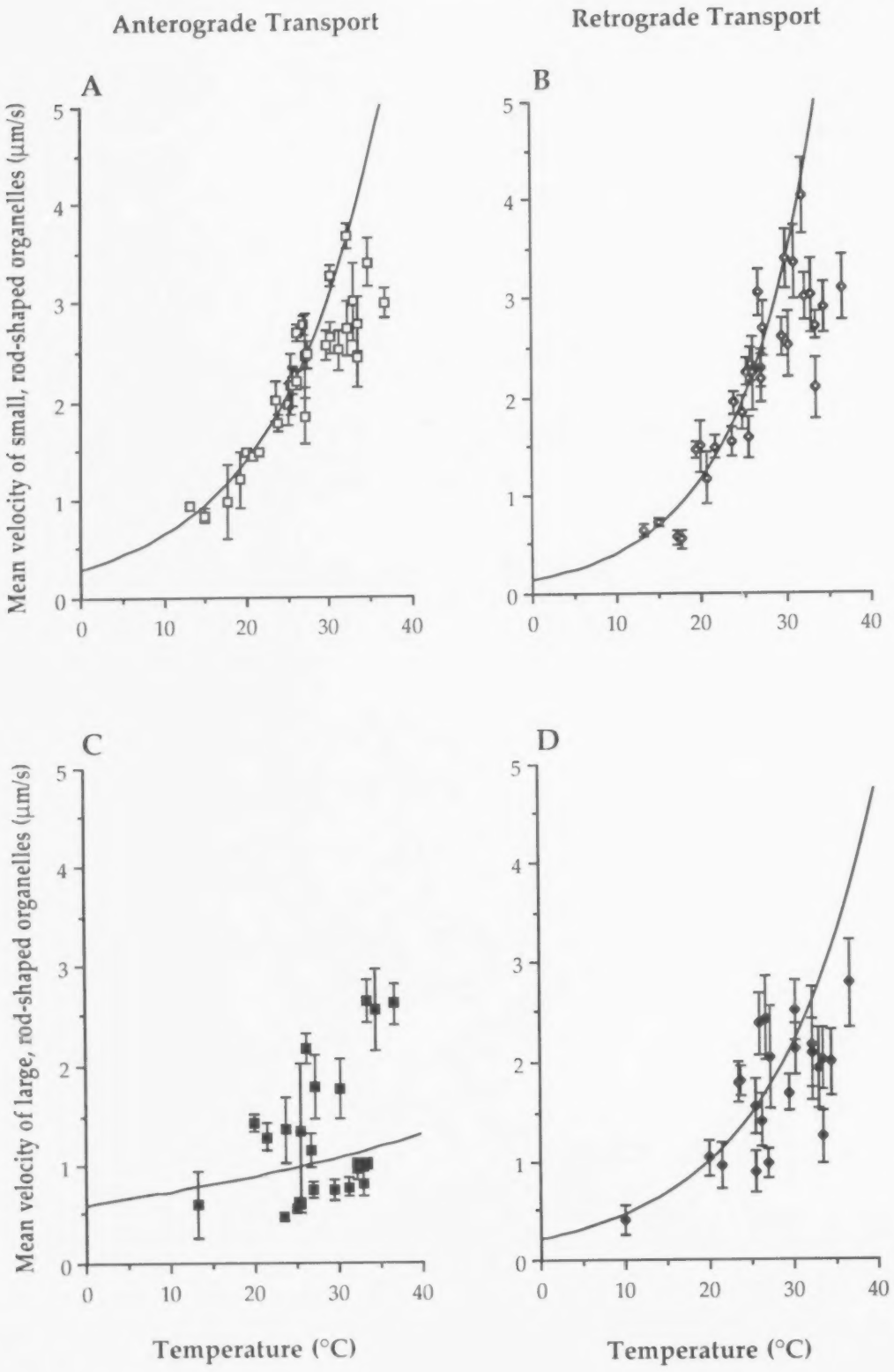
Anterograde Transport
Retrograde Transport
A
B
C
D
Mean velocity of small, rod-shaped organelles (μm/s)
Mean velocity of large, rod-shaped organelles (μm/s)
0
1
2
3
4
5
0
10
20
30
40
Temperature (°C)
Temperature (°C)

Figure 4. 4.

Semilog plot of the data from Figure 4.3. Mean velocities of anterogradely- (A) and retrogradely-transported (B) rod-shaped organelles were plotted on a logarithmic scale against temperature.

A: The open and solid squares represent the mean velocities of small and large rod-shaped organelles, respectively. Their relationship with temperature is described by the dotted and solid lines, respectively. Note that the mean velocity of anterogradely-transported small rod-shaped organelles was exponentially related to temperature over a range of 10°-30°C. Similar to circular vesicles, a possible discontinuity in the relationship between velocity and temperature occurred above 27°-30°C. The velocity of large rod-shaped organelles was only poorly described by an exponential fit. Very few small or large rod-shaped organelles were transported below 10°C.

B: The open and solid diamonds represent the same classes of organelles as in A with the relationships indicated by the dotted and solid lines, respectively. Here the mean velocity of retrogradely-transported small rod-shaped organelles was approximately exponentially related with temperature over a temperature range of about 12°-30°C. The velocity of large rod-shaped organelles with temperature was poorly described by an exponential fit.

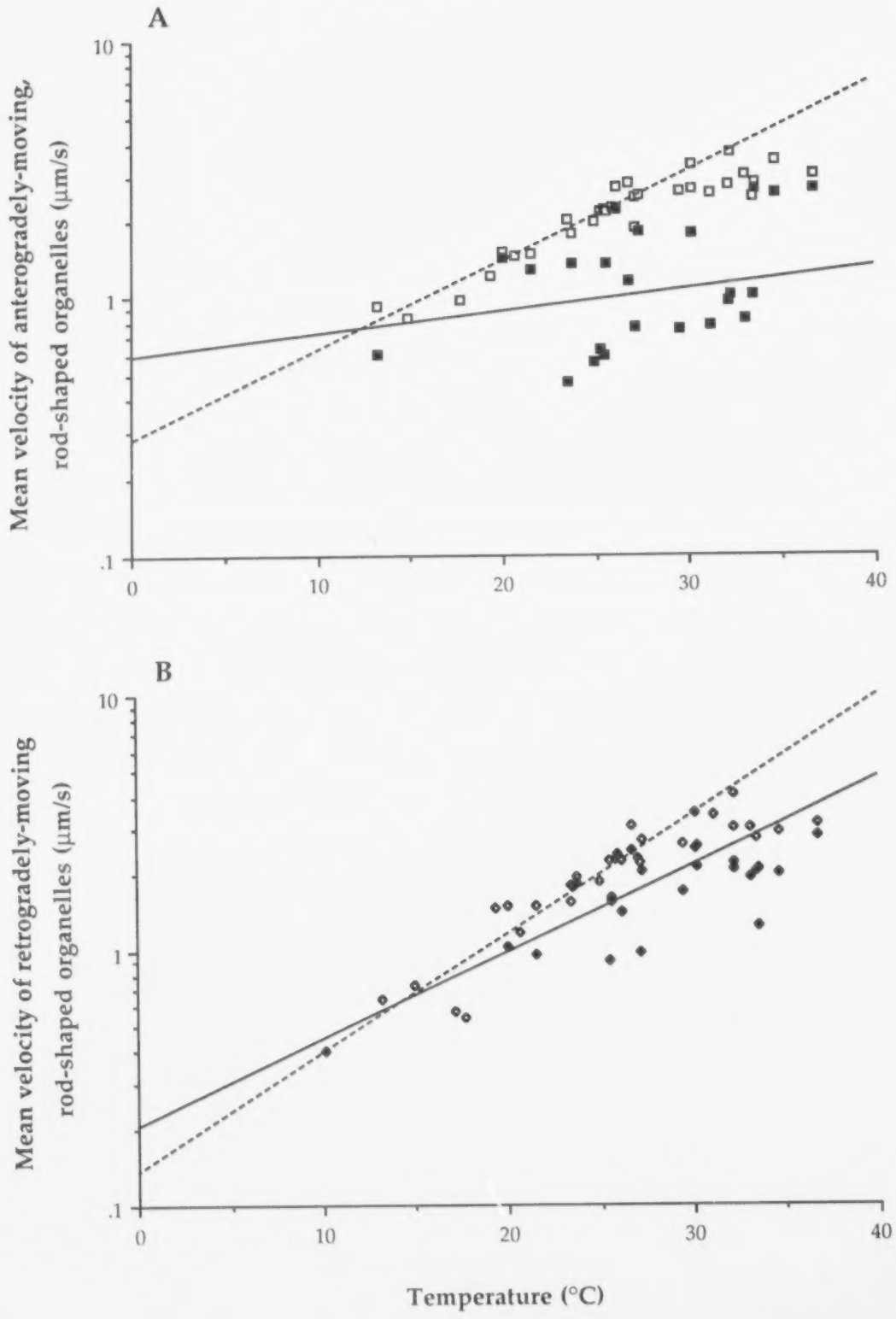
A
Mean velocity of anterogradely-moving, rod-shaped organelles (μm/s)
10
1
.1
0
10
20
30
40
B
Mean velocity of retrogradely-moving rod-shaped organelles (μm/s)
10
1
.1
0
10
20
30
40
Temperature (°C)

4. 2. 2 Q_{10} values and the E_a values

Table 4.2 lists the Q_{10} values calculated between 10° and 20°C and the E_a values of the different classes of organelles. With the exception of LR organelles, anterogradely-moving SC, LC, and SR organelles possess similar Q_{10} values ranging between 2.2 and 2.8, while their retrogradely-moving counterparts have slightly higher Q_{10} values between 2.9 and 3.1. The subsequent E_a values appear to follow a similar trend. Activation energies of 13-17 kcal/mole were observed for anterogradely-moving organelles, excluding LR organelles. Activation energies of 17-19 kcal/mol were calculated for retrogradely-moving organelles.

4. 2. 3 Organelle transport after 14 hours cooling

The results from Figures 4.1A and B and from 18 nerve preparations treated according to the methods outlined in Section 4.1.3 are illustrated as semilog plots in Figure 4.5. Particular attention was directed towards the temperature range of 0-10°C in order to determine whether the variation in the conditions to which the nerve preparation was subjected affected mean vesicle velocities similarly to protein transport rates. Unlike Figures 2.5 and 2.7, mean SC vesicle velocities obtained from nerves cooled for 14 hours with or without the press and MPC were not statistically significant ($p>0.05$). This indicated that unlike the transport of radiolabelled proteins, the transport of vesicles is not affected by the presence of the press and the MPC. In addition, Figure 4.5 shows that in both 2- and 14-hour cooled nerves, no sudden drop in vesicle velocity occurred between 5-10°C, the critical temperature at which protein transport drops rapidly to zero. To investigate whether the gradual drop observed in the mean velocity of SC vesicle transport resulted from a loss of microtubules, amphibian sciatic nerves were incubated in taxol prior to cooling and during the

Table 4. 2.

Activation energies and Q_{10} values over 6.5-25°C for different types of organelles rapidly transported in either the anterograde or the retrograde direction

Organelle type	Q_{10} (± SEM)	Activation energy (kcal/mole ± SEM)
Anterograde, small, circular	2.4 ± 0.1	14.8 ± 0.8
Retrograde, small, circular	3.0 ± 0.1	18.2 ± 0.8
Anterograde, large, circular	2.8 ± 0.4	17.1 ± 2.7
Retrograde, large, circular	2.9 ± 0.3	17.8 ± 1.5
Anterograde, small, rod-shaped	2.2 ± 0.2	12.9 ± 1.5
Retrograde, small, rod-shaped	3.1 ± 0.7	18.6 ± 3.8
Anterograde, large, rod-shaped	1.1 ± 0.6	1.1 ± 9.9
Retrograde, large, rod-shaped	2.9 ± 0.5	17.5 ± 3.0

Figure 4. 5.

Semilog plots of mean velocities of anterogradely- (A) and retrogradely-transported (B) small vesicles versus temperature.

A: The open circles represent the mean velocities obtained from nerves acclimated at a desired temperature for a maximum of 30 minutes. The relationship of these mean velocities with temperature is described by the broken line. The red circles represent mean vesicle velocities from nerves cooled for 14-20 hours in the absence of the press and MPC; green triangles represent those velocities from nerves cooled for 14-20 hours in the presence of the press and MPC. The mean vesicle velocities designated by the coloured data points (green and red) were not statistically different ($p>0.05$). The transport of organelles after 14 hours cooling occurred at slightly lower velocities than after a 30 minute acclimation, but the main point is that no sudden drop in vesicle velocity occurred at around the critical temperature at which protein transport drops.

B: The representation of open circles and coloured data points is similar to above. Similar observations as above can be made concerning the mean velocity of retrogradely-transported vesicles.

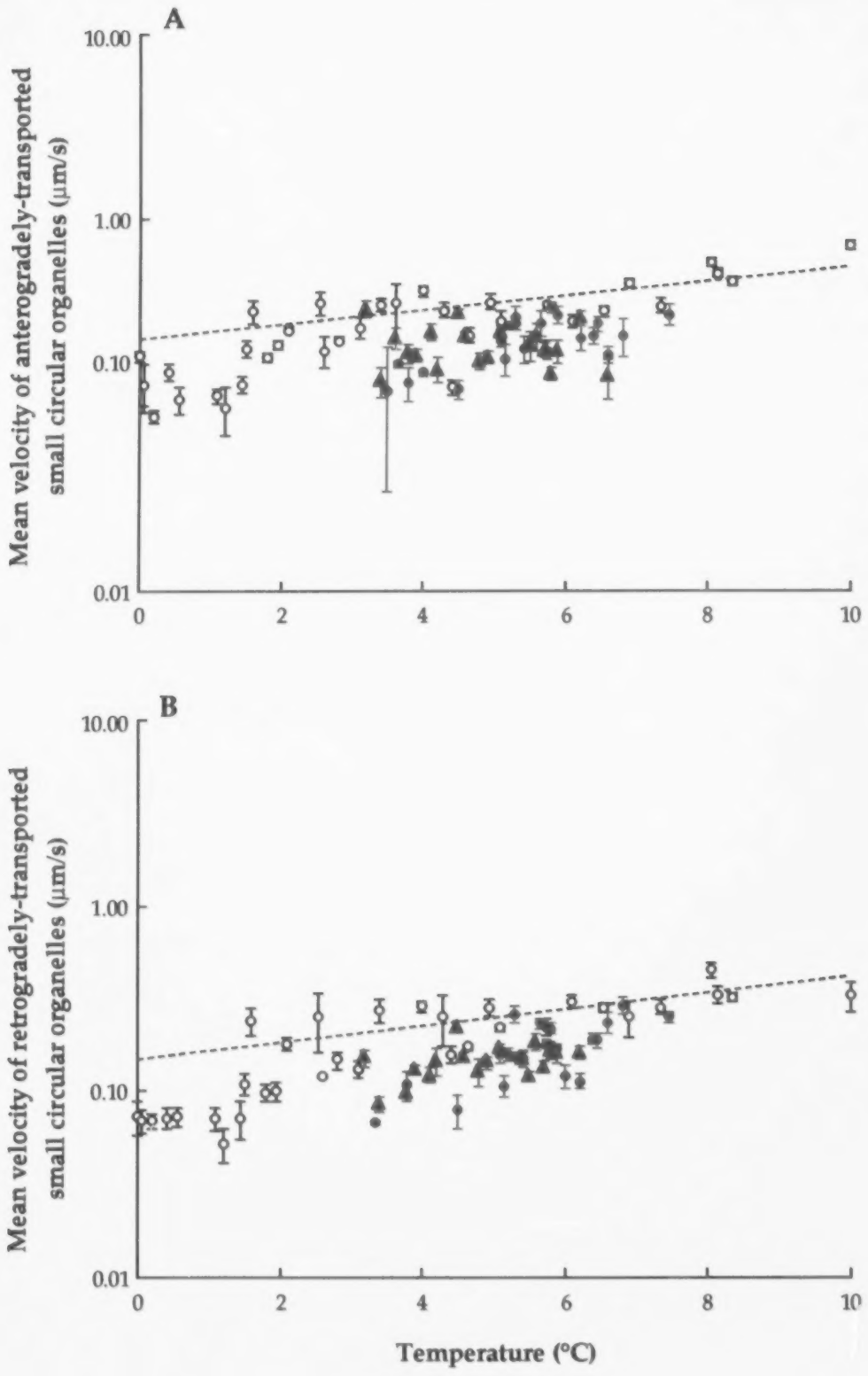
A
10.00
1.00
0.10
0.01
Mean velocity of anterogradely-transported small circular organelles (μm/s)
0
2
4
6
8
10
B
10.00
1.00
0.10
0.01
Mean velocity of retrogradely-transported small circular organelles (μm/s)
0
2
4
6
8
10
Temperature (°C)

16-20 hour cooling period. Taxol has been shown to prevent the cold depolymerization of microtubules in *Xenopus* axons (Smith and Snyder, 1995). Vesicle velocity in both the anterograde and retrograde directions was similar in taxol-treated and -untreated axons (Figure 4.6), indicating that the number of microtubules does not affect the velocity of vesicles.

4. 3 Summary

Anterograde and retrograde organelle transport was detected by video microscopy at temperatures down to 0°C. With the exception of large rod-shaped organelles, the velocities of anterogradely and retrogradely transported organelles increased with increasing temperature in an approximately exponential manner. Deviations from the exponential relationship occurred below approximately 5°C and above approximately 30°C. For anterogradely-moving SC vesicles, there was no statistically significant difference in vesicle traffic above and below 6.5°C. Any reduction in the vesicle traffic below 6.5°C was less than 15%. This indicates that the sudden drop in protein transport rate at 6.5°C is not due to a loss of vesicles. Comparison of Q_{10} and E_a values over 6.5-25°C revealed that anterogradely-moving SC, LC, and SR organelles had lower Q_{10} and E_a values than their retrogradely-moving counterparts.

Unlike the transport of radiolabelled proteins, the transport of organelles under the two conditions (Methods 1 and 2) was not statistically different. It did appear that the transport of SC vesicles in 14-hour cooled nerves was slower than in nerves cooled for no longer than 2 hours, but unlike protein transport, no sudden drop in vesicle transport occurred at around 5-10°C in either 2-hour or 14-hour cooled nerves. Prevention of cold depolymerization by taxol did not change the observed drop in vesicle velocity, indicating that the number of microtubules does not affect the velocity of vesicles.

Figure 4. 6.

Semilog plot of mean velocities of anterogradely-and retrogradely-moving vesicles in taxol-untreated and -treated nerves at different temperatures.

A: The solid circles represent mean velocities of anterogradely-moving vesicles in nerves cooled for no greater than 2 hours. The relationship of these velocities and temperature is described by the solid line over 5°-30°C. The open squares represent mean anterograde velocities in nerves bathed in oxygenated physiological saline containing 10 μmol/L taxol at room temperature before cooling the saline for 16-20 hours. Note that despite the length of the cooling period, the mean vesicle velocity is similar in both taxol-untreated and -treated nerves.

B: The solid squares represent mean velocities of retrogradely-moving vesicles in nerves cooled for no greater than 2 hours. The relationship of these velocities and temperature is described by the solid line over 5°-30°C. The open triangles represent mean retrograde velocities in nerves incubated in taxol for 1 hour at room temperature before cooling fo 16-20 hours. The mean retrograde velocity is similar in both taxol-untreated and -treated nerves.

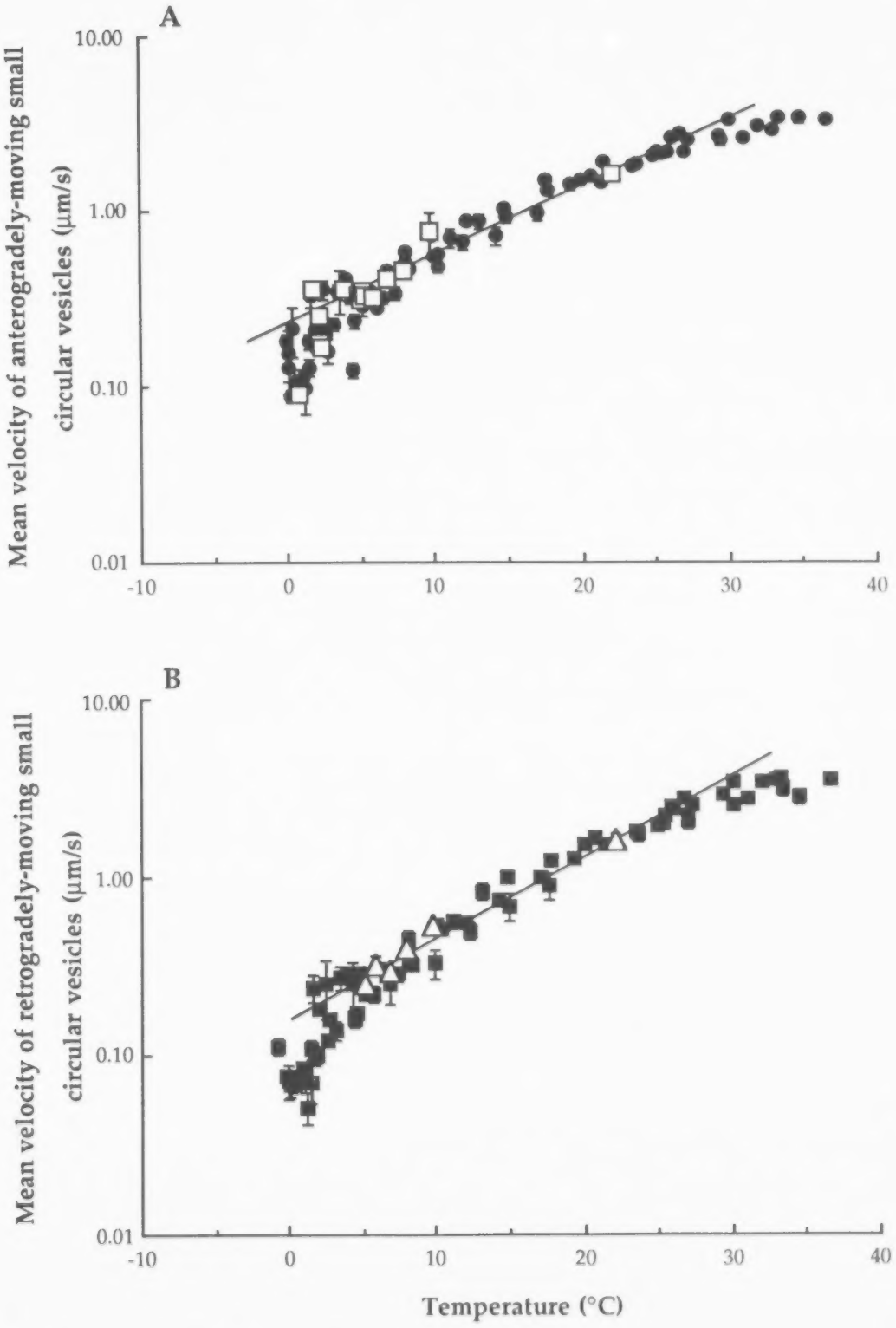
A
Mean velocity of anterogradely-moving small circular vesicles (μm/s)
10.00
1.00
0.10
0.01
-10
0
10
20
30
40
B
Mean velocity of retrogradely-moving small circular vesicles (μm/s)
10.00
1.00
0.10
0.01
-10
0
10
20
30
40
Temperature (°C)

5 DISCUSSION

5. 0 Main findings

In this work, the temperature dependence of the fast anterograde transport of newly synthesized proteins and their carrier vesicles was studied in axons from the sciatic nerve of *Xenopus laevis*. The objectives were to confirm the presence of the reported discontinuity in the velocity-temperature relationship of rapidly anterogradely-transported proteins, and then to test whether this discontinuity was caused by either a loss of proteins to a non-transportable, stationary phase or a loss of both organelles and their cargo of proteins. The results show that an approximately exponential relationship exists between the velocity of protein transport and temperature and that a sudden drop in this relationship occurs at about 6.5°C. Below this low critical temperature, protein transport ceases. These findings are in agreement with previous studies (Edström and Hanson, 1973; Ochs and Smith, 1975; Cosens *et al.*, 1976; Brimijoin *et al.*, 1979) as shown in Figure 5.1A. However, the sudden drop at around 5-10°C that was observed in the results of Method 1 and previous studies was not observed in the results of Method 2 (Figure 5.1B), a discrepancy which will be discussed later. It was also shown that upon rewarming from all low temperatures, the migration of most newly synthesized proteins resumes at about the same, or slightly lower, velocity as before cooling and leaves behind a trail of proteins to a stationary phase. These findings were also observed in previous studies (Edström and Hanson, 1973; Brimijoin, 1975; Ochs and Smith, 1975; Cosens *et al.*, 1976; Hanson, 1978; Hanson, 1979; Snyder *et al.*, 1990) and indicate that newly synthesized proteins are not entirely off-loaded to a non-transportable, stationary phase.

Figure 5. 1.

Comparison of protein transport rates observed in this work with those of previous studies.

A: Anterograde protein transport rates from Method 1 analysis and previous studies were plotted on a logarithmic scale against temperature. Note that in all studies the velocity of protein transport is exponentially related to temperature. There is a sudden drop in this relationship at around 5-10°C (depending upon the animal).

- ■ DBH transport rate in rabbit taken from Cosens *et al.* (1976)
- • Protein transport rate in bullfrog derived from Edstrom & Hanson (1973)
- △ Protein transport rate in cat taken from Ochs & Smith (1975)
- ■ Protein transport rate in *X. laevis*

B: Anterograde protein transport vs. temperature. The solid blue squares and exponential curve represent the protein transport rate derived from Method 1 analysis and its relationship to temperature. This shows that unlike the results from Method 1 analysis and previous studies, a sudden drop did not occur in the results of Method 2 (open circles) at the critical temperature of around 5-10°C.

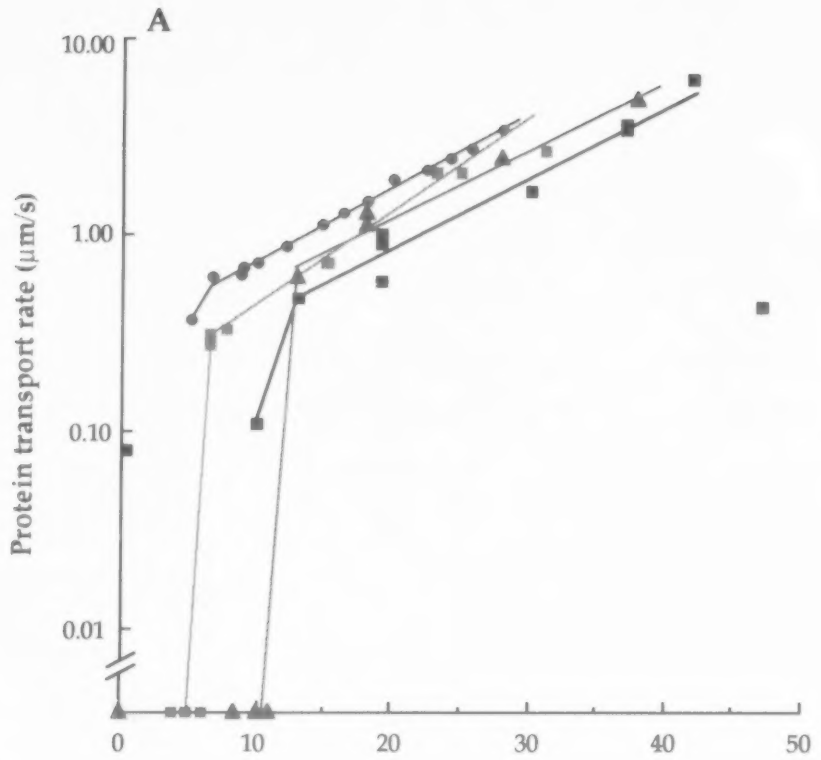
A
10.00
1.00
0.10
0.01
Protein transport rate (μm/s)
0
10
20
30
40
50

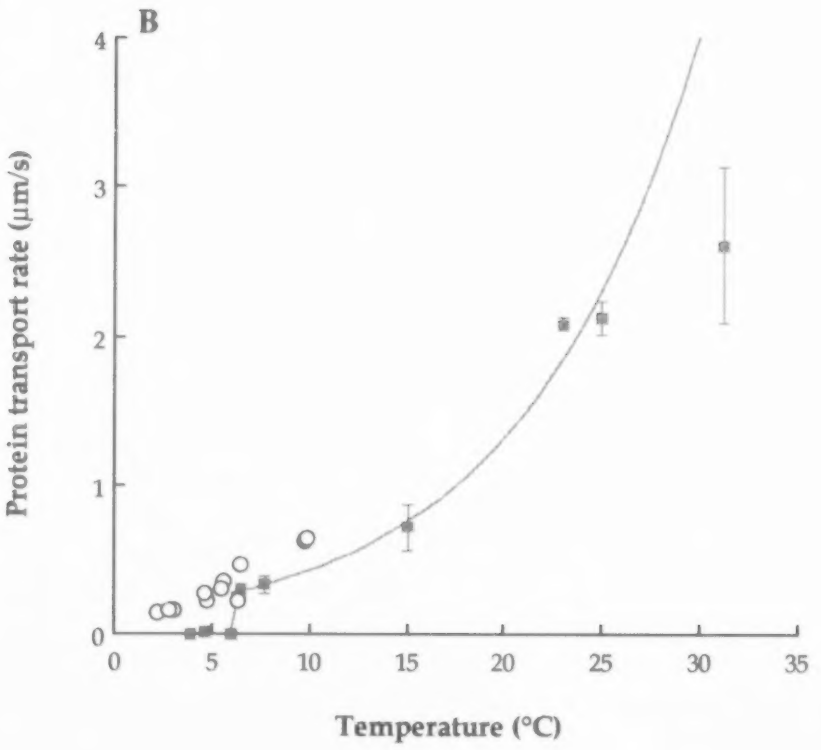
B
4
3
2
1
0
Protein transport rate (μm/s)
0
5
10
15
20
25
30
35
Temperature (°C)

This work suggests that subresolution vesicles with small, circular images (SC vesicles) are most likely the carriers of newly synthesized proteins despite the difference in temporal and spatial scales of measuring protein and vesicle transport velocities. The results show that the velocity of SC vesicle transport is exponentially related to temperature over a range of 5-30°C and smoothly drops below and above these temperatures. Over the range of 6.5-25°C, the velocity of protein transport (Method 1) closely matches the mean velocity of SC vesicle transport, suggesting that proteins are associated with their carrier vesicles. However, the significant difference in this close protein-vesicle velocity-temperature relationship is at about 6.5°C. The results of this work show that below 6.5°C, the protein transport rate rapidly drops to zero while vesicles continue to move to 0°C, indicating that the discontinuity, both reported and confirmed here, is not caused by a cessation of anterograde vesicle transport at 6.5°C. This is supported by the observation that there was no statistically significant difference in the SC vesicle traffic below and above 6.5°C. If there was a difference, it was less than 15%, indicating that the sudden drop in protein transport rate is not due to a loss of carrier vesicles. Analysis of deposition rates (Method 1) shows that the drop in protein transport at the low critical temperature of 6.5°C coincides with an increase in the amount of protein off-loaded by the migrating wave of radiolabelled proteins (Figure 5.2A). SC vesicles, however, continue to move (Figure 5.2B). Thus, these results support the second model that a loose association exists between newly synthesized proteins and their carrier vesicles such that around the critical temperature newly synthesized proteins are lost from their moving carrier vesicles, and upon rewarming reassociate with other moving vesicles.

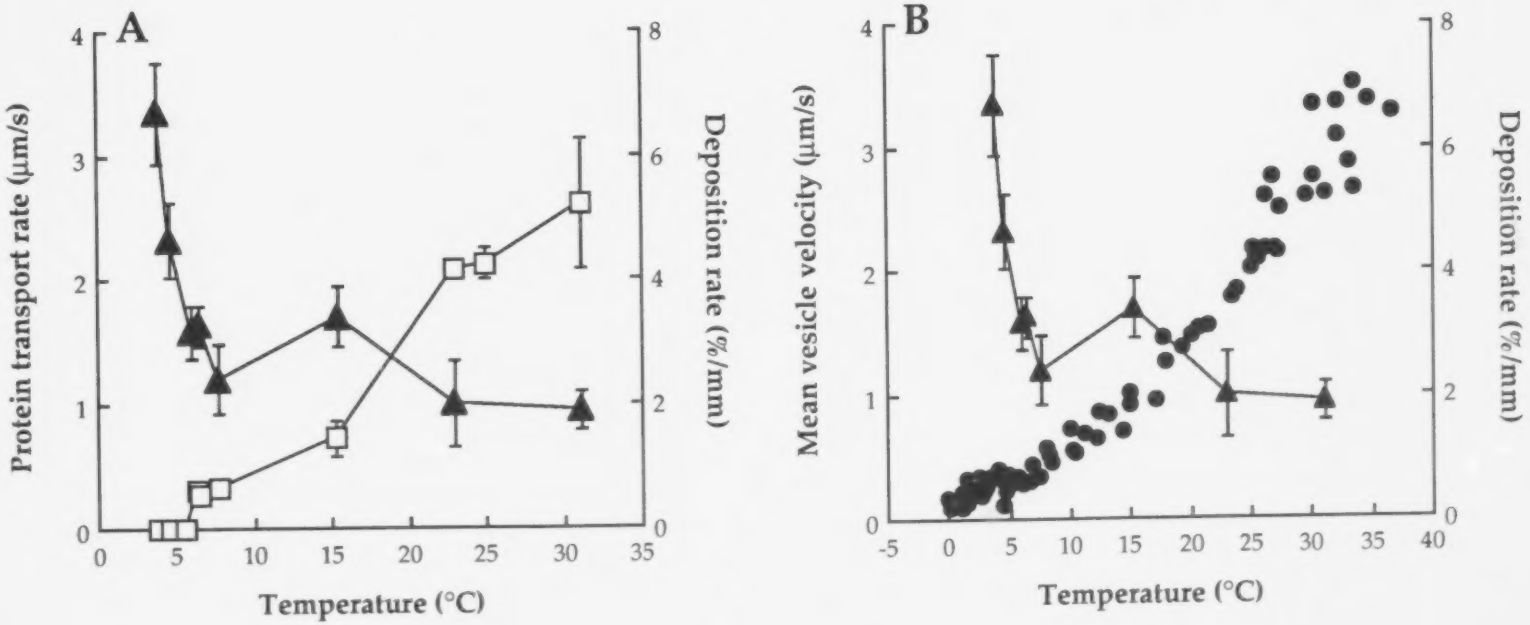

Figure 5. 2. Anterograde protein and vesicle transport at different temperatures in relation to the deposition of protein to a stationary state. **A:** Protein transport and deposition rates vs. temperature. The error bar of each point indicates ± 1 SEM. Note that at the critical temperature of approximately 6.5°C when protein transport from Method 1 analysis (open squares) drops, the amount of protein deposited by the migrating wave of radiolabelled proteins (solid triangles) increases, reaching 7%/mm at around 2-3°C. **B:** Mean vesicle velocity and protein deposition rate vs. temperature. This shows that vesicles (velocities represented by solid circles) continue to move despite the loss of their cargo (solid triangles).

5. 1 Protein transport

As stated in the account above, the approximately exponential relationship between the velocity of protein transport and temperature is seen both in the results of Method 1 and in previous studies (Edström and Hanson, 1973; Ochs and Smith, 1975; Cosens *et al.*, 1976; Brimijoin *et al.*, 1979). However, in contrast to the reported 2%/mm (Edström and Hanson, 1973; Gross and Beidler, 1975; Muñoz-Martínez, 1982; Snyder *et al.*, 1990), the proportion of radiolabelled proteins off-loaded to a stationary phase in this work was 4.8%/mm at room temperature. This proportion may represent proteins and glycoproteins that are deposited to renew membrane components undergoing turnover, while the remainder is destined for the nerve terminals. It is also possible that the amount of protein off-loaded may depend upon the physiological state of the axon (Snyder *et al.*, 1990; Smith and Snyder, 1991). Unlike the work conducted by Snyder and his colleagues (1990), the work here involved nerves that were warmed, cooled, and rewarmed for a considerable length of time. Some of the radiolabelled proteins may have been relocated and redistributed after warm-up. This explanation may be supported by the fact that in double-ligation studies, deposited radiolabelled material is capable of undergoing further transport and relocation, resulting in an increase in the amount of label deposited to the stationary phase between the two ligations (Ochs, 1975).

The low critical temperature at which the velocity of protein transport drops appears to be species-specific. This temperature ranges from 4°C in mollusc (Heslop and Howes, 1972) to 10-13°C in bullfrog (Brimijoin *et al.*, 1979), cat (Ochs and Smith, 1975; Cosens *et al.*, 1976), and rabbit (Brimijoin *et al.*, 1979) sciatic nerves. In Edström and Hanson's work (1973) on frog (*R. temporaria*) and here in toad (*X. laevis*), the sudden drop occurs at about 6.5°C. Muñoz-Martínez

(1982) suggested that the sudden drop in protein velocity at low temperatures is related to an increase in the amount of material that is deposited from the rapidly moving phase to a stationary phase. Indeed, the analysis of deposition rates (Method 1) in this work appears to support such a suggestion. The amount of radiolabelled material deposited by the pulse after rewarming was nonlinearly related to temperature. Particularly, at the critical temperature when the velocity of protein transport dropped, the amount of material deposited by the migrating wave upon rewarming increased, reaching 7%/mm at 2°C. This implies that the lower the temperature, the more protein is off-loaded to a stationary phase; this off-loading is then observed as a reduction in the velocity of protein transport. So, it appears that low temperatures reduce the velocity of protein transport and this reduction may be associated with increased protein deposition, particularly at the critical temperature. However, the question is in what form is this deposition occurring? Are proteins lost from their carrier vesicles at this critical temperature or are protein-vesicle complexes lost from the rapidly moving phase?

5. 2 Organelle transport

The temperature dependence of fast anterograde and retrograde organelle transport was examined since they have not been compared previously in the same axons. Two main groups of optically detectable organelles have been identified previously: round or elliptical and rod-shaped (Cooper and Smith, 1974; Hammond and Smith, 1977; Allen *et al.*, 1981; Brady *et al.*, 1982; Forman *et al.*, 1983; Forman *et al.*, 1984). In this work, organelles were classified on the basis of their direction of transport and their apparent size. With the exception of large rod-shaped organelles, the finding that the transport velocities of most organelles are exponentially related to temperature in both the anterograde and

retrograde directions is not entirely unexpected (See Section 1.1.2). In particular, anterogradely-moving organelles moved faster than their retrogradely-moving counterparts. These findings are in agreement with work done in extruded squid axoplasm (Brady *et al.*, 1982; Gilbert and Sloboda, 1984; Fahim *et al.*, 1985; Vale *et al.*, 1985c) and in bullfrog and toad sciatic nerve (Cooper and Smith, 1974; Forman *et al.*, 1977b; Smith and Snyder, 1991). This observation appears to be reflected in the Q_{10} and E_a values (Table 4.2). Anterogradely-moving SC, LC, and SR organelles, on the whole, had lower Q_{10} and E_a values over 6.5-25°C than their retrogradely-moving counterparts. The high E_a values calculated for retrogradely-moving organelles indicate that the process of retrograde transport is more sensitive to temperature than anterogradely-moving organelles. Thus, anterograde and retrograde transport motors can not only be identified pharmacologically as observed by Forman and his colleagues (1983) and Smith and Forman (1988), but also on the basis of their temperature-dependent properties.

The results of this work also show that in both directions, small organelles move faster than large organelles, supporting the results of Forman *et al.* (1977a) and Okabe and Hirokawa (1989). The difference in velocity between small and large organelles may be explained by understanding the forces acting on an organelle. A more detailed description is given by Smith (1991). Briefly, the motion of an organelle is described by $F_c = bv$, where F_c is the chemical driving force, v is the velocity of the organelle, and b is the viscous drag coefficient. The viscous drag coefficient depends upon the geometry of the organelle and the viscosity of the axoplasm. If F_c remains constant, then to compensate for the increase in organelle size, the velocity of the organelle must decrease. Hence, small vesicles move faster than large organelles at all temperatures observed in this work.

In this work deviations in the exponential relationship were not observed as reported by Forman *et al.* (1977b) and Smith and Cooper (1981). These investigators reported that above 36°C the transport of mainly retrogradely-moving organelles ceased. Transport of microscopically visible anterogradely-moving organelles ceased at 37.3°C (Smith and Cooper, 1981). The velocity of organelle transport in either direction was not measured below 5°C. In contrast, this work shows that vesicle transport continued to drop smoothly to 0°C or less, and above 30°C the velocity of SC and LC vesicle transport reached a plateau. The discrepancy between this work and previous findings may, in part, be explained by the development of optical and digital processing techniques which are now capable of detecting subresolution structures (Smith, 1989). Greater than 90% of anterogradely-moving organelles and 63% of retrogradely-moving organelles consist of the small vesicles (50-100 nm in diameter) (Smith and Snyder, 1991). This population of organelles may not have been detected by the optical techniques used by Forman *et al.* (1977b) and Smith and Cooper (1981) and thus may not have been reflected in their observed velocity-temperature relationship.

It is reported that the speeds of rod-shaped organelles, assumed to be mostly mitochondria (Kirkpatrick *et al.*, 1972; Cooper and Smith, 1974), increase at higher temperatures (Forman *et al.*, 1977b), but the exact relationship between the velocity of these organelles and temperature has not been extensively studied. This work shows that the mean velocity of small, rod-shaped (SR) organelles increased exponentially with temperature over a range of 10°-30°C in both anterograde and retrograde directions, but LR (large, rod-shaped) organelles follow this trend poorly. Nevertheless, rod-shaped organelles of either size were not observed to move below 10°C, indicating that they are not likely responsible for carrying newly synthesized proteins. Ochs (1983) has

observed mitochondria to be more sensitive to changes in ATP level. It is therefore possible that the cessation of SR and LR organelle transport at 10°C (higher than other vesicles) may be due to the rate of ATP utilization.

5. 3 Possible mechanisms of organelle and protein transport

The existing evidence and this work imply that under most conditions newly synthesized proteins are carried by small, anterogradely-moving vesicles. It then follows that the transport of these proteins and vesicles (as well as other organelles) may be guided by similar driving mechanisms. Vesicle and protein anterograde transport require microtubules and the microtubule-based, ATP-driven transport motor, kinesin (Smith, 1971; Gilbert and Sloboda, 1984; Fahim *et al.*, 1985; Miller and Lasek, 1985; Smith, 1991). In that case, the relationship between the velocity of vesicle and protein transport and temperature observed from this work may have resulted from an alteration in microtubule structural integrity and/or from the availability and utilization of ATP. The sudden drop in protein transport at 6.5°C, however, would seem to suggest that an additional factor is affecting the association between newly synthesized proteins and their carrier vesicles.

Microtubule depolymerization induced by antimitotic drugs, such as colchicine and vinblastine, reduces or inhibits organelle movement (Chang, 1972; Hammond and Smith, 1977; Forman, 1982; Kendal *et al.*, 1983; Smith and Kendal, 1985) and protein transport (Edström and Mattsson, 1972; Heslop and Howes, 1972; Hanson and Edström, 1977; Dahlström *et al.*, 1982; Forman, 1982). Lowering temperature also induces microtubule depolymerization (Gaskin *et al.*, 1975; Brimijoin *et al.*, 1979; Alvarez and Fadic, 1992; Smith and Snyder, 1995), especially at around 4°C, which completely depolymerizes cold-labile microtubules, resulting in a reduction in both the length and number of

microtubules (Sahenk and Brady, 1987). Since microtubule disassembly by antimitotic drugs and low temperatures results in a shortening and then a loss of intact microtubules, and microtubules are required to stimulate the action of the ATP-driven motors and act as transport tracks, it may be inferred that the action of the transport motors depends upon the length and number of microtubules present. The results from the taxol experiments in this work indicate that the number of microtubules does not affect the vesicle velocity. From this, it can be inferred that the velocity of protein transport would also not be affected by the number of microtubules. Furthermore, Brimijoin *et al.* (1979) noted no correspondence between the relationship of protein transport and temperature and of microtubules and temperature. Nevertheless, the observation of sustained organelle velocities below 4°C may be explained by the presence of cold-stable microtubules which are known to exist in a small pool, but whose physiological significance is not known (Black *et al.*, 1984; Brady *et al.*, 1984; Sahenk and Brady, 1987).

The reduced transport velocities may be due to the availability and utilization of ATP. Organelle movement involves a two-step process: the utilization of ATP and the conversion of chemical to mechanical energy. Transport motors require ATP to allow the vesicle-motor complexes to associate with microtubules; hydrolysis of ATP facilitates the energy required by the motors to generate movement along microtubules (Adams, 1982; Lasek and Brady, 1985; Miller and Lasek, 1985). Lasek and Brady (1985) demonstrated that the non-hydrolyzable analogue of ATP, AMP-PNP, competes with ATP for the critical ATP binding site of kinesin, thus preventing translocation, but not binding to microtubules. A decline in ATP levels leads to a decline in organelle movement (Adams, 1982; Forman *et al.*, 1984; Smith and Forman, 1988). It is possible that lowering temperatures would reduce the level of ATP and energy-

rich creatine phosphate (~P) available for translocation. However, these levels remain unchanged at low temperatures, even after a 64-hour cooling period (Ochs, 1971; Ochs and Hollingsworth, 1971; Ochs and Smith, 1975).

Varying the experimental conditions to which the nerve was subjected could explain the difference in behaviour of protein and vesicle transport below 6.5°C. Mean vesicle velocities were determined from nerves cooled for no longer than 2 hours whereas protein transport rates were derived from nerves cooled for about 14 hours. Could the temperature sensitivity of vesicle transport behave similarly to that of protein transport after a 14-hour cooling interval? Nerves were prepared according to the two methodological approaches, but then video recorded to examine the effect of prolonged cooling on organelle velocities. Over 2-10°C no sudden drop in mean vesicle velocity was observed in either nerves cooled for 2 hours or nerves cooled for 14 hours with or without being under the press. Thus, it may be that the critical temperature of 6.5°C alters the association between newly synthesized proteins and their carrier vesicles, as indicated by the deposition rates, the vesicle numbers, and possibly the Q_{10} and E_a values, but does not alter temporarily deposited proteins in such a way that they cannot be reassociated with other moving vesicles. Levine and Willard (1980) noted that two polypeptides associate with two groups of organelles, but travel at different velocities, indicating that interactions of these polypeptides with other transported proteins in that group of organelles and/or with the lipid molecules of the organelles themselves may imply different velocity rates. In their study of the effects of leupeptin upon reversal of transport, Smith and Snyder (1991) suggested that axonally transported proteins undergo an anterograde-to-retrograde conversion via a protein phosphorylation/ dephosphorylation process. So, it may be that the critical temperature, besides affecting the velocity of protein and vesicle transport, also affects the interaction between the proteins

and their carrier vesicles. Since the identity of many rapidly transported polypeptides has not yet been determined, it would be very interesting to investigate this possibility.

5. 4 Difference in results obtained from Methods 1 and 2

The relationship between protein transport velocity and temperature was approximately exponential in both the results from the two different methodologies (Methods 1 and 2). The main difference, however, was the sudden discontinuity at 6.5°C observed using Method 1 (Figure 5.3). Since these results are in agreement with previous studies, the question was raised as to what factors may have caused this internal discrepancy. The difference may have involved a higher percentage of radiolabelled protein being deposited during the cooling period in Method 1 than in Method 2, implying that perhaps the nerves in Method 1 were exposed to cold temperatures more than those in Method 2. However, no statistically significant difference in deposition rates at 6°C, 10°C, and 23°C was observed. Analysis of liquid scintillation counting, however, did show that the rate of deposition was affected by the nerve exposure time to low temperatures and by a 2-5°C cooling.

Temperature differences along the length of the nerve may account for the observed discrepancies. In Method 2 experiments the nerves remained on the MPC for a considerable length of time at a desired cooled temperature in comparison to those in Method 1 experiments. Despite the recorded cooling temperatures at the proximal and distal ends of the nerve, the temperature along the length of the nerve may been have sufficiently "warm" to allow for continued protein transport below 6°C. However, no statistically significant differences in temperature were recorded.

It has been shown that the manner in which a receptor-ligand complex is

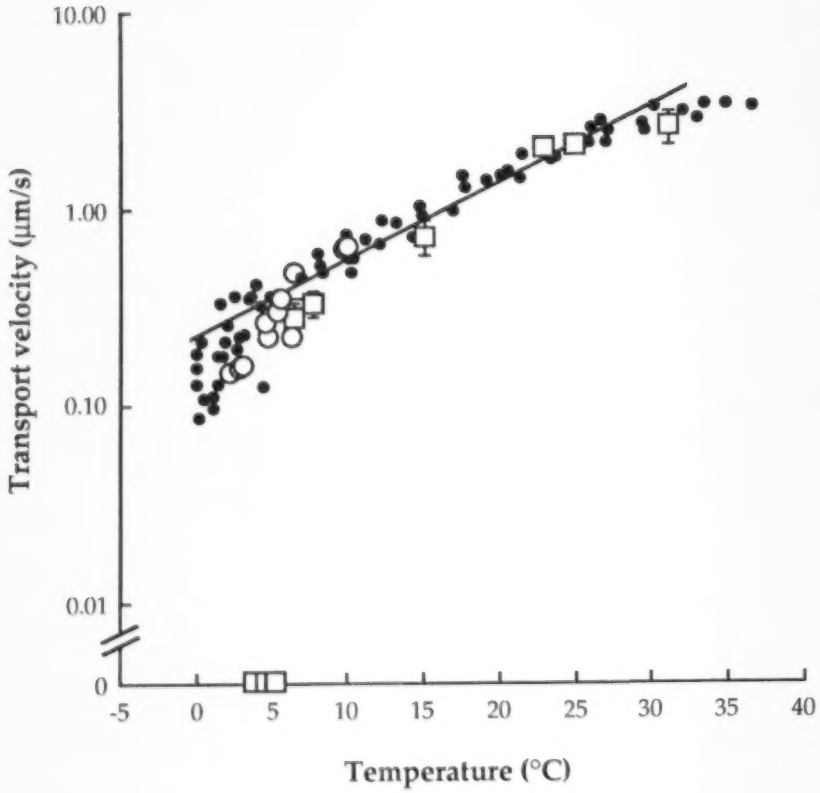

Figure 5. 3. Semilog plot of anterograde protein and vesicle transport as a function of temperature. The open squares and circles represent protein transport rates observed in Methods 1 and 2, respectively. The solid circles and line represent mean vesicle velocities and their relationship to temperature. The velocity of protein transport closely matched the mean velocity of SC vesicles over a range of 6.5-25°C. Below 6.5°C, however, the protein transport rate in Method 1 rapidly dropped to zero while vesicle transport and the protein transport rate in Method 2 continued to drop smoothly to 0°C.

formed depends upon pH (Nilsson and Warren, 1994). For instance, early in the endocytic and lysosomal pathways a low pH of 6.2 is required for the dissociation and separation of a receptor-ligand complex. This dissociation and separation could be prevented with an increase in pH (Griffiths and Simons, 1986; Parton and Dotti, 1993). In these experiments, a gaseous mixture of argon/carbon dioxide was flushed through the detector. As mentioned, the nerves in Method 2 experiments were in contact with the thin mylar of the MPC for a considerable length of time. With the mylar being very thin, carbon dioxide gas may have diffused into the physiological saline and the axoplasm of the sciatic nerve itself, shifting the pH. Hence, it was thought that a pH shift in may affect the charge of the newly synthesized proteins such that their ability to be rapidly transported is optimized, even at low temperatures. Alternatively, protein interaction with their carrier vesicles could be stabilized so that proteins could continue to be transported at low temperatures. The pH of the saline solution at the beginning and at the end of the experiment was recorded, but no significant variation was noted. Thus, the carbon dioxide may have altered the microenvironment of the nerve itself. It would be interesting to test whether altering the pH of the saline to one or 2 pH units or changing the gas mixture would affect protein transport. No statistically significant difference was noted between mean organelle velocities of nerves cooled for 2 hours and those treated similarly to those prepared for protein transport. This indicates that, unlike the transport of vesicles, the transport of radiolabelled proteins was somehow affected by the presence of the press and the MPC.

A series of experiments was performed to mimic both approaches simultaneously. No migration or redistribution of radioactivity was seen in nerves cooled in the absence of the MPC, but with the press and MPC present, some movement of protein transport was seen in the pressed region of the nerve

and not in the free mid-region. This suggested that the press alone was not responsible for the reduced protein transport observed below 6.5°C in Method 2. It must be assumed that the combined presence of the press and the MPC affected the results seen in Method 2 by some unknown means. Nevertheless, as already described, it is possible that the release of recently synthesized protein from vesicles may be regulated by local cellular conditions (Ochs, 1971; Snyder *et al.*, 1990). If the results of Method 2 were not artifactual, then there must be some component not yet determined, possibly pH-sensitive, that protects the protein-vesicle association because similar velocities of protein and vesicle transport are observed below the critical temperature.

5. 5 General conclusion

This work provides evidence to support the second model, namely that a loose association exists between newly synthesized proteins and their carrier vesicles so that under certain circumstances these proteins may be lost from the vesicles. In this work, to further understand this association, the temperature dependence of both fast anterograde protein and vesicle transport was studied in axons of the amphibian sciatic nerve. The velocity of both protein (Method 1 analysis) and vesicle transport was exponentially related to temperature, but below 6.5°C protein transport rapidly dropped to zero. Vesicle transport continued to 0°C. This drop in protein transport appeared to be caused by an increase in the off-loading of proteins from their rapidly moving phase to a stationary phase. This is supported by the observation that no statistically significant difference in vesicle traffic was observed above and below 6.5°C, indicating that newly synthesized proteins must be lost from their carrier vesicles. Upon rewarming from low temperatures, the fast anterograde transport of proteins and vesicles resumed at about the same, or slightly lower, velocity as

before cooling. In addition, the off-loading of a portion of radiolabelled proteins from the migrating wave also resumed at the same rate as before cooling. These findings suggest that in line with the second model, proteins are capable of reassociating with other moving vesicles.

In addition, two experimental approaches, one of which was adopted to verify the results of the first approach (Method 2), were used to examine the temperature dependence of fast anterograde protein transport. The result that the sudden drop observed in Method 1 and previous studies did not occur in Method 2 led to the design of a series of experiments to mimic both approaches simultaneously. Since temperature differences and solution pH could not account for the observed discrepancy between the two experimental approaches, it is possible that the MPC somehow permitted protein transport to continue to 2°C.

REFERENCES

Abe, T., Haga, T., and Kurokawa, M. 1973. Rapid transport of phosphatidylcholine occurring simultaneously with protein transport in the frog sciatic nerve. *Biochem. J.* **136**: 731-740.

Adams, R. J. 1982. Organelle movement in axons depends on ATP. *Nature* **297**: 327-329.

Allen, R. D., Allen, N. S., and Travis, J. L. 1981. Video-enhanced contrast, differential interference contrast (AVEC-DIC) microscopy: A new method capable of analyzing microtubule-related motility in the reticulopodial network of *Allogromia laticollaris*. *Cell Motil.* **1**: 291-302.

Alvarez, J., and Fadic, R. 1992. Assembly and disassembly of axonal microtubules of the toad *Xenopus laevis* under the effect of temperature. *J. Exp. Zool.* **264**: 261-266.

Ambron, R. T., Schmied, R., Huang, C.-C., and Smedman, M. 1992. A signal sequence mediates the retrograde transport of proteins from the axon periphery to the cell body and then into the nucleus. *J. Neurosci.* **12**: 2813-2818.

Bauerfeind, R., and Huttner, W. B. 1993. Biogenesis of constitutive secretory vesicles, secretory granules and synaptic vesicles. *Curr. Op. Cell Biol.* **5**: 628-635.

Bennett, G., Giamberardino, L. D., Koenig, H. L., and Bernard, D. 1973. Axonal migration of protein and glycoprotein to nerve endings. II. Radioautographic analysis of the renewal of glycoproteins in nerve endings of chicken ciliary ganglion after intracerebral injection of [^{3}H] fucose and [^{3}H]glucosamine. *Brain Res.* **60**: 129-146.

Bisby, M. A. 1985. Retrograde axonal transport of phospholipid in rat sciatic nerve. *J. Neurochem.* **45**: 1941-1947.

Black, M. M., Cochran, J. M., and Kurdyla, J. T. 1984. Solubility properties of neuronal tubulin: Evidence for labile and stable microtubules. *Brain Res.* **295**: 255-263.

Brady, S. T., Lasek, R. J., and Allen, R. D. 1982. Fast axonal transport in extruded axoplasm from squid giant axon. *Science* **218**: 1129-1131.

Brady, S. T., Tytell, M., and Lasek, R. J. 1984. Axonal tubulin and microtubules: Biochemical evidence for cold stability. *J. Cell Biol.* **99**: 1716-1724.

Brimijoin, S. 1975. Stop-flow: A new technique for measuring axonal transport, and its application to the transport of dopamine-β-hydroxylase. J. *Neurobiol.* **6**: 379-394.

Brimijoin, S. 1981. Transport of defined endogenous molecules. *Neurosci. Res. Prog. Bull.* **20**: 31-39.

Brimijoin, S., and Helland, L. 1976. Rapid retrograde transport of dopamine-β-hydroxylase as examined by the stop-flow technique. *Brain Res.* **102**: 217-228.

Brimijoin, S., Olsen, J., and Rosenson, R. 1979. Comparison of the temperature-dependence of rapid axonal transport and microtubules in nerves of the rabbit and bullfrog. *J. Physiol.* **287**: 303-314.

Brimijoin, S., Skau, K., and Weirmaa, M. J. 1978. On the origin and fate of external acetylcholinesterase in peripheral nerve. *J. Physiol.* **285**: 143-158.

Chan, S. Y., Ochs, S., and Worth, R. M. 1980. The requirement for calcium ions and the effects of ions on axoplasmic transport in mammalian nerve. *J. Physiol.* **301**: 477-504.

Chang, C- M. 1972. Effect of colchicine and cytochalasin B on axonal particle movement and outgrowth *in vitro*. *J. Cell Biol.* **55**: 37a.

Cleveland, W. S. 1985. The elements of graphing data. Wadsworth Advanced Books and Software, Monterey, California, 170-178.

Cooper, P. D., and Smith, R. S. 1974. The movement of optically detectable organelles in myelinated axons of *Xenopus laevis*. *J. Physiol.* **242**: 77-97.

Cosens, B., Thacker, D., and Brimijoin, S. 1976. Temperature dependence of rapid axonal transport in sympathetic nerves of the rabbit. *J. Neurobiol.* 7: 339-354.

Dahlström, A., Bööj, S., and Larsson, P-A. 1982. Axonal transport of enzymes and transmitter organelles in cholinergic neurons. IN *Axoplasmic Transport*. (ed. D. G. Weiss) Springer-Verlag, Berlin, 131-138.

Droz, B., Koenig, H. L. and Giamberardino, L. D. 1973. Axonal migration of protein and glycoprotein to nerve endings. I. Radioautographic analysis of the renewal of protein in nerve endings of chicken ciliary ganglion after intracerebral injection of [^{3}H] lysine. *Brain Res.* **60**: 93-127.

Edström, A., and Hanson, M. 1973. Temperature effects on fast axonal transport of proteins *in vitro* in frog sciatic nerves. *Brain Res.* **58**: 345-354.

Edström, A., and Mattsson, H. 1972. Fast axonal transport *in vitro* in the sciatic system of the frog. *J. Neurochem.* **19**: 205-221.

Elam, J. S., and Agranoff, B. W. 1971. Rapid transport of protein in the optic system of the goldfish. *J. Neurochem.* **18**: 375-387.

Fahim, M. A., Lasek, R. J., Brady, S. T., and Hodge, A. J. 1985. AVEC-DIC and electron microscopic analyses of axonally transported particles in cold-blocked squid giant axons. *J. Neurocytol.* **14**: 689-704.

Forman, D. S. 1982. Saltatory organelle movement and the mechanism of fast axonal transport. IN *Axoplasmic Transport*. (ed. D. G. Weiss) Springer-Verlag, Berlin, 234-240.

Forman, D. S., Brown, K. J., and Livengood, D. R. 1983. Fast axonal transport in permeabilized lobster giant axons is inhibited by vanadate. *J. Neurosci.* **3**: 1279-1288.

Forman, D. S., Brown, K. J., Promersberger, M. W., and Adelman, M. R. 1984. Nucleotide specificity for reactivation of organelle movements in permeablized axons. *Cell Motil.* **4**: 121-128.

Forman, D. S., Padjen, A. L., and Siggins, G. R. 1977a. Axonal transport of organelles visualized by light microscopy: Cinemicrographic and computer analysis. *Brain Res.* **136**: 197-213.

Forman, D. S., Padjen, A. L., and Siggins, G. R. 1977b. Effect of temperature on the rapid retrograde transport of microscopically visible intra-axonal organelles. *Brain Res.* **136**: 215-226.

Gaskin, F., Cantor, C. R., and Shelanski, M. L. 1975. Biochemical studies on the in vitro assembly and disassembly of microtubules. *Ann. N. Y. Acad. Sci.* **253**: 133-146.

Giamberardino, L. D., Bennett, G., Koenig, H. L., and Droz, B. 1973. Axonal migration of protein and glycoprotein to nerve endings. III. Cell fractionation analysis of chicken ciliary ganglion after intracerebral injection of labeled precursors of proteins and glycoproteins. *Brain Res.* **60**: 147-159.

Gilbert, S. P., and Sloboda, R. D. 1984. Bidirectional transport of fluorescently labeled vesicles introduced into extruded axoplasm of squid *Loligo pealei*. *J. Cell Biol.* **99**: 445-452.

Grafstein, B., and Forman, D. S. 1980. Intracellular transport in neurons. *Physiol. Rev.* **60**: 1167-1283.

Griffiths, G., and Simons, K. 1986. The *trans* Golgi network: Sorting at the exit site of the Golgi complex. *Science* **23**: 438-443.

Gross, G. W. 1973. The effect of temperature on the rapid axoplasmic transport in C-fibers. *Brain Res.* **56**: 359-363.

Gross, G. W., and Beidler, L. M. 1973. Fast axonal transport in the C-fibers of the garfish olfactory nerve. *J. Neurobiol.* **4**: 413-428.

Gross, G. W., and Beidler, L. M. 1975. A quantitative analysis of isotope concentration profiles and rapid transport velocities in the C-fibers of the garfish olfactory nerve. *J. Neurobiol.* **6**: 213-232.

Hammerschlag, R., Stone, G. C., Bolen, F. A., Lindsey, J. D., and Ellisman, M. H. 1982. Evidence that all newly synthesized proteins destined for fast axonal transport pass through the Golgi apparatus. *J. Cell Biol.* **93**: 568-575.

Hammond, G. R., and Smith, R. S. 1977. Inhibition of the rapid movement of optically detectable axonal particles by colchicine and vinblastine. *Brain Res.* **128**: 227-242.

Hanson, M. 1978. A new method to study fast axonal transport *in vivo*. *Brain Res.* **153**: 121-126.

Hanson, M. 1979. Fast axonal transport of acetylcholinesterase and protein in cold-blocked frog sciatic nerves *in vitro*. *Neurosci.* **4**: 413-416.

Hanson, M., and Edström, A. 1977. Fast axonal transport: Effect of antimitotic drugs and inhibitors of energy metabolism on the rate and amount of transported protein in frog sciatic nerves. *J. Neurobiol.* **8**: 97-108.

Hendrickson, A. E. 1972. Electron microscopic distribution of axoplasmic transport. *J. Comp. Neurol.* **144**: 381-397.

Heslop, J. P., and Howes, E. A. 1972. Temperature and inhibitor effects on fast axonal transport in a molluscan nerve. *J. Neurochem.* **19**: 1709-1716.

Hirokawa, N., Sato-Yoshitake, R., Kobayashi, N., Pfister, K. K., Bloom, G. S., and Brady, S. T. 1991. Kinesin associates with anterogradely transported membranous organelles *in vivo*. *J. Cell Biol.* **114**: 295-302.

Inoué, S. 1986. Video Microscopy. New York. Plenum Press.

Kendal, W. S., Koles, Z. J., and Smith, R. S. 1983. Oscillatory motion of intra-axonal organelles of *Xenopus laevis* following inhibition of their rapid transport. *J. Physiol.* **345**: 501-513.

Kirkpatrick, J. B., Bray, J. J., and Palmer, S. M. 1972. Visualization of axoplasmic flow *in vitro* by Nomarski microscopy. Comparison to rapid flow of radioactive proteins. *Brain Res.* **43**: 1-10.

Lasek, R. 1968. Axoplasmic transport in cat dorsal root ganglion cells: As studied with [^{3}H]-L-leucine. *Brain Res.* **7**: 360-377.

Lasek, R. J., and Brady, S. T. 1985. Attachment of transported vesicles to microtubules in axoplasm is facilitated by AMP-PNP. *Nature* **316**: 645-647.

LaVail, J. H., Rapisardi, S., and Sugino, I. K. 1980. Evidence against the smooth endoplasmic reticulum as a continuous channel for the retrograde axonal transport of horseradish peroxidase. *Brain Res.* **191**: 3-20.

Levine, J., and Willard, M. 1980. The composition and organization of axonally transported proteins in the retinal ganglion cells of the guinea pig. *Brain Res.* **194**: 137-154.

Longo, F. M., and Hammerschlag, R. 1980. Relation of somal lipid synthesis to the fast axonal transport of protein and lipid. *Brain Res.* **193**: 471-485.

Luzio, J. P., and Banting, G. 1993. Eukaryotic membrane traffic: Retrieval and retention mechanisms to achieve organelle residence. *TIBS* **18**: 395-397.

Miller, R. H, and Lasek, R. J. 1985. Cross-bridges mediate anterograde and retrograde vesicle transport along microtubules in squid axoplasm. *J. Cell Biol.* **101**: 2181-2193.

Miller, R. H, Lasek, R. J., and Katz, M. J. 1987. Preferred microtubules for vesicle transport in lobster axons. *Science* **235**: 220-222.

Morin, P. J., Liu, N., Johnson, R. J., Leeman, S. E., and Fine, R. E. 1991. Isolation and characterization of rapid transport vesicle subtypes from rabbit optic nerve. *J. Neurochem.* **56**: 415-427.

Muñoz-Martínez, E. J. 1982. Axonal retention of transported material and the lability of nerve terminals. IN *Axoplasmic Transport*. (ed. D. G. Weiss) Springer-Verlag, Berlin, 256-274.

Nilsson, T., and Warren, G. 1994. Retention and retrieval in the endoplasmic reticulum and the Golgi apparatus. *Curr. Op. Cell Biol.* **6**: 517-521.

Ochs, S. 1971. Characteristics and a model for fast axoplasmic transport in nerve. *J. Neurobiol.* **2**: 331-345.

Ochs, S. 1975. Retention and redistribution of proteins in mammalian nerve fibres by axoplasmic transport. *J. Physiol.* **253**: 459-475.

Ochs, S. 1983. Axoplasmic transport. IN *Handbook of Neurochemistry*, 2nd edition. (ed. A. Lajtha) Plenum Press, New York, 355-379.

Ochs, S., and Hollingsworth, D. 1971. Dependence of fast axoplasmic transport in nerve on oxidative metabolism. *J. Neurochem.* **18**: 107-114.

Ochs, S., and Ranish, N. 1969. Characteristics of the fast transport system in mammalian nerve fibers. *J. Neurobiol.* **2**: 247-261.

Ochs, S., and Smith, C. 1971. Fast axoplasmic transport in mammalian nerve *in vitro* after block of glycolysis with iodoacetic acid. *J. Neurochem.* **18**: 833-843.

Ochs, S., and Smith, C. 1975. Low temperature slowing and cold-block of fast axoplasmic transport in mammalian nerves *in vitro*. *J. Neurobiol.* **6**: 85-102.

Okabe, S., and Hirokawa, N. 1989. Axonal transport. *Curr. Op. Cell Biol.* **1**: 91-97.

Parton, R. G. and Dotti, C. G. 1993. Cell biology of neuronal endocytosis. *J. Neurosci. Res.* **36**: 1-9.

Ranish, N., and Ochs, S. 1972. Fast axoplasmic transport of acetylcholinesterase in mammalian nerve fibres. *J. Neurochem.* **19**: 2641-2649.

Rothman, J. E. 1994. Mechanisms of intracellular protein transport. *Nature* **372**: 55-63.

Sahenk, Z., and Brady, S. T. 1987. Axonal tubulin and microtubules: Morphologic evidence for stable regions on axonal microtubules. *Cell Motil. Cytoskeleton* **8**: 155-164.

Sahenk, Z., and Lasek, R. J. 1988. Inhibition of proteolysis blocks anterograde-retrograde conversion of axonally transported vesicles. *Brain Res.* **460**: 199-203.

Schnapp, B. J., and Reese, T. S. 1989. Dynein is the motor for retrograde axonal transport of organelles. *Proc. Natl. Acad. Sci. USA.* **86**: 1548-1552.

Schroer, T. A., Steuer, E. R., and Sheetz, M. P. 1989. Cytoplasmic dynein is a minus end-directed motor for membranous organelles. *Cell* **56**: 937-946.

Schwab, M. E., and Thoenen, H. 1978. Selective binding, uptake, and retrograde transport of tetanus toxin by nerve terminals in the rat iris. An electron microscope study using colloidal gold as a tracer. *J. Cell Biol.* **77**: 1-13.

Schwab, M. E., and Thoenen, H. 1983. Retrograde axonal transport. IN *Handbook of Neurochemistry*, 2nd edition. (ed. A. Lajtha) Plenum Press, New York, 381-404.

Smith, D. S. 1971. On the significance of cross-bridges between microtubules and synaptic vesicles. *Phil. Trans. Roy. Soc. Lond. B.* **261**: 395-405.

Smith, R. S. 1980. The short term accumulation of axonally transported organelles in the region of localized lesions of single myelinated axons. *J. Neurocytol.* **9**: 36-65.

Smith, R. S. 1988. Studies on the mechanism of the reversal of rapid organelle transport in myelinated axons of *Xenopus laevis*. *Cell Motil. Cytoskel.* **10**: 296-308.

Smith, R. S. 1989. Real-time imaging of axonally transported subresolution organelles in vertebrate myelinated axons. *J. Neurosci. Methods* **26**: 203-209.

Smith, R. S. 1991. Rapid organelle transport in axons. IN *Advances in Structural Biology*, Vol. 1. JAI Press Inc., 91-116.

Smith, R. S., and Cooper, P. D. 1981. Variability and temperature dependence of the velocity of retrograde particle transport in myelinated axons. *Can. J. Physiol. Pharmacol.* **59**: 857-863.

Smith, R. S., and Forman, D. S. 1988. Organelle dynamics in lobster axons: anterograde and retrograde particulate organelles. *Brain Res.* **446**: 26-36.

Smith, R. S., Hammerschlag, R., Snyder, R. E., Chan, H., and Bobinski, J. 1994. Action of brefeldin A on amphibian neurons: Passage of newly synthesized proteins through the Golgi complex is not required for continued fast organelle transport in axons. *J. Neurochem.* **62**: 1698-1706.

Smith, R. S., and Kendal, W. S. 1985. The recovery of organelle transport and microtubule integrity in myelinated axons that are frozen and thawed. *Can. J. Physiol. Pharmacol.* **63**: 292-297.

Smith, R. S., and Snyder, R. E. 1991. Reversal of rapid axonal transport at a lesion: Leupeptin inhibits reversed protein transport, but does not inhibit reversed organelle transport. *Brain Res.* **552**: 215-227.

Smith, R. S., and Snyder, R. E. 1992. Relationships between the rapid axonal transport of newly synthesized proteins and membranous organelles. *Mol. Neurobiol.* **6**: 285-300.

Smith, R. S., and Snyder, R. E. 1995. Anterograde to retrograde reversal of fast axonal transport within cold blocked and rewarmed intact axons. *Brain Res.* **672**: 205-213.

Snyder, R. E. 1986a. The kinematics of turnaround and retrograde axonal transport. *J. Neurobiol.* **17**: 637-647.

Snyder, R. E. 1986b. A radiolabelled pulse for the simultaneous study of anterograde and retrograde axonal transport. *J. Neurosci. Meth.* **17**: 109-119.

Snyder, R. E. 1989. Loss of material from the retrograde axonal transport system in frog sciatic nerve. *J. Neurobiol.* **20**: 81-94.

Snyder, R. E., Chen, X., and Smith, R. S. 1990. Protein loss from axonal transport occurs without diminution of vesicle traffic. *Neuroreport* **1**: 259-262.

Snyder, R. E., Reynolds, R. S., Smith, R. S., and Kendal, W. S. 1976. Application of a multiwire proportional chamber to the detection of axoplasmic transport. *Can. J. Physiol. Pharmacol.* **54**: 238-244.

Snyder, R. E., and Smith, R. S. 1982. Application of position-sensitive radioactivity detectors to the study of the axonal transport of β-emitting isotopes. IN *Axoplasmic Transport*. (ed. D. G. Weiss) Springer-Verlag, Berlin, 442-453.

Snyder, R. E., Smith, R. S., and Chen, X. 1994. Reversal of rapidly transported protein and organelles at an axonal lesion. *Brain Res.* **635**: 49-58.

Stone, G. C., and Hammerschlag, R. 1987. Molecular mechanisms involved in sorting of fast-transported proteins. IN *Neurology and Neurobiology*.

Volume 25, Axonal Transport. (eds. R. S. Smith and M. A. Bisby) A. R. Liss, Inc., New York, 15-36.

Takenaka, T., Horie, H., Sugita, T. 1978. New technique for measuring dynamic axonal transport and its application to temperature effects. *J. Neurobiol.* **9**: 317-324.

Tsukita, S., and Ishikawa, H. 1980. The movement of membranous organelles in axons: Electron microscopic identification of anterogradely and retrogradely transported organelles. *J. Cell Biol.* **84**: 513-530.

Tytell, M., Black, M. M., Garner, J. A., and Lasek, R. J. 1981. Axonal transport: Each major rate component reflects the movement of distinct macromolecular complexes. *Science* **214**: 179-181.

Vale, R. D., Reese, T. S., and Sheetz, M. P. 1985a. Identification of a novel force-generating protein, kinesin, involved in microtubule-based motility. *Cell* **42**: 39-50.

Vale, R. D., Schnapp, B. J., Mitchison, T., Steuer, E., Reese, T. S., and Sheetz, M. P. 1985b. Different axoplasmic proteins generate movement in opposite directions along microtubules *in vitro*. *Cell* **43**: 623-632.

Vale, R. D., Schnapp, B. J., Reese, T. S., and Sheetz, M. P. 1985c. Movement of organelles along filaments dissociated from the axoplasm of the squid giant axon. *Cell* **40**: 449-454

Vale, R. D., Schnapp, B. J., Reese, T. S., and Sheetz, M. P. 1985d. Organelle, bead, and microtubule movement translocations promoted by soluble factors from the squid giant axon. *Cell* **40**: 559-569.